

Matej Bel University

Acta Universitatis Matthiae Belii
series Mathematics
Volume 28

 BELIANUM

2020

ACTA UNIVERSITATIS MATTHIAE BELII, SERIES MATHEMATICS
ISSN 1338-712X

- Editor-in-chief:** Miroslav Haviar, Matej Bel University, B. Bystrica, Slovakia
- Executive editor:** Ján Karabáš, Matej Bel University, B. Bystrica, Slovakia
- Editorial board:** A. Breda d’Azevedo, Univesidade de Aveiro, Aveiro, Portugal
B. A. Davey, La Trobe University, Melbourne, Australia
M. Dirbák, Matej Bel University, B. Bystrica, Slovakia
M. Haviar, Matej Bel University, B. Bystrica, Slovakia
V. Janiš, Matej Bel University, B. Bystrica, Slovakia
J. Karabáš, Matej Bel University, B. Bystrica, Slovakia
M. Klin, Ben-Gurion University of the Negev, Be’er Sheva, Israel
J. Kratochvíl, Charles University, Prague, Czech republic
P. Kráľ, Matej Bel University, B. Bystrica, Slovakia
V. Jiménez López, Universidad de Murcia, Murcia, Spain
R. Nedela, University of West Bohemia, Pilsen, Czech republic
A. Sergyeyev, Silesian University in Opava, Czech republic
Ľ. Snoha, Matej Bel University, B. Bystrica, Slovakia
- Editorial office:** Acta Universitatis Matthiae Belii, ser. Mathematics
Department of Mathematics, Faculty of Natural Sciences
Matej Bel University
Tajovského 40
974 01 Banská Bystrica
Slovakia
E-mail: actamath@savbb.sk
- Scope of Journal:** Acta Universitatis Matthiae Belii, series Mathematics, publishes original research articles and survey papers in all areas of mathematics and theoretical computer science. Occasionally valuable papers dealing with applications of mathematics in other fields can be published.
- Manuscripts:** We only consider original articles not under consideration in other journal and written in English. For the preparation of your manuscript use please `ambart` L^AT_EX document class, available from <https://actamath.savbb.sk>. Send the source file and figures needed to compile the output form as an attachment via e-mail to the address actamath@savbb.sk.
- Subscriptions:** Acta Universitatis Matthiae Belii series Mathematics is usually published once a year. The journal is available for exchange. Information on the exchange is available from the Editorial Office. On-line version of the journal is available at <https://actamath.savbb.sk>.

Matej Bel University
Faculty of Natural Sciences

Acta Universitatis Matthiae Belii
series Mathematics

Volume 28



Banská Bystrica, 2020

Degree 5 polynomials and Descartes' rule of signs

Hassen Cheriha

Université Côte d'Azur, LJAD, France

University of Carthage, EPT - LIM, Tunisia

hassen.cheriha@gmail.com, hassan.cheriha@unice.fr

Yousra Gati

University of Carthage, EPT - LIM, Tunisia

yousra.gati@gmail.com

Vladimir Petrov Kostov

Université Côte d'Azur, LJAD, France

vladimir.kostov@unice.fr

Abstract

For a univariate real polynomial without zero coefficients, Descartes' rule of signs (completed by an observation of Fourier) says that its numbers *pos* of positive and *neg* of negative roots (counted with multiplicity) are majorized respectively by the numbers *c* and *p* of sign changes and sign preservations in the sequence of its coefficients, and that the differences $c - pos$ and $p - neg$ are even numbers. For degree 5 polynomials, it has been proved by A. Albouy and Y. Fu that there exist no such polynomials having three distinct positive and no negative roots and whose signs of the coefficients are $(+, +, -, +, -, -)$ (or having three distinct negative and no positive roots and whose signs of the coefficients are $(+, -, -, -, -, +)$). For degree 5 and when the leading coefficient is positive, these are all cases of numbers of positive and negative roots (all distinct) and signs of the coefficients which are compatible with Descartes' rule of signs, but for which there exist no such polynomials. We explain this non-existence and the existence in all other cases with $d = 5$ by means of pictures showing the discriminant set of the family of polynomials $x^5 + x^4 + ax^3 + bx^2 + cx + d$ together with the coordinate axes.

Received May 4, 2020

Accepted in final form September 30, 2020

Communicated with Miroslav Haviar.

Keywords real polynomial in one variable, sign pattern, Descartes' rule of signs.

MSC(2010) Primary: 26C10; Secondary: 12D05.

1 Introduction

Consider a univariate real polynomial $P(x) := \sum_{j=0}^d a_j x^j$, $a_d \neq 0$, with c sign changes in the sequence of its coefficients. The classical Descartes' rule of signs says that the number *pos* of its positive roots is not larger than c , see [10]. Fourier (see [8]) has observed also that if roots are counted with multiplicity, then the number $c - pos$ is even. In the present paper we consider polynomials with all coefficients nonzero. In this case if one considers the polynomial $P(-x)$ and applies Descartes' rule to it, one finds that for the number *neg* of negative roots of P , (counted with multiplicity) one obtains $neg \leq p$, where p is the number of sign preservations in the sequence of coefficients (hence $c + p = d$); moreover, the number $p - neg$ is even. Descartes' rule of signs gives only necessary conditions about the possible values of the numbers *pos* and *neg* when the numbers c and p are known. To explain what sufficient conditions means we need the following definition:

Definition 1. For a given degree d , a *sign pattern (SP)* is a sequence of $d + 1$ signs (+ or -). We assume the first of them to be a +, because without loss of generality we consider only monic polynomials. Given the degree d and a SP, we denote by c and p the numbers of sign changes and sign preservations in the SP and we call the pair (c, p) *Descartes' pair*. Any pair (pos, neg) satisfying the conditions

$$pos \leq c \quad , \quad c - pos \in 2\mathbb{Z} \quad , \quad neg \leq p \quad , \quad p - neg \in 2\mathbb{Z} \quad (1.1)$$

is called *admissible pair (AP)* for the given SP. In particular, the Descartes' pair is an AP. A given couple (SP, AP) is *realizable* if there exists a monic degree d polynomial the signs of whose coefficients define the given SP and which has exactly pos positive and exactly neg negative roots, all of them simple.

To give sufficient conditions in the context of Descartes' rule of signs means to give the answer to the following realization problem:

Problem 2. For a given degree d , which couples (SP, AP) are realizable and which are not?

The answer to this problem is known for $d \leq 8$. For $d \leq 3$, all couples (SP, AP) are realizable. For $d = 4$, the answer to it is due to D. Grabiner, see [9], for $d = 5$ and 6 it is due to A. Albouy and Y. Fu, see [1], and for $d = 7$ and 8, it was given by J. Forsgård, V. P. Kostov and B. Z. Shapiro, see [6], [7] and [12].

Remark 3. In order to reduce the number of couples (SP, AP) to be considered one can use the following $\mathbb{Z}_2 \times \mathbb{Z}_2$ -action. Its first generator g_1 changes a given polynomial $P(x)$ to $(-1)^d P(-x)$ thereby changing every second sign of the SP and replacing the AP (pos, neg) by the AP (neg, pos) . The second generator g_2 changes $P(x)$ to $P^R(x) := x^d P(1/x)/P(0)$ which means reading the SP backward and preserving the AP (the roots of the *reverted polynomial* P^R are the reciprocals of the roots of P). The generators g_1 and g_2 are commuting involutions. Given a couple (SP, AP) (denoted by λ), the couples λ and $g_1(\lambda)$ are always different, because the second signs of their SPs are different, but one might have $g_2(\lambda) = \lambda$ or $g_1 g_2(\lambda) = \lambda$.

Thus orbits of the $\mathbb{Z}_2 \times \mathbb{Z}_2$ -action consist of 4 or 2 couples (SP, AP). E.g. for $d = 2$, one has the orbit $((+, -, -), (1, 1)), ((+, +, -), (1, 1))$ of length 2; for $d = 3$, the orbit

$$\begin{aligned} & ((+, +, +, -), (1, 2)) \quad , \quad ((+, -, +, +), (2, 1)) \quad , \\ & ((+, -, -, -), (1, 2)) \quad , \quad ((+, +, -, +), (2, 1)) \end{aligned}$$

is of length 4. It is clear that all 4 or 2 couples (SP, AP) of a given orbit are simultaneously (non)realizable.

In each of the cases $d = 4$ and $d = 5$ there is exactly one example of non-realizability of a couple (SP, AP) modulo the $\mathbb{Z}_2 \times \mathbb{Z}_2$ -action, namely

$$\left((+, +, -, +, +), (2, 0) \right) \quad \text{and} \quad \left((+, +, -, +, -, -), (3, 0) \right) \quad , \quad (1.2)$$

see [9] and [1] respectively. For each of these two couples (SP, AP) one has $g_2(\lambda) = \lambda$, see Remark 3, so they define orbits of length 2. For $d = 6, 7$ and 8, there are respectively 4, 6 and 19 non-realizable cases modulo the $\mathbb{Z}_2 \times \mathbb{Z}_2$ -action, see [1], [6], [7] and [12].

Proposition 4. For $d = 5$, there are 22 realizable and no non-realizable orbits of the $\mathbb{Z}_2 \times \mathbb{Z}_2$ -action of length 4 and 13 realizable and one non-realizable orbits of length 2.

The proposition is proved in Section 3 after Remarks 14.

In [13] the *discriminant set* of the family of polynomials $x^4 + x^3 + ax^2 + bx + c$ is represented (i.e. the set of values of the triple (a, b, c) for which the polynomial has a multiple real root) and thus the non-realizability of the first of the two cases (1.2) is explained geometrically. In the present paper we give such an explanation for the non-realizability of the second of these cases and of the realizability of all other cases with $d = 5$. One can assume that the first two signs of the SP are $(+, +)$. Recall that $a_d = 1$. The change $P(x) \mapsto P(a_{d-1}x)/a_{d-1}^d$ transforms $P(x)$ into $x^d + x^{d-1} + \dots$, i.e. one can normalize the first two coefficients. So we consider the 4-parameter family of polynomials

$$P(x, a, b, c, d) := x^5 + x^4 + ax^3 + bx^2 + cx + d, \quad (1.3)$$

with $a, b, c, d \in \mathbb{R}$. We denote by Δ the *discriminant set*

$$\Delta := \{ (a, b, c, d) \in \mathbb{R}^4 \mid \text{Res}(P, \partial P/\partial x, x) = 0 \}, \quad (1.4)$$

where $\text{Res}(P, \partial P/\partial x, x)$ is the resultant of the polynomials P and $\partial P/\partial x$ when considered as polynomials in x , i.e. the determinant of the corresponding Sylvester matrix. A polynomial of the family P has a multiple real root exactly when $(a, b, c, d) \in \Delta$. Our aim is to explain by means of pictures of the set Δ why the second of the cases (1.2) is not realizable. These pictures are given in Section 3. In Section 2 we remind some properties of the set Δ and we explain the notation used in the pictures.

2 Properties of the discriminant set

The set Δ partitions $\mathbb{R}^4 \setminus \Delta$ into three open domains, in which a polynomial of the family P has 5, 3 or 1 simple real roots and hence 0, 1 or 2 conjugate pairs respectively (for properties of discriminants see [2]). In the figures these domains are indicated by the letters h , t and s respectively. We remind that polynomials of the domain h (i.e. with all roots real) are called *hyperbolic*; the set of values of the parameters (a, b, c, d) for which the polynomial P is hyperbolic is called the *hyperbolicity domain* of the family (1.3). The domain h , contrary to the domains t and s , is not present in all figures, and when it is present, it is bounded; it is a curvilinear quadrigon or triangle, see part (2) of Remarks 12. The set Δ and the coordinate hyperplanes together partition the set

$$\mathbb{R}^4 \setminus \{ \Delta \cup \{ a = 0 \} \cup \{ b = 0 \} \cup \{ c = 0 \} \cup \{ d = 0 \} \} \quad (2.1)$$

into open domains in each of which both the number of real roots and the signs of the coefficients of the polynomial P remain the same, see the first paragraph of the Introduction; in fact, the real roots are distinct and nonzero hence the number of positive and negative roots is the same in each of the domains. The non-realizability of the second of the cases (1.2) is explained by the absence of the corresponding domain.

Remark 5. It would be interesting to (dis)prove that each of the open domains of the set (2.1) is contractible and that to each realizable case (SP, AP) there corresponds exactly one of these domains.

Remark 6. For $d = 6, 7$ and 8 , the following *neighbouring property* holds true (the property can be checked directly using the results of [1], [6], [7] and [12]): For each two non-realizable orbits C_0, C_* of the $\mathbb{Z}_2 \times \mathbb{Z}_2$ -action one can find a finite string of such orbits $C_1, C_2, \dots, C_s = C_*$ such that for each two of the orbits C_i and C_{i+1} of this string there exist couples (SP, AP) $C_i^0 \in C_i, C_{i+1}^0 \in C_{i+1}$, such that either the SPs of C_i^0 and C_{i+1}^0 differ only by one sign and their APs are the same, or their SPs and one of the

components of their APs are the same while the other components of the APs differ by ± 2 .

Example: for $d = 6$, the non-realizable cases are the ones of the orbits of the following couples (SP, AP), see [1]:

$$\begin{aligned} & ((+, +, -, +, -, -, +), (4, 0)) \quad , \quad ((+, +, -, +, -, +, +), (2, 0)) \\ & ((+, +, -, +, -, +, +), (4, 0)) \quad \text{and} \quad ((+, +, -, +, +, +, +), (2, 0)) . \end{aligned}$$

It is clear that they are neighbouring.

If the couples C_i^0 and C_{i+1}^0 were realizable, then they would correspond to two domains of the set (2.1) separated by a hypersurface, either by Δ or by one of the coordinate hyperplanes.

For $d = 9$, the neighbouring property does not hold true. Indeed, there exists a single non-realizable case (modulo the $\mathbb{Z}_2 \times \mathbb{Z}_2$ -action) with both components of the AP nonzero, this is the couple $C_{\sharp} := ((+, -, -, -, -, +, +, +, +, -), (1, 6))$, see [3]. There exist non-realizable cases in which one of the components of the AP equals 0, see [4]. However there are no non-realizable couples in which the AP equals $(1, 8)$, $(1, 4)$, $(3, 6)$, $(8, 1)$, $(4, 1)$ or $(6, 3)$. Hence if C_0 is an orbit of a couple (SP, AP) with one of the components of the AP equal to 0 and C_* is the orbit of the couple C_{\sharp} , then one cannot construct the string of orbits C_i .

The set Δ is *stratified*. Its strata are defined by the *multiplicity vectors* of the real roots of the polynomials of the family P (in the case of two conjugate pairs, we do not specify whether these pairs are distinct or not). The notation which we use for the strata should be clear from the following example:

Example 7. There is a single stratum \mathcal{T}_5 corresponding to a polynomial with a five-fold real root. This polynomial is

$$(x + 1/5)^5 = x^5 + x^4 + 2x^3/5 + 2x^2/25 + x/125 + 1/3125 \quad (2.2)$$

and the stratum \mathcal{T}_5 is of dimension 0 in \mathbb{R}^4 (we remind that the coefficients of x^5 and x^4 are both 1). The strata $\mathcal{T}_{4,1}$, $\mathcal{T}_{3,2}$, $\mathcal{T}_{2,3}$ and $\mathcal{T}_{1,4}$ are of dimension 1 in \mathbb{R}^4 ; they correspond to polynomials of the form $(x - x_1)^m(x - x_2)^{5-m}$, where $x_1 < x_2$ and $m = 4, 3, 2$ and 1 respectively; hence $mx_1 + (5 - m)x_2 = -1$. The stratum \mathcal{T}_3 is of dimension 2 and corresponds to polynomials $(x - x_1)^3(x^2 + ux + v)$, where $u^2 < 4v$.

Remark 8.

- (1) The dimension of a stratum is equal to the number of distinct roots (real or complex) minus 1; we subtract 1, because the sum of all roots equals (-1) . Thus $\mathcal{T}_{4,1}$, $\mathcal{T}_{3,2}$, $\mathcal{T}_{2,3}$ and $\mathcal{T}_{1,4}$ are the only strata of dimension 1. As $d = 5$, i.e. as d is odd, there is always at least one real root, so a stratum corresponding to polynomials having at least one conjugate pair (hence to polynomials having ≥ 3 distinct roots) is of dimension ≥ 2 . This is the case of the stratum \mathcal{T}_3 .
- (2) The tangent space at any point of any stratum of dimension 1, 2 or 3 is transversal to the space $Obcd$, Ocd or Od respectively. This follows from [11, Theorem 2].

In Fig. 1 and Fig. 2 we show the projections in the (a, b) -plane of the strata \mathcal{T}_5 , $\mathcal{T}_{4,1}$, $\mathcal{T}_{3,2}$, $\mathcal{T}_{2,3}$ and $\mathcal{T}_{1,4}$. The union of the projections of the three strata $\mathcal{T}_{4,1}$, \mathcal{T}_5 and $\mathcal{T}_{1,4}$ (resp. $\mathcal{T}_{3,2}$, \mathcal{T}_5 and $\mathcal{T}_{2,3}$) is an algebraic curve drawn by a solid (resp. dashed) line and

having a cusp at the projection of \mathcal{T}_5 ; the coordinates of the projection of \mathcal{T}_5 are $(2/5, 2/25)$, see (2.2). When following a vertical line (i.e. parallel to the b -axis) from below to above, the projections of the strata are intersected in the following order: $\mathcal{T}_{4,1}, \mathcal{T}_{3,2}, \mathcal{T}_{2,3}, \mathcal{T}_{1,4}$. These projections and the a - and b -axes define 15 open zones in \mathbb{R}^2 (the space Oab), denoted by A, B, \dots, M, N and P .

The SPs which we use begin with $(+, +)$. In the right upper corner of Fig. 1 the notation $\sigma = (+, +, +, +, \bar{\sigma})$ means that when one chooses the values of the variables (a, b) from the first quadrant, then this defines the SP σ , in which $\bar{\sigma}$ stands for the couple of signs of the variables (c, d) (and similarly for the other three corners of Fig. 1). Recall that in the plane, the four open quadrants correspond to the following couples of signs of the two coordinates:

$$\text{I : } (+, +), \text{ II : } (-, +), \text{ III : } (-, -) \text{ and IV : } (+, -) .$$

Notation 9. Further in the text, we use the following notation: $\sigma_{i,j}$ means that the signs of the variables (a, b) correspond to the i th and the ones of the variables (c, d) to the j th quadrant. Thus the SPs $(+, +, -, +, +, -)$ and $(+, +, +, +, -, -)$ are denoted by $\sigma_{2,4}$ and $\sigma_{1,3}$ respectively.

We explain now the meaning of the pictures. In Fig. 1, 2, 3 and 4 we represent the plane (a, b) ; the a -axis is horizontal and the b -axis is vertical. In the rest of the figures we represent the plane (c, d) ; the c -axis is horizontal and the d -axis is vertical. We fix a value (a_0, b_0) of the couple (a, b) from one of the domains A, \dots, N, P , and we draw the set $\Delta^\sharp := \Delta|_{(a,b)=(a_0,b_0)}$. The figures thus obtained resemble the ones given in [15] in relationship with the butterfly catastrophe. Indeed, in the definition of the latter one uses a degree 5 monic polynomial family S with vanishing coefficient of x^4 . The family $P(x, a, b, c, d)$, see (1.3), is obtained from S via the shift $x \mapsto x+1/5$ which means making an upper-triangular affine transformation in the space of coefficients. The convexity of the curves shown in the figures results from the following theorem of I. Méguerditchian, see [14, Proposition 1.3.3], which is a generalization of a result of B. Chevallier, see [5].

Theorem 10. *Locally the discriminant set Δ at a point, where it is smooth, belongs entirely to one of the two half-spaces defined by its tangent hyperplane, namely, the one, where the polynomial P has two more real roots.*

We use also another result of [14]:

Lemma 11 (Lemma about the product). *Suppose that P_1, \dots, P_s are monic polynomials, where for $i \neq j$, the polynomials P_i and P_j have no root in common. Set $P := P_1 \cdots P_s$. Then there exist open neighbourhoods U_k of P_k and U of P such that for $Q_k \in U_k$, the mapping*

$$U_1 \times \cdots \times U_s \rightarrow U \quad , \quad (Q_1, \dots, Q_s) \mapsto Q_1 \cdots Q_s$$

is a diffeomorphism.

Remark 12.

(1) From Lemma 11 one can deduce what local singularities of the sets Δ^\sharp can be encountered. At a point (a, b, c, d) for which the polynomial $\tilde{P} := P(x, a, b, c, d)$ has one double and one or three simple roots the set Δ^\sharp is smooth. Indeed, according to Lemma 11 in this case the set Δ^\sharp is locally diffeomorphic to the cartesian product of the discriminant set of the family $x^2 + ux + v$, $u, v \in \mathbb{R}$ (which is the curve $u^2 = 4v$), and \mathbb{R}^2 .

At a point where \tilde{P} has a triple real root and 2 or 0 simple real roots, the set Δ^\sharp is diffeomorphic to the cartesian product of a semi-cubic parabola (i.e. a cusp) and \mathbb{R}^2 . Indeed, the discriminant set of the family of polynomials $S_1 := x^3 + ux + v$, $u, v \in \mathbb{R}$, is the curve $27v^2 + 4u^3 = 0$. The family $S_2 := x^3 + wx^2 + u^*x + v^*$ is obtained from S_1 via the shift $x \mapsto x + w/3$; here $u^* = u + w^2/3$ and $v^* = v + uw/3 + w^3/27$. In the figures cusp points are denoted by κ , λ and μ .

At a point where \tilde{P} has one simple and two double roots, the set Δ^\sharp is locally diffeomorphic to the cartesian product of two transversally intersecting smooth curves and \mathbb{R}^2 , see Lemma 11. In the figures, such points are denoted by ϕ , ψ or θ .

At a point where \tilde{P} has a triple and a double real roots, the set Δ^\sharp is locally diffeomorphic to a cartesian product of \mathbb{R}^2 and the union of a semi-cubic parabola and a smooth arc passing through the cusp point and transversal to the geometric tangent at the cusp point. Such points belong to the strata $\mathcal{T}_{2,3}$ and $\mathcal{T}_{3,2}$. We do not show such sets Δ^\sharp in the pictures.

Finally, if \tilde{P} has a quadruple and a simple real roots (such points belong to the strata $\mathcal{T}_{1,4}$ and $\mathcal{T}_{4,1}$), then locally the set Δ^\sharp is diffeomorphic to the cartesian product of a swallowtail and \mathbb{R} . For a picture of a swallowtail see [15].

In the figures the letters α and ω denote the "infinite branches" of the sets Δ^\sharp .

There are no vertical tangent lines at any point of any of the sets Δ^\sharp , see part (2) of Remarks 8.

- (2) In the figures the hyperbolicity domain (denoted by h) is represented by the following curvilinear triangles or quadrilaterals:

$\lambda\mu\phi$	Figures	6 (right),	8 (left),	16	and 17 (right)	;
$\lambda\theta\psi\phi$	Figures	7 (left),	9 (left),	15	and 18 (left)	;
$\lambda\theta\kappa$	Figures	11,	14,	19 (left)	.	

How the set Δ looks like near the origin is justified by the following lemma:

Lemma 13. *In the space of the parameters (a, b, c, d) , a point with $c = d = 0$ belongs to the discriminant set Δ . If $b \neq 0 = c = d$, then the set Δ is tangent to the hyperplane $d = 0$. For $b > 0$ and $b < 0$ the set belongs locally to the half-plane $d \geq 0$ and $d \leq 0$ respectively.*

Proof. For $c = d = 0$, the number 0 is a double root of P which proves the first claim of the lemma. For $b \neq 0 = c = d$, the polynomial P is locally representable in the form $(x + \varepsilon)^2(g + hx + ux^2 + x^3)$, where $g \neq 0$. Hence $c = 2\varepsilon g + \varepsilon^2 h$ and $d = g\varepsilon^2$, i.e. the set Δ is locally defined by an equation of the form $d = c^2/4g + o(c^2)$ which proves the second claim. For $b > 0$ and $b < 0$ one has $g > 0$ and $g < 0$ respectively which proves the last statement of the lemma. \square

3 Pictures representing the discriminant set

In Figures 5-20 we show the set Δ^\sharp for values of (a, b) from the different zones shown in Figures 1 and 2. After each figure we indicate which cases are realizable in the domains h , t and s , see Notation 9. Whenever a figure consists of two pictures, the one on the right is a detailed picture close to the origin. Under each of Fig. 5-20 we indicate the cases which are realizable in the different parts of the plane (c, d) delimited by the coordinate axes and the corresponding set Δ^\sharp . E.g. when after Fig. 4 under "domain t " we write " $5, 9 \sigma_{2,1} (2,1), (0,3)$ ", this means that in the two parts of the domain t in the first

quadrant the cases $(\sigma_{2,1}, (2,1))$ and $(\sigma_{2,1}, (0,3))$ are realizable. The numbers 5 and 9 are numbers of different cases. These numbers are attributed in the order of appearance of the cases. When one and the same case appears in different zones, then it bears the same number. There are two figures corresponding to zone E, see the lines following Fig. 9.

Remark 14.

(1) The following six rules hold true. They allow to define by continuity the case (SP, AP) which is realizable in any domain of the (c, d) -plane for (a, b) fixed.

i) When the c -axis is crossed at a point not belonging to the set $\Delta^\#$ and different from the origin, then exactly one real root changes sign. When a hyperplane $a = 0$, $b = 0$ or $c = 0$ is crossed, then only the corresponding sign in the SP changes.

ii) In all pictures, in the part of the domain s which is above the c -axis, the only real root of the polynomial P is negative. Indeed, for a , b and c fixed and $d > 0$ large enough, the polynomial P has only one real root which is simple and negative.

iii) At a cusp point belonging to the closure of the domain t (but not h) the triple root of P has the same sign as the single real root in the adjacent s -domain.

iv) Suppose that a point follows the arc of the set $\Delta^\#$ which passes through the point $(0, 0)$ in the plane (c, d) . Then when the point passes from the first into the second quadrant or vice versa, a double real root of P changes sign.

v) The AP corresponding to a point of the set (2.1) and belonging to the domain h is the Descartes' pair which is defined by the SP. This allows, for each of the Figures 5-20 containing the domain h , to find the cases realizable in each of the parts of the domain h .

vi) At a self-intersection point ϕ or ψ one of the open sectors defined by the two intersecting arcs of $\Delta^\#$ belongs to the domain s and its opposite sector belongs to the domain h . The other two sectors (denoted here by S_1 and S_2) belong to the domain t . When a point moves from ϕ or ψ into S_1 , then one of the two double roots of P gives birth to a complex conjugate pair of roots. When a point moves from ϕ or ψ into S_2 , then the other one of the two double roots of P gives birth to such a pair. This follows from Lemma 11.

(2) To the possible Descartes' pairs of the SPs beginning with $(+, +)$, i.e. to $(0, 5)$, $(1, 4)$, $(2, 3)$, $(3, 2)$ and $(4, 1)$, there correspond 3, 3, 4, 4 and 3 possible APs respectively. E.g. to the Descartes' pair $(2, 3)$ there correspond the possible APs $(2, 3)$, $(0, 3)$, $(2, 1)$ and $(0, 1)$. This means that for the four quadrants in the plane (a, b) one obtains the following numbers of a priori possible couples (SP, AP) (we list also the zones of each quadrant in Fig. 1-2 and the possible couples (SP, Descartes' pair) for the given quadrant):

$$\text{I: } 13 \quad L, M, N, P \quad (\sigma_{1,1}, (0, 5)), (\sigma_{1,2}, (2, 3)), (\sigma_{1,3}, (1, 4)), (\sigma_{1,4}, (1, 4)) ,$$

$$\text{II: } 15 \quad A, B, C \quad (\sigma_{2,1}, (2, 3)), (\sigma_{2,2}, (4, 1)), (\sigma_{2,3}, (3, 2)), (\sigma_{2,4}, (3, 2)) ,$$

$$\text{III: } 15 \quad D, E, F, G \quad (\sigma_{3,1}, (2, 3)), (\sigma_{3,2}, (2, 3)), (\sigma_{3,3}, (1, 4)), (\sigma_{3,4}, (3, 2)) ,$$

$$\text{IV: } 15 \quad H, I, J, K \quad (\sigma_{4,1}, (2, 3)), (\sigma_{4,2}, (2, 3)), (\sigma_{4,3}, (1, 4)), (\sigma_{4,4}, (3, 2)) .$$

The non-realizable couple (the second of couples (1.2)) corresponds to quadrant II.

- (3) In Fig. 3-4 we show the projections in the plane (a, b) of the strata \mathcal{T}_5 and $\mathcal{T}_{i,j}$, $1 \leq i, j \leq 4$, $i + j = 5$, (see Fig. 1-2), and of the set \mathcal{M} of values of (a, b) for which the set Δ^\sharp has a self-intersection at $c = d = 0$. This is the set for which the polynomial $x^3 + x^2 + ax + b$ has a multiple root. It is drawn by a dotted line. It

(a) has a cusp point $(1/3, 1/27)$ situated on the projection of the stratum $\mathcal{T}_{3,2}$;

(b) is tangent to the projection of $\mathcal{T}_{2,3}$ at $(a, b) = (1/4, 0)$;

(c) is tangent to the projection of $\mathcal{T}_{1,4}$ at $(a, b) = (0, 0)$;

(d) intersects the projection of $\mathcal{T}_{3,2}$ and $\mathcal{T}_{2,3}$ at $(a, b) =$

$$(-8 - 4\sqrt{10})/15, (-152(2 + \sqrt{10}) + 52)/675) = (-1.37\dots, -1.39\dots) \quad \text{and}$$

$$(-8 + 4\sqrt{10})/15, (-152(2 - \sqrt{10}) + 52)/675) = (0.30\dots, 0.03\dots)$$

respectively;

(e) has no point in common with the projection of the stratum $\mathcal{T}_{4,1}$.

At these points the polynomial P and the set Δ^\sharp have respectively

(a) P : a triple negative root and a double root at 0, Δ^\sharp : a cusp point at $c = d = 0$ with a non-horizontal tangent line at it and a smooth arc with a horizontal tangent line at $c = d = 0$;

(b) P : a double negative root and a triple root at 0, Δ^\sharp : a cusp at $c = d = 0$ with a horizontal tangent line at it and a smooth arc with a non-horizontal tangent line at $c = d = 0$;

(c) P : a negative a simple root and a quadruple root at 0, Δ^\sharp : a 4/3-singularity with a horizontal tangent line at $c = d = 0$;

(d) at $\mathcal{T}_{3,2}$: P : a simple positive, a double negative and a double 0 root, Δ^\sharp : two transversally intersecting arcs at $(0; 0)$ one of which with a horizontal tangent line; at $\mathcal{T}_{2,3}$: P : a simple and a double negative and a double 0 root, Δ^\sharp : two transversally intersecting arcs at $(0; 0)$ one of which with a horizontal tangent line.

We do not include the set \mathcal{M} in the partition of the plane (a, b) into zones in order to keep the number of figures to be drawn reasonably low. Some changes of the relative position of the cusps of the set Δ^\sharp and the coordinate axes c and d as the values of a and b change are commented between the figures.

- (4) Two SPs, one corresponding to the third and one to the fourth quadrant in the (a, b) -plane, begin by $(+, +, -, -)$ and $(+, +, +, -)$ respectively. Hence if their last two signs are the same, then they contain one and the same number of sign changes and sign preservations. This means that one and the same APs correspond to them. Therefore the two couples (SP, AP), $(\sigma_{3,j}, (k_1, k_2))$ and $(\sigma_{4,j}, (k_1, k_2))$, are simultaneously realizable.

Proof of Proposition 4. We use Notation 9 and the definition of the generators g_1 and g_2 of the $\mathbb{Z}_2 \times \mathbb{Z}_2$ -action, see Remark 3. We consider only SPs beginning with $(+, +)$ which means that we deal with halves of orbits (the other halves are with SPs beginning with $(+, -)$, see Remark 3). We consider the action of g_1 and g_2 not only on couples (SP, AP), but also just on SPs. Thus

$$g_2(\sigma_{2,1}) = \sigma_{4,1} \quad \text{and} \quad g_2(\sigma_{1,3}) = \sigma_{3,3} . \quad (3.1)$$

The Descartes' pair corresponding to $\sigma_{2,1}$ (resp. $\sigma_{1,3}$) equals $(2, 3)$ (resp. $(1, 4)$), see part (2) of Remarks 14. We denote by ρ any of the APs, so $\rho = (2, 3), (0, 3), (2, 1)$ or $(0, 1)$ (resp. $\rho = (1, 4), (1, 2)$ or $(1, 0)$). Thus $((\sigma_{2,1}, \rho), (\sigma_{4,1}, \rho))$ (resp. $((\sigma_{1,3}, \rho), (\sigma_{3,3}, \rho))$) are half-orbits; the other halves are of the form $(g_1((\sigma_{2,1}, \rho)), g_1((\sigma_{4,1}, \rho)))$ (resp. $(g_1((\sigma_{1,3}, \rho)), g_1((\sigma_{3,3}, \rho)))$), see Remark 3. Thus we have described $4 + 3 = 7$ orbits of length 4. Next, one has

$$g_1g_2(\sigma_{1,2}) = \sigma_{4,4}, \quad g_1g_2(\sigma_{2,2}) = \sigma_{1,4}, \quad g_1g_2(\sigma_{3,2}) = \sigma_{2,4} \quad \text{and} \quad g_1g_2(\sigma_{4,2}) = \sigma_{3,4}. \quad (3.2)$$

The half-orbits in the case of $\sigma_{1,2}$ are of the form $((\sigma_{1,2}, \rho), (\sigma_{4,4}, \rho^R))$, where ρ^R is obtained from ρ by exchanging the two components, similarly for the other cases in (3.2). Thus one obtains $4 + 3 + 4 + 4 = 15$ more orbits of length 4, see part (2) of Remarks 14.

Finally, one obtains

$$g_2(\sigma_{1,1}) = \sigma_{1,1}, \quad g_2(\sigma_{2,3}) = \sigma_{2,3}, \quad g_2(\sigma_{3,1}) = \sigma_{3,1} \quad \text{and} \quad g_2(\sigma_{4,3}) = \sigma_{4,3}, \quad (3.3)$$

so by analogy with the SPs involved in (3.1) one obtains half-orbits of length 1 hence orbits of length 2. Their quantity is $3 + 4 + 4 + 3 = 14$. One of them is the only non-realizable orbit, see the second couple in (1.2). There remains to notice that each possible SP $\sigma_{i,j}$ participates in exactly one of the equalities (3.1), (3.2) and (3.3), and to remind that the generators g_1 and g_2 are commuting involutions. Hence we have described all orbits of the $\mathbb{Z}_2 \times \mathbb{Z}_2$ -action. \square

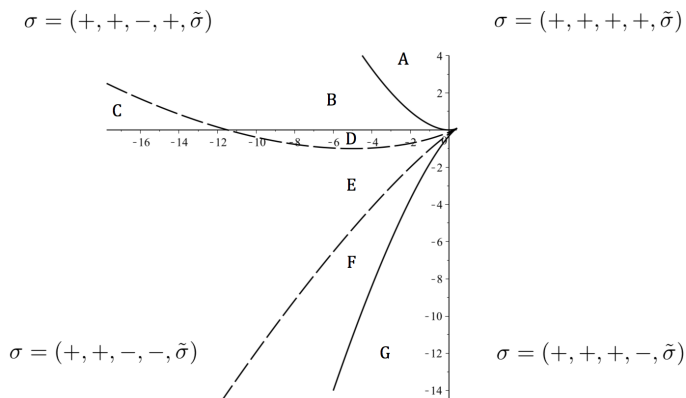


Figure 1. The projection of the discriminant locus of P to the plane of the parameters (a, b) .

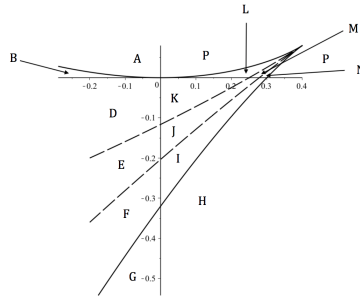


Figure 2. Picture of the projection in the plane (a, b) of the discriminant locus of P with an enlarged portion near the cusp point.

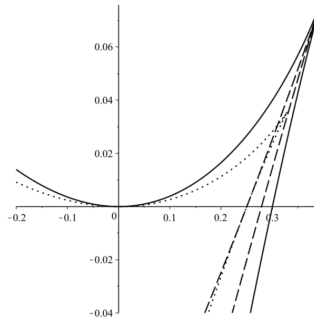


Figure 3. The projections in the plane (a, b) of the strata \mathcal{T}_5 and $\mathcal{T}_{i,j}$, $1 \leq i, j \leq 4$, $i + j = 5$, and of the set \mathcal{M} .

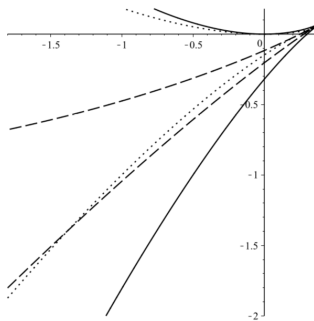


Figure 4. The projections in the plane (a, b) of the strata \mathcal{T}_5 and $\mathcal{T}_{i,j}$, $1 \leq i, j \leq 4$, $i + j = 5$, and of the set \mathcal{M} (with enlarged portion near the cusp points).

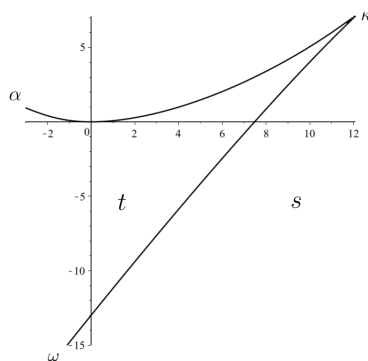


Figure 5. Zone A: The set Δ^\sharp for $a = -2$ and $b = 3$.

	domain s	domain t
1	$\sigma_{2,1} (0,1)$	5 $\sigma_{2,1} (0,3)$
2	$\sigma_{2,2} (0,1)$	6 $\sigma_{2,2} (2,1)$
3	$\sigma_{2,3} (1,0)$	7 $\sigma_{2,3} (1,2)$
4	$\sigma_{2,4} (1,0)$	8 $\sigma_{2,4} (1,2)$

Cases 2 and 6 are realizable in the open second quadrant, above and below the set Δ^\sharp respectively; cases 3 and 7 in the open third quadrant, below and above Δ^\sharp respectively; cases 4 and 8 in the open fourth quadrant, below and above Δ^\sharp respectively. Cases 1 and 5 occupy the open first quadrant minus the set Δ^\sharp , case 5 the curvilinear triangle and case 1 the rest of the quadrant.

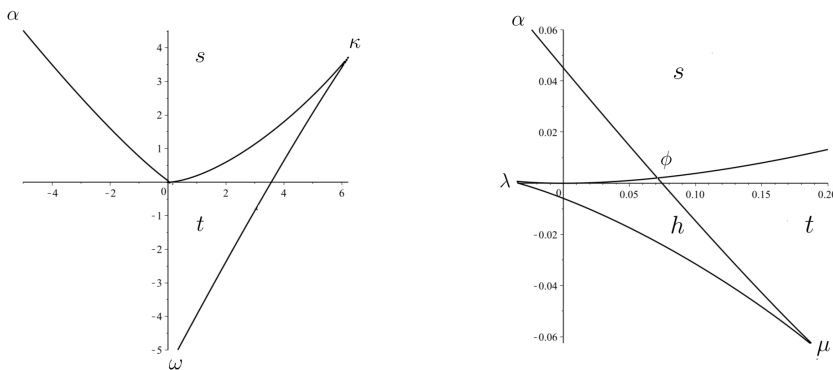


Figure 6. Zone B: The set Δ^\sharp for $a = -2$ and $b = 0.5$.

	domain s	domain t	domain h
1	$\sigma_{2,1} (0,1)$	5, 9 $\sigma_{2,1} (0,3), (2,1)$	10 $\sigma_{2,1} (2,3)$
2	$\sigma_{2,2} (0,1)$	6 $\sigma_{2,2} (2,1)$	11 $\sigma_{2,2} (4,1)$
3	$\sigma_{2,3} (1,0)$	7 $\sigma_{2,3} (1,2)$	12 $\sigma_{2,3} (3,2)$
4	$\sigma_{2,4} (1,0)$	8 $\sigma_{2,4} (1,2)$	13 $\sigma_{2,4} (3,2)$

The infinite branch ω intersects the negative d -half-axis.

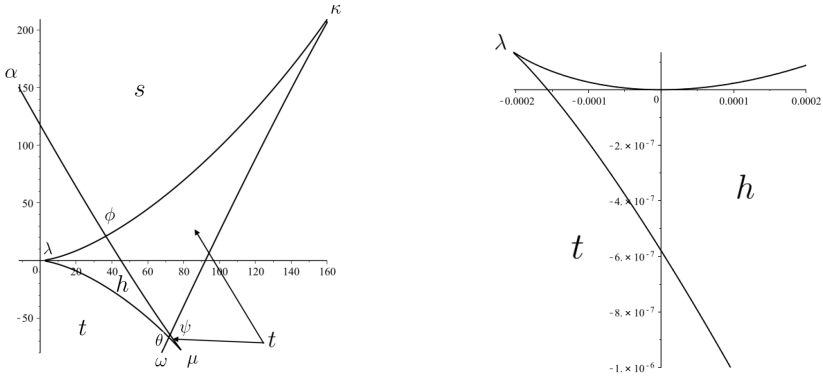


Figure 7. Zone C: The set Δ^\sharp for $a = -16$ and $b = 0.1$.

domain s		domain t		domain h	
1	$\sigma_{2,1} (0,1)$	5, 9	$\sigma_{2,1} (0,3), (2,1)$	10	$\sigma_{2,1} (2,3)$
2	$\sigma_{2,2} (0,1)$	6	$\sigma_{2,2} (2,1)$	11	$\sigma_{2,2} (4,1)$
3	$\sigma_{2,3} (1,0)$	7	$\sigma_{2,3} (1,2)$	12	$\sigma_{2,3} (3,2)$
4	$\sigma_{2,4} (1,0)$	8, 14	$\sigma_{2,4} (1,2), (3,0)$	13	$\sigma_{2,4} (3,2)$

In Fig. 7, the infinite branch ω intersects the negative d -half-axis. The intersection of the domain t with the fourth quadrant consists of three curvilinear triangles. In the one which borders the third quadrant the AP is $(1, 2)$ (as in the intersection of the domain t with the third quadrant), in the one which belongs entirely to the interior of the fourth quadrant it is $(3, 0)$ and in the one which borders the first quadrant it is again $(1, 2)$.

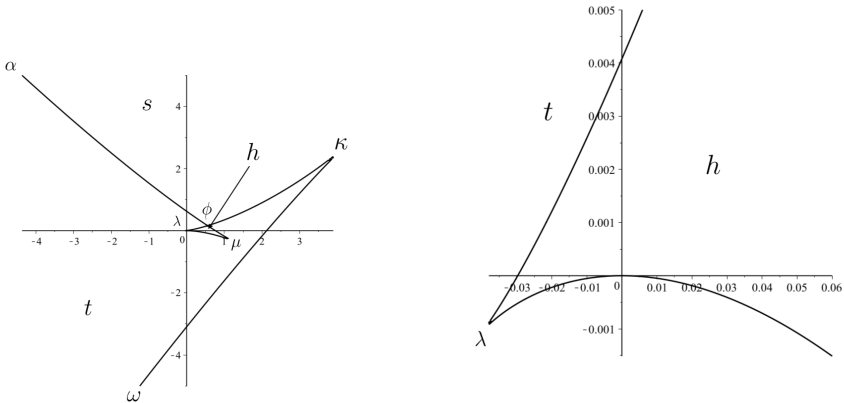


Figure 8. Zone D: The set Δ^\sharp for $a = -2$ and $b = -0.5$.

	domain s		domain t		domain h
15	$\sigma_{3,1}$ (0,1)	19 , 20	$\sigma_{3,1}$ (0,3) , (2,1)	24	$\sigma_{3,1}$ (2,3)
16	$\sigma_{3,2}$ (0,1)	21	$\sigma_{3,2}$ (2,1)	25	$\sigma_{3,2}$ (2,3)
17	$\sigma_{3,3}$ (1,0)	22	$\sigma_{3,3}$ (1,2)	26	$\sigma_{3,3}$ (1,4)
18	$\sigma_{3,4}$ (1,0)	23	$\sigma_{3,4}$ (1,2)	27	$\sigma_{3,4}$ (3,2)

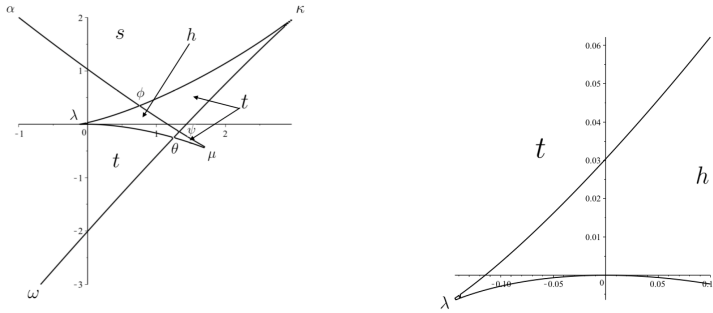


Figure 9. Zone E: The set $\Delta^\#$ for $a = -2$ and $b = -1$.

	domain s		domain t		domain h
15	$\sigma_{3,1}$ (0,1)	19 , 20	$\sigma_{3,1}$ (0,3) , (2,1)	24	$\sigma_{3,1}$ (2,3)
16	$\sigma_{3,2}$ (0,1)	21	$\sigma_{3,2}$ (2,1)	25	$\sigma_{3,2}$ (2,3)
17	$\sigma_{3,3}$ (1,0)	22	$\sigma_{3,3}$ (1,2)	26	$\sigma_{3,3}$ (1,4)
18	$\sigma_{3,4}$ (1,0)	23 , 28	$\sigma_{3,4}$ (1,2) , (3,0)	27	$\sigma_{3,4}$ (3,2)

In Fig. 9 the self-intersection point ϕ is to the right while in Fig. 10 it is to the left of the d -axis. This is why case 29 is present only in the second of these figures. In Fig. 9 there are two domains corresponding to case 23. If one compares Fig. 9 with Fig. 8 one sees that for $a = -2$, as b increases from -1 to -0.5 , the two domains of case 23 fuse in one single domain.

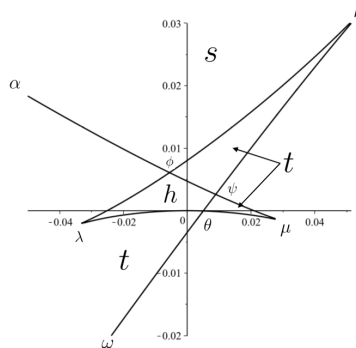


Figure 10. Zone E: The set $\Delta^\#$ for $a = -0.014$ and $b = -0.15$.

	domain s		domain t		domain h
15	$\sigma_{3,1} (0,1)$	19 , 20	$\sigma_{3,1} (0,3) , (2,1)$	24	$\sigma_{3,1} (2,3)$
16	$\sigma_{3,2} (0,1)$	21 , 29	$\sigma_{3,2} (2,1) , (0,3)$	25	$\sigma_{3,2} (2,3)$
17	$\sigma_{3,3} (1,0)$	22	$\sigma_{3,3} (1,2)$	26	$\sigma_{3,3} (1,4)$
18	$\sigma_{3,4} (1,0)$	23 , 28	$\sigma_{3,4} (1,2) , (3,0)$	27	$\sigma_{3,4} (3,2)$

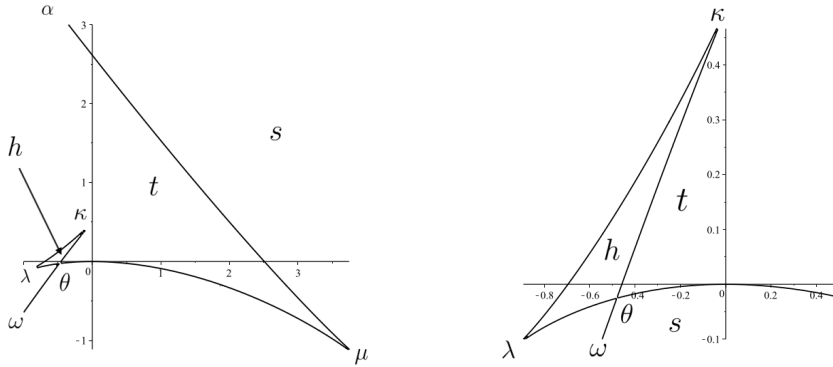


Figure 11. Zone F: The set Δ^\sharp for $a = -2$ and $b = -2.5$.

	domain s		domain t		domain h
15	$\sigma_{3,1} (0,1)$	20	$\sigma_{3,1} (2,1)$	25	$\sigma_{3,2} (2,3)$
16	$\sigma_{3,2} (0,1)$	21	$\sigma_{3,2} (2,1)$	26	$\sigma_{3,3} (1,4)$
17	$\sigma_{3,3} (1,0)$	22	$\sigma_{3,3} (1,2)$		
18	$\sigma_{3,4} (1,0)$	28	$\sigma_{3,4} (3,0)$		

The intersection of the domain t with the second quadrant consists of two parts. In both of them one and the same case is realizable.

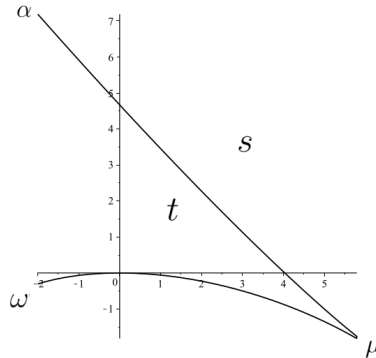


Figure 12. Zone G: The set Δ^\sharp for $a = -2$ and $b = -4$.

domain s			domain t		
15	$\sigma_{3,1}$	(0,1)	20	$\sigma_{3,1}$	(2,1)
16	$\sigma_{3,2}$	(0,1)	21	$\sigma_{3,2}$	(2,1)
17	$\sigma_{3,3}$	(1,0)	22	$\sigma_{3,3}$	(1,2)
18	$\sigma_{3,4}$	(1,0)	28	$\sigma_{3,4}$	(3,0)

When comparing Fig. 11 and Fig. 12 it becomes clear that for $a = -2$ and for some $b = b_* \in (-4, -2.5)$, in the corresponding picture of the set Δ^\sharp , the domain h intersects only the third, but not the second quadrant.

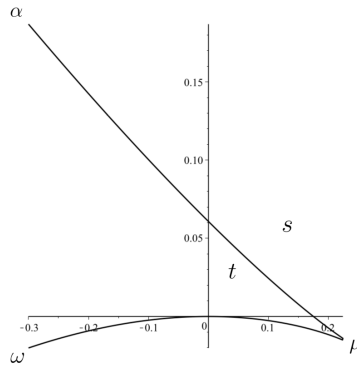


Figure 13. Zone H: The set Δ^\sharp for $a = 1$ and $b = -1$.

domain s			domain t		
30	$\sigma_{4,1}$	(0,1)	34	$\sigma_{4,1}$	(2,1)
31	$\sigma_{4,2}$	(0,1)	35	$\sigma_{4,2}$	(2,1)
32	$\sigma_{4,3}$	(1,0)	36	$\sigma_{4,3}$	(1,2)
33	$\sigma_{4,4}$	(1,0)	37	$\sigma_{4,4}$	(3,0)

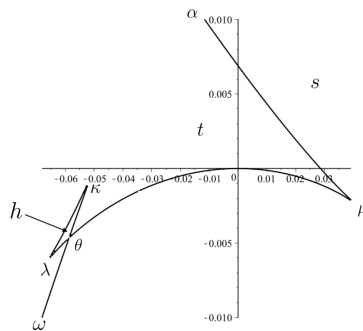


Figure 14. Zone I: The set Δ^\sharp for $a = 0.05$ and $b = -0.2$.

	domain s		domain t		domain h
30	$\sigma_{4,1}$ (0,1)		34	$\sigma_{4,1}$ (2,1)	
31	$\sigma_{4,2}$ (0,1)		35	$\sigma_{4,2}$ (2,1)	
32	$\sigma_{4,3}$ (1,0)		36	$\sigma_{4,3}$ (1,2)	38
33	$\sigma_{4,4}$ (1,0)		37	$\sigma_{4,4}$ (3,0)	$\sigma_{4,3}$ (1,4)

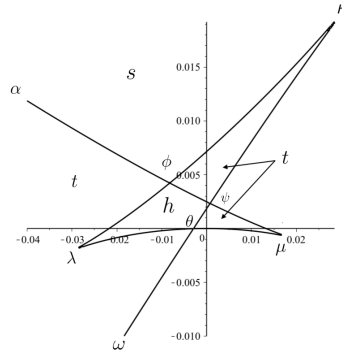


Figure 15. Zone J: The set $\Delta^\#$ for $a = 0.05$ and $b = -0.12$.

	domain s		domain t		domain h
30	$\sigma_{4,1}$ (0,1)		34 , 39	$\sigma_{4,1}$ (2,1) , (0,3)	41
31	$\sigma_{4,2}$ (0,1)		35 , 40	$\sigma_{4,2}$ (2,1) , (0,3)	42
32	$\sigma_{4,3}$ (1,0)		36	$\sigma_{4,3}$ (1,2)	38
33	$\sigma_{4,4}$ (1,0)		37	$\sigma_{4,4}$ (3,0)	$\sigma_{4,3}$ (1,4)

By comparing Figures 14 and 15 it becomes clear that for $a = 0.05$ and for some $b = b^b \in (-0.2, -0.12)$, the domain h intersects the second and the third, but not the first quadrant.

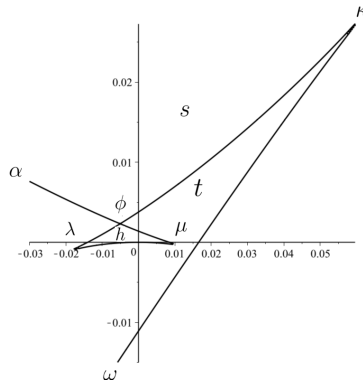


Figure 16. Zone K: The set $\Delta^\#$ for $a = 0.05$ and $b = -0.09$.

	domain s		domain t		domain h
30	$\sigma_{4,1}$ (0,1)	39	$\sigma_{4,1}$ (0,3)	41	$\sigma_{4,1}$ (2,3)
31	$\sigma_{4,2}$ (0,1)	35, 40	$\sigma_{4,2}$ (2,1), (0,3)	42	$\sigma_{4,2}$ (2,3)
32	$\sigma_{4,3}$ (1,0)	36	$\sigma_{4,3}$ (1,2)	38	$\sigma_{4,3}$ (1,4)
33	$\sigma_{4,4}$ (1,0)	43	$\sigma_{4,4}$ (1,2)	44	$\sigma_{4,4}$ (3,2)

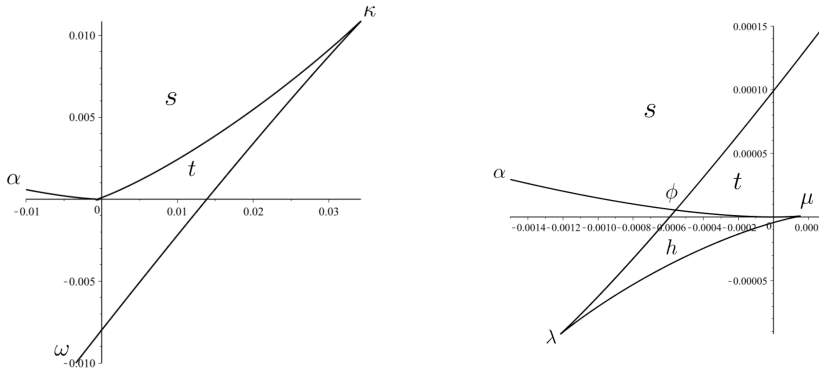


Figure 17. Zone L: The set Δ^\sharp for $a = 0.22$ and $b = 0.01$.

	domain s		domain t		domain h
45	$\sigma_{1,1}$ (0,1)	49	$\sigma_{1,1}$ (0,3)	54	$\sigma_{1,1}$ (0,5)
46	$\sigma_{1,2}$ (0,1)	50, 51	$\sigma_{1,2}$ (0,3), (2,1)	55	$\sigma_{1,2}$ (2,3)
47	$\sigma_{1,3}$ (1,0)	52	$\sigma_{1,3}$ (1,2)	56	$\sigma_{1,3}$ (1,4)
48	$\sigma_{1,4}$ (1,0)	53	$\sigma_{1,4}$ (1,2)	57	$\sigma_{1,4}$ (1,4)

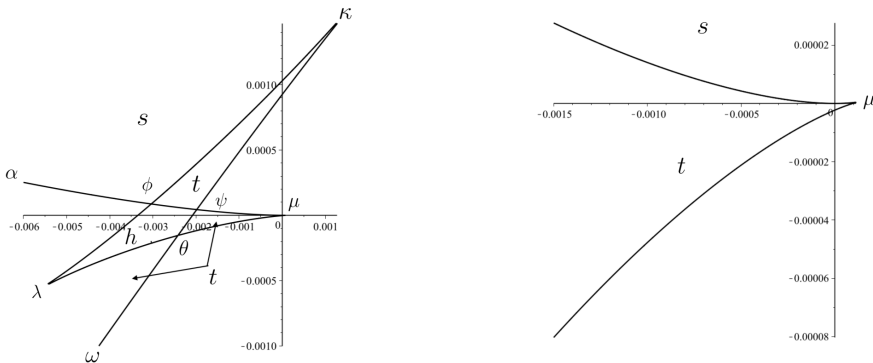


Figure 18. Zone M: The set Δ^\sharp for $a = 0.28$ and $b = 0.01$.

	domain s		domain t		domain h
45	$\sigma_{1,1} (0,1)$	49	$\sigma_{1,1} (0,3)$		
46	$\sigma_{1,2} (0,1)$	50 , 51	$\sigma_{1,2} (0,3) , (2,1)$	55	$\sigma_{1,2} (2,3)$
47	$\sigma_{1,3} (1,0)$	52	$\sigma_{1,3} (1,2)$	56	$\sigma_{1,3} (1,4)$
48	$\sigma_{1,4} (1,0)$	53	$\sigma_{1,4} (1,2)$		

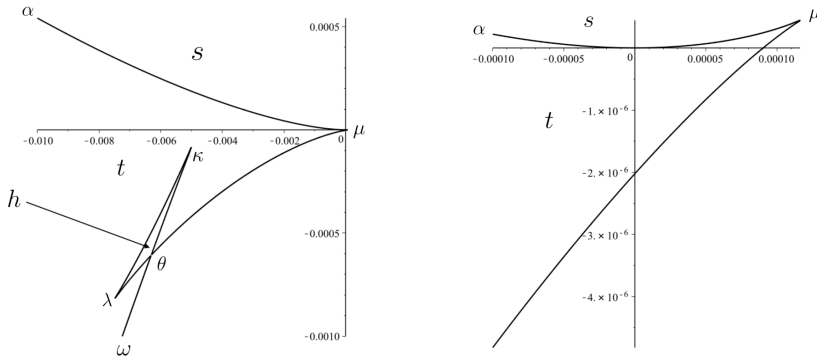


Figure 19. Zone N: The set $\Delta^\#$ for $a = 0.295$ and $b = 0.01$.

	domain s		domain t		domain h
45	$\sigma_{1,1} (0,1)$	49	$\sigma_{1,1} (0,3)$		
46	$\sigma_{1,2} (0,1)$	51	$\sigma_{1,2} (2,1)$		
47	$\sigma_{1,3} (1,0)$	52	$\sigma_{1,3} (1,2)$	56	$\sigma_{1,3} (1,4)$
48	$\sigma_{1,4} (1,0)$	53	$\sigma_{1,4} (1,2)$		

When comparing Figures 18 and 19 it becomes clear that for $b = 0.01$, there exist two values $0.28 < a_\dagger < a_{\ddagger} < 0.295$ of a such that for $a = a_\dagger$, the cusp κ is in the second quadrant, but still above the arc $\mu\alpha$ (so the self-intersection points ϕ and ψ exist), and for $a = a_{\ddagger}$, the cusp point κ is in the second quadrant and under the arc $\mu\alpha$.

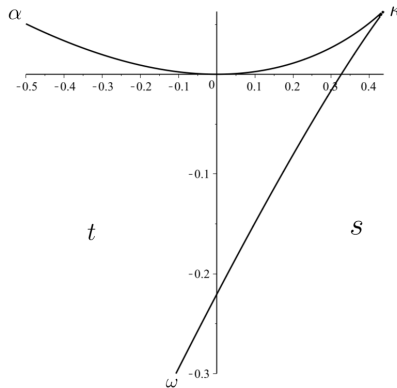


Figure 20. Zone P: The set $\Delta^\#$ for $a = 1$ and $b = 1$.

	domain s		domain t
45	$\sigma_{1,1}$ (0,1)	49	$\sigma_{1,1}$ (0,3)
46	$\sigma_{1,2}$ (0,1)	51	$\sigma_{1,2}$ (2,1)
47	$\sigma_{1,3}$ (1,0)	52	$\sigma_{1,3}$ (1,2)
48	$\sigma_{1,4}$ (1,0)	53	$\sigma_{1,4}$ (1,2)

References

- [1] A. Albouy and Y. Fu, Some remarks about Descartes' rule of signs. *Elem. Math.*, 69 (2014), 186–194.
- [2] V. I. Arnold, S. M. Gusein-Zade and A. N. Varchenko, *Singularities of Differentiable Maps*, Birkhäuser (2012).
- [3] H. Cheriha, Y. Gati and V. P. Kostov, A nonrealization theorem in the context of Descartes' rule of signs, *St. Kliment Ohridski – Faculty of Mathematics and Informatics* 106 (2019), 25–51.
- [4] H. Cheriha, Y. Gati and V. P. Kostov, On Descartes' rule for polynomials with two variations of signs *Lithuanian Math. J.* (to appear).
- [5] B. Chevallier, Courbes maximales de Harnack et discriminant. (French) [Maximal Harnack curves and the discriminant] *Séminaire sur la géométrie algébrique réelle*, Tome I, II, 41–65, *Publ. Math. Univ. Paris VII*, 24, Univ. Paris VII, Paris, 1986.
- [6] J. Forsgård, B. Shapiro and V. P. Kostov, Could René Descartes have known this? *Exp. Math.* 24 (4) (2015), 438–448.
- [7] J. Forsgård, B. Shapiro and V. P. Kostov, Corrigendum: Could René Descartes have known this? *Exp. Math.* 28 (2) (2019), 255–256.
- [8] J. Fourier, Sur l'usage du théorème de Descartes dans la recherche des limites des racines. *Bulletin des sciences par la Société philomatique de Paris* (1820) 156–165, 181–187; *œuvres* 2, 291–309, Gauthier-Villars, 1890.
- [9] D. J. Grabiner, Descartes' Rule of Signs: Another Construction. *Am. Math. Mon.* 106 (1999), 854–856.
- [10] V. Jullien, Descartes La "Geometrie" de 1637.
- [11] V. P. Kostov, On a stratification defined by real roots of polynomials, *Serdica Math. J.* 29 (2) (2003), 177–186.
- [12] V. P. Kostov, On realizability of sign patterns by real polynomials, *Czechoslovak Math. J.* 68 (2018), 853–874.
- [13] V. P. Kostov and B. Shapiro, Polynomials, sign patterns and Descartes' rule, *Acta Universitatis Matthiae Belii, series Mathematics* (2019), 1–11.
- [14] I. Méguerditchian, Thesis - Géométrie du discriminant réel et des polynômes hyperboliques, thesis defended in 1991 at the University Rennes 1.
- [15] T. Poston and I. Stewart, *Catastrophe theory and its applications*. With an appendix by D. R. Olsen, S. R. Carter and A. Rockwood. *Surveys and Reference Works in Mathematics*, No. 2. Pitman, London-San Francisco, Calif.-Melbourne: distributed by Fearon-Pitman Publishers, Inc., Belmont, Calif., 1978. xviii+491 pp. ISBN: 0-273-01029-8.

An accurate approximation method for solving fractional order boundary value problems

Mohammad Izadi

Department of Applied Mathematics,
Faculty of Mathematics and Computer,
Shahid Bahonar University of Kerman, Kerman, Iran
izadi@uk.ac.ir

Abstract

In the present work, the generalized Chebyshev polynomials are used as basis functions in a collocation scheme to solve a class of fractional differential equations along with boundary conditions arising in science, engineering, and mathematical physics. By means of the collocation points and the matrix operations, the proposed scheme transforms the fractional boundary value problems (FBVPs) into a matrix equation, and this matrix equation corresponds to a set of linear algebraic equations consist of polynomial coefficients. An error estimation based on the residual function is performed to show the accuracy of the results. Hence, an improvement of the approximate solutions are obtained based upon this error estimation. Illustrative examples are given to demonstrate the validity and applicability of the method. Comparisons between the numerical results of the proposed method with existing results are done in order to show that the new method is efficient.

Received July 2, 2020

Accepted in final form October 19, 2020

Communicated with Víctor Jiménez López.

Keywords boundary value problem, Caputo fractional derivative, Chebyshev polynomials, collocation method.

MSC(2010) 34B05, 26A33, 41A10, 34A08, 65M70.

1 Introduction

In the present work, a new simple but accurate collocation algorithm based on Chebyshev polynomials is developed to obtain an approximate solution of the following fractional differential equation [1]

$$Y''(x) + \mathcal{D}_*^{(\gamma)}Y(x) = f(x), \quad 0 \leq x \leq 1, \quad (1.1)$$

supplemented with the boundary conditions

$$Y(0) = \beta_0, \quad Y(1) = \beta_1, \quad (1.2)$$

with given β_0, β_1 as real constants. Here, the function $f(x)$ is assumed to be continuous on $[0, 1]$ and $\mathcal{D}_*^{(\gamma)}$ the standard Caputo fractional derivative operator and $n - 1 < \gamma < n$, $n \in \mathbb{N}$. The discussion about the existence and uniqueness of the solution of fractional two-point boundary value problems can be found in [2], [36], [23], [32], [35]. The fractional order boundary value problems appear in the description of many physical stochastic-transport processes and in the inspection of liquid filtration which arises in a strongly porous's medium [33], see also the monographs of Kilbas et al. [17] and the references therein.

Although, the appearance of the fractional calculus as well as the fractional differential equations (FDEs) are as old as the classical calculus, but they have recently proved to be powerful and valuable in the modeling of many phenomena in various fields of science and engineering [21, 26, 17]. To model many real world problems, it has turned out the use of the fractional-order derivatives are more adequate than the integer-order ones. That is due to the fact that the fractional derivatives and integrals enable the description of the memory properties of various materials and processes [26]. Therefore, one needs to extend the concept of the ordinary differentiation as well as the integration to an arbitrary non-integer order. However, most of the resulting FDEs do not have an exact analytical solution, so the approximative and numerical techniques are preferred in identifying the solutions behaviour of such fractional equations. Numerous analytical and numerical methods have been developed to solve the FDEs. Among others, we mention some schemes such as the fractional linear multistep method [18], the adomian decomposition method [29, 16], the variational iteration method [19], the generalized Taylor method [20], the spline techniques [35, 1], the Adams-type predictor-corrector method [6], the spectral collocation approach [8, 9, 11, 14, 12], the local discontinuous Galerkin method [10, 13, 15], and the sinc-Galerkin method [28], to name but a few.

The following approximative and numerical schemes have been proposed for the model problem (1.1)-(1.2) and closely related problems, to the best of our knowledge. These include the quadratic spline method [35], exponential spline technique [1], and sinc-Galerkin scheme [28]. Recently, considerable attention has been given to the establishment of techniques to solve the fractional differential equations using the orthogonal functions. The main characteristic of this technique is that it reduces the solution of the differential equations to the solution of a system of algebraic equations. Historically this approach was originated from the use of Fourier [25], Walsh [5] and block-pulse functions [27] and was later extended to other classical orthogonal polynomials such as Chebyshev, Legendre, Hermite, and Laguerre polynomials [31]. In most of the presented works, the use of the numerical techniques in conjunction with the operational matrices in differentiation and integration operators of some orthogonal polynomials, to solve the fractional differential equations on finite and infinite intervals, produced highly accurate solutions for such equations, see [3] for a recent review.

In this work, we are aiming to propose an approximation algorithm as an extension of the above mentioned papers. Our approach is based on the generalized fractional order of the Chebyshev orthogonal functions of the first kind to get an approximative solution of (1.1) accurately on the interval $[0, 1]$. The main idea of the proposed technique based on using these (orthogonal) functions along with the collocation points is that, it converts the differential or integral operator involved in (1.1) (1.2) to an algebraic form, thus greatly reduces the computational effort.

The content of this work is organized as follows. In the next section 2, some preliminary definitions of the fractional calculus and the relevant properties are introduced. Hence, we define the Chebyshev polynomials of fractional order and their properties. Section 3 is devoted to the presentation of the proposed collocation scheme applied to the fractional boundary value problems. Section 4 is devoted to the error analysis technique based on the residual function for the present method. Improving the Chebyshev collocation method is then introduced with the aid of the residual error function. In Section 5, we perform some experiments to illustrate the high accuracy and efficiency of the scheme. Finally, Section 5 provides a conclusion.

2 Basic definitions

In this section, first, some definitions and fundamental facts of the fractional calculus are given. Hence, some basic definitions of (generalized) Chebyshev polynomials and theorems, which are useful for our subsequent sections have been introduced.

2.1 Fractional calculus

Definition 1. Assuming that $g(x)$ is n -times continuously differentiable, the fractional derivative $\mathcal{D}_\star^{(\gamma)}$ of $g(x)$ of order $\gamma > 0$ in the Caputo's sense is defined as

$$\mathcal{D}_\star^{(\gamma)}g(x) = \begin{cases} I^{n-\gamma}g^{(n)}(x) & \text{if } n-1 < \gamma < n, \\ g^{(n)}(x), & \text{if } \gamma = n, \quad n \in \mathbb{N}, \end{cases} \quad (2.1)$$

where

$$I^\gamma g(x) = \frac{1}{\Gamma(\gamma)} \int_0^x \frac{g(s)}{(x-s)^{1-\gamma}} ds, \quad x > 0.$$

The properties of the operator $\mathcal{D}_\star^{(\gamma)}$ can be found in [26]. We make use of the followings

$$\mathcal{D}_\star^{(\gamma)}(C) = 0 \quad (C \text{ is a constant}), \quad (2.2)$$

$$\mathcal{D}_\star^{(\gamma)}x^\beta = \begin{cases} \frac{\Gamma(\beta+1)}{\Gamma(\beta+1-\gamma)}x^{\beta-\gamma}, & \text{for } \beta \in \mathbb{N}_0 \text{ and } \beta \geq \lceil \gamma \rceil, \text{ or } \beta \notin \mathbb{N}_0 \text{ and } \beta > \lceil \gamma \rceil, \\ 0, & \text{for } \beta \in \mathbb{N}_0 \text{ and } \beta < \lceil \gamma \rceil. \end{cases} \quad (2.3)$$

2.2 Chebyshev functions

The Chebyshev polynomials play an outstanding role in classical as well as modern numerical computation [7]. It is known that the classical Chebyshev polynomials (of the first kind) are defined on $[-1, 1]$. Starting with $\mathcal{T}_0(t) = 1$ and $\mathcal{T}_1(t) = t$, these polynomials satisfy the following recurrence relation

$$\mathcal{T}_{n+1}(t) = 2t\mathcal{T}_n(t) - \mathcal{T}_{n-1}(t), \quad n = 1, 2, \dots$$

By introducing the change of variable, $x = 1 - 2(\frac{t}{L})^\alpha$, $\alpha > 0$, $L > 0$, one obtains the shifted version of the polynomials defined on $[0, L]$ will be denoted as $\mathcal{T}_n^\alpha(x) = \mathcal{T}_n(t)$. This transformation was introduced in [24]. The explicit analytical form of $\mathcal{T}_n^\alpha(x)$ of degree $(n\alpha)$ is given for $n = 0, 1, \dots$

$$\mathcal{T}_n^\alpha(x) = \sum_{k=0}^n t_{n,k} x^{\alpha k}, \quad t_{n,k} = (-1)^k \frac{n 2^{2k} (n+k-1)!}{(n-k)! L^{\alpha k} (2k)!}, \quad k = 0, 1, \dots, n, \quad (2.4)$$

with $t_{0,k} = 1$ for all $k = 0, 1, \dots, n$. It is proved in [24] that the set of the fractional polynomial functions $\{\mathcal{T}_0^\alpha, \mathcal{T}_1^\alpha, \dots\}$ is orthogonal on $[0, L]$ with respect to the weight function, $w_{L,\alpha}(x) = \frac{x^{\alpha/2-1}}{\sqrt{L^\alpha-x^\alpha}}$; i.e.

$$\int_0^L \mathcal{T}_n^\alpha(x) \mathcal{T}_m^\alpha(x) w_{L,\alpha}(x) dx = \frac{\pi}{2\alpha} d_n \delta_{mn}, \quad n, m \geq 0.$$

Here, δ_{mn} is the Kronecker delta function, $d_0 = 2$ while $d_n = 1$ for $n \geq 1$. These polynomials also satisfy the following properties

$$\mathcal{T}_n^\alpha(0) = 1, \quad \mathcal{T}_n^\alpha(L) = (-1)^n.$$

2.2.1 Approximation of functions

Any square integrable function $u(x)$ in $(0, L)$, may be expanded in terms of shifted Chebyshev polynomials as

$$u(x) = \sum_0^{\infty} a_n \mathcal{T}_n^{\alpha}(x),$$

where the unknown coefficients a_n are obtained through the orthogonality properties of the shifted Chebyshev polynomials as follows

$$a_n = \frac{2\alpha}{\pi d_n} \int_0^L u(x) \mathcal{T}_n^{\alpha}(x) w_{L,\alpha}(x) dx, \quad n = 0, 1, \dots$$

However, in practice, one needs to deal with only the first $(N+1)$ -terms shifted Chebyshev polynomials to find an approximate solution of model (1.1) expressed as

$$u_{N,\alpha}(x) = \sum_{n=0}^N a_n \mathcal{T}_n^{\alpha}(x), \quad 0 \leq x \leq L, \quad (2.5)$$

where the unknown coefficients a_n , $n = 0, 1, \dots, N$ are sought. To proceed, we write $\mathcal{T}_n^{\alpha}(x)$, $n = 0, 1, \dots, N$ in the matrix form as follows

$$\mathbb{T}_{\alpha}(x) = \mathbb{B}_{\alpha}(x) \mathbb{D}, \quad (2.6)$$

where

$$\begin{aligned} \mathbb{T}_{\alpha}(x) &= [\mathcal{T}_0^{\alpha}(x) \quad \mathcal{T}_1^{\alpha}(x) \quad \dots \quad \mathcal{T}_N^{\alpha}(x)], \\ \mathbb{B}_{\alpha}(x) &= [1 \quad x^{\alpha} \quad x^{2\alpha} \quad \dots \quad x^{N\alpha}], \end{aligned}$$

and the upper triangular $(N+1) \times (N+1)$ matrix \mathbb{D} takes the form

$$\mathbb{D} = \begin{bmatrix} 1 & 1 & 1 & 1 & \dots & 1 & 1 \\ 0 & t_{1,1} & t_{2,1} & t_{3,1} & \dots & t_{N-1,1} & t_{N,1} \\ 0 & 0 & t_{2,2} & t_{3,2} & \dots & t_{N-1,2} & t_{N,2} \\ \vdots & \vdots & \ddots & \ddots & \ddots & \vdots & \vdots \\ 0 & 0 & 0 & \dots & 0 & t_{N-1,N-1} & t_{N,N-1} \\ 0 & 0 & 0 & \dots & 0 & 0 & t_{N,N} \end{bmatrix}.$$

By means of (2.6) one can write the relation (2.5) in the matrix form

$$u_{N,\alpha}(x) = \mathbb{T}_{\alpha}(x) \mathbb{A} = \mathbb{B}_{\alpha}(x) \mathbb{D} \mathbb{A}, \quad (2.7)$$

where the vector of unknown is defined as

$$\mathbb{A} = [a_0 \quad a_1 \quad \dots \quad a_N]^t.$$

We conclude the discussion about the shifted Chebyshev polynomials by considering their convergence result. The following theorem states that the approximation solution $u_{N,\alpha}(x)$ is convergent to $u(x)$ exponentially, if one increases the number of basis functions N [24].

Theorem 2. Assuming that $\mathcal{D}_{\star}^{(k\alpha)} u(x) \in C[0, L]$ for $k = 0, 1, \dots, N$ and let

$$CT_N^{\alpha} = \text{Span}\langle \mathcal{T}_0^{\alpha}(x), \mathcal{T}_1^{\alpha}(x), \dots, \mathcal{T}_{N-1}^{\alpha}(x) \rangle.$$

If $u_{N,\alpha} = \mathbb{T}_\alpha \mathbb{A}$ is the best approximation to u from CT_N^α , then the error bound is presented as follows:

$$\|u(x) - u_{N,\alpha}(x)\|_w \leq \frac{L^{N\alpha} M_\alpha}{2^N \Gamma(N\alpha + 1)} \left(\frac{\pi}{\alpha N!} \right)^{1/2},$$

where $M_\alpha \geq |\mathcal{D}_\star^{(N\alpha)} u(x)|$, $x \in [0, L]$.

Ultimately, to obtain a solution in the form (2.5) for the problem (1.1) on the interval $0 < x \leq L$, we use the spectral collocation points as the roots of the generalized fractional order of the Chebyshev functions. According to [24], the following points are used

$$x_k = L \left(\frac{1 - t_k}{2} \right)^{\frac{1}{\alpha}}, \quad k = 0, 1, \dots, N, \quad (2.8)$$

where $t_k = \cos \left(\frac{2k+1}{N+1} \frac{\pi}{2} \right)$ are the zeros of the usual Chebyshev polynomials of degree $N + 1$ on $(-1, 1)$.

3 Chebyshev-collocation method

Now, suppose the approximation of the solution $Y(x)$ of the linear BVPs (1.1) in terms of $(N + 1)$ -terms Chebyshev polynomials series denoted by $Y_{N,\alpha}(x)$ on the interval $[0, L]$. As previously stated, in the vector form one may write

$$Y(x) \approx Y_{N,\alpha}(x) = \mathbb{B}_\alpha(x) \mathbb{D} \mathbb{A}. \quad (3.1)$$

By inserting the collocation points (2.8) into (3.1), we get a system of matrix equations in the form

$$Y_{N,\alpha}(x_k) = \mathbb{B}_\alpha(x_k) \mathbb{D} \mathbb{A}, \quad k = 0, 1, \dots, N.$$

These equations can be expressed in the following compact representation

$$\mathbf{Y} = \mathbf{B} \mathbb{D} \mathbb{A}, \quad \mathbf{Y} = \begin{bmatrix} Y_{N,\alpha}(x_0) \\ Y_{N,\alpha}(x_1) \\ \vdots \\ Y_{N,\alpha}(x_N) \end{bmatrix}, \quad \mathbf{B} = \begin{bmatrix} \mathbb{B}_\alpha(x_0) \\ \mathbb{B}_\alpha(x_1) \\ \vdots \\ \mathbb{B}_\alpha(x_N) \end{bmatrix}. \quad (3.2)$$

To proceed, we take the fractional derivative of order γ from both sides of (3.1) to get

$$\mathcal{D}_\star^{(\gamma)} Y_{N,\alpha}(x) = \mathcal{D}_\star^{(\gamma)} \mathbb{B}_\alpha(x) \mathbb{D} \mathbb{A}. \quad (3.3)$$

The computation of $\mathcal{D}_\star^{(\gamma)} \mathbb{B}_\alpha(x)$ can be easily obtained via the property (2.2) and (2.3) as follows

$$\mathbb{B}_\alpha^{(\gamma)}(x) = \mathcal{D}_\star^{(\gamma)} \mathbb{B}_\alpha(x) = [0 \quad \mathcal{D}_\star^{(\gamma)} x^\alpha \quad \dots \quad \mathcal{D}_\star^{(\gamma)} x^{\alpha N}].$$

To obtain a system of matrix equations for the fractional derivative, we substitute the collocation points (2.8) into (3.3) to get

$$\mathcal{D}_\star^{(\gamma)} Y_{N,\alpha}(x_k) = \mathbb{B}_\alpha^{(\gamma)}(x_k) \mathbb{D} \mathbb{A}, \quad k = 0, 1, \dots, N,$$

which can also be expressed in the matrix form

$$\mathbf{Y}^{(\gamma)} = \mathbf{B}^{(\gamma)} \mathbb{D} \mathbb{A}, \quad \mathbf{Y}^{(\gamma)} = \begin{bmatrix} \mathcal{D}_\star^{(\gamma)} Y_{N,\alpha}(x_0) \\ \mathcal{D}_\star^{(\gamma)} Y_{N,\alpha}(x_1) \\ \vdots \\ \mathcal{D}_\star^{(\gamma)} Y_{N,\alpha}(x_N) \end{bmatrix}, \quad \mathbf{B}^{(\gamma)} = \begin{bmatrix} \mathbb{B}_\alpha^{(\gamma)}(x_0) \\ \mathbb{B}_\alpha^{(\gamma)}(x_1) \\ \vdots \\ \mathbb{B}_\alpha^{(\gamma)}(x_N) \end{bmatrix}. \quad (3.4)$$

Our next goal is to find a relationship between $Y_{N,\alpha}(x)$ and its second derivative. To this end, it suffices to compute $\frac{d^2}{dx^2}\mathbb{B}_\alpha(x)$. Evidently, the calculation of integer-order derivatives of $\mathbb{B}_\alpha(x)$ strictly depends on the values of α and N . These tasks are also obtainable through the properties (2.2)-(2.3) using integer values of $\gamma = 1, 2$. For instance, by choosing $\alpha = 1/2$ and $N = 7$ we get

$$\mathbb{B}_{\frac{1}{2}}(x) = \left[1 \quad x^{1/2} \quad x \quad x^{3/2} \quad x^2 \quad x^{5/2} \quad x^3 \quad x^{7/2} \right].$$

Differentiation two times with respect to x reveals that

$$\begin{aligned} \frac{d}{dx}\mathbb{B}_{\frac{1}{2}}(x) &= \left[0 \quad 0 \quad 1 \quad \frac{3}{2}x^{1/2} \quad 2x \quad \frac{5}{2}x^{3/2} \quad 3x^2 \quad \frac{7}{2}x^{5/2} \right], \\ \frac{d^2}{dx^2}\mathbb{B}_{\frac{1}{2}}(x) &= \left[0 \quad 0 \quad 0 \quad 0 \quad 2 \quad \frac{15}{4}x^{1/2} \quad 6x \quad \frac{35}{4}x^{3/2} \right]. \end{aligned}$$

Now, by defining

$$\ddot{\mathbb{B}}_\alpha(x) := \frac{d^2}{dx^2}\mathbb{B}_\alpha(x),$$

and using the relation (3.1) one obtains that

$$Y''_{N,\alpha}(x) = \ddot{\mathbb{B}}_\alpha(x) \mathbb{D} \mathbb{A}. \quad (3.5)$$

If we place the collocation points (2.8) into (3.5), we arrive at the following matrix expression

$$\ddot{\mathbf{Y}} = \ddot{\mathbf{B}} \mathbb{D} \mathbb{A}, \quad \ddot{\mathbf{Y}} = \begin{bmatrix} Y''_{N,\alpha}(x_0) \\ Y''_{N,\alpha}(x_1) \\ \vdots \\ Y''_{N,\alpha}(x_N) \end{bmatrix}, \quad \ddot{\mathbf{B}} = \begin{bmatrix} \ddot{\mathbb{B}}_\alpha(x_0) \\ \ddot{\mathbb{B}}_\alpha(x_1) \\ \vdots \\ \ddot{\mathbb{B}}_\alpha(x_N) \end{bmatrix}. \quad (3.6)$$

Now, we are in place to calculate the Chebyshev solutions of (1.1). The collocation procedure is based on computing these polynomial coefficients by the aid of collocation points defined in (2.8). This can be done by inserting the collocation points into the fractional BVPs to get the system

$$Y''(x_k) + \mathcal{D}_*^{(\gamma)} Y(x_k) = f(x_k), \quad k = 0, 1, \dots, N.$$

In the matrix form we may write the above equations as

$$\ddot{\mathbf{Y}} + \mathbf{Y}^{(\gamma)} = \mathbf{F}, \quad (3.7)$$

where the right-hand side vector \mathbf{F} of size $(N+1) \times 1$ takes the form

$$\mathbf{F} = \begin{bmatrix} f(x_0) \\ f(x_1) \\ \vdots \\ f(x_N) \end{bmatrix}.$$

Substituting the relations (3.4) and (3.6) into (3.7), the fundamental matrix equation is obtained

$$\mathbf{W} \mathbb{A} = \mathbf{F}, \quad (3.8)$$

where

$$\mathbf{W} := \left(\ddot{\mathbf{B}} + \mathbf{B}^{(\gamma)} \right) \mathbb{D}.$$

Obviously, (3.8) is a linear matrix equation with a_n , $n = 0, 1, \dots, N$, being the unknown Chebyshev coefficients to be sought.

We are left with the task of entering the boundary conditions (1.2) into the former matrix equation. To take into account the first condition $Y(0) = \beta_0$, we tend $x \rightarrow 0$ in (3.1) to get the following matrix representation

$$\widehat{\mathbf{W}}_0 \mathbb{A} = \beta_0, \quad \widehat{\mathbf{W}}_0 := \mathbb{B}_\alpha(0) \mathbb{D} = [1 \quad 1 \quad \dots \quad 1].$$

Similarly, for the second condition $Y(1) = \beta_1$ we obtain the matrix expression

$$\widehat{\mathbf{W}}_1 \mathbb{A} = \beta_1, \quad \widehat{\mathbf{W}}_1 := \mathbb{B}_\alpha(1) \mathbb{D} = [\hat{w}_{1,0} \quad \hat{w}_{1,1} \quad \dots \quad \hat{w}_{1,N}].$$

Consequently, by replacing the first and last rows of the augmented matrix $[\mathbf{W}; \mathbf{F}]$ by the row matrices $[\widehat{\mathbf{W}}_0; \beta_0]$ and $[\widehat{\mathbf{W}}_1; \beta_1]$ we arrive at the new augmented system

$$[\widehat{\mathbf{W}}; \widehat{\mathbf{F}}] = \begin{bmatrix} 1 & 1 & 1 & 1 & \dots & 1 & ; & \beta_0 \\ w_{1,0} & w_{1,1} & w_{1,2} & w_{1,3} & \dots & w_{1,N} & ; & f(x_1) \\ w_{2,0} & w_{2,1} & w_{2,2} & w_{2,3} & \dots & w_{2,N} & ; & f(x_2) \\ \vdots & \vdots & \vdots & \ddots & \vdots & \vdots & ; & \vdots \\ w_{N-1,0} & w_{N-1,1} & w_{N-1,2} & w_{N-1,3} & \dots & w_{N-1,N} & ; & f(x_{N-1}) \\ \hat{w}_{1,0} & \hat{w}_{1,1} & \hat{w}_{1,2} & \hat{w}_{1,3} & \dots & \hat{w}_{1,N} & ; & \beta_1 \end{bmatrix}. \quad (3.9)$$

Thus, the unknown Chebyshev coefficients in (3.1) will be calculated via solving this linear system of equations. This task can be easily performed by means of the linear solvers.

4 Error estimation based on residual functions and improvement of solutions

In this section, the error estimation based on the residual function is introduced for the method and thus the approximate solution (1.1) is corrected by the residual correction technique. This technique were previously used in [22, 4, 30] and recently in [34]. This error estimation is useful, in particular, when the exact solution of the boundary value problems is not yet known and requires some tools to measure the accuracy of the proposed collocation scheme. Briefly speaking, our goal is to construct an approximate solution based on the already calculated Chebyshev solution $Y_{N,\alpha}(x)$ in the form

$$Y_{N,M,\alpha}(x) = Y_{N,\alpha}(x) + \widetilde{\mathcal{E}}_{N,M,\alpha}(x), \quad (4.1)$$

where $\widetilde{\mathcal{E}}_{N,M,\alpha}(x)$ is the Chebyshev solution of the error problem obtained using the residual error function as described below. Here, the positive constant M is selected such that $M > N$.

To continue, let us define the residual function for the present method as

$$\mathcal{R}_{N,\alpha}(x) := \mathcal{L}[Y_{N,\alpha}](x) - f(x) = Y_{N,\alpha}''(x) + \mathcal{D}_\star^{(\gamma)} Y_{N,\alpha}(x) - f(x). \quad (4.2)$$

Clearly, the approximate solution $Y_{N,\alpha}(x)$ is satisfied the following problem

$$\mathcal{L}[Y_{N,\alpha}](x) = f(x) + \mathcal{R}_{N,\alpha}(x), \quad Y_{N,\alpha}(0) = \beta_0, \quad Y_{N,\alpha}(1) = \beta_1. \quad (4.3)$$

Assuming that the function $Y(x)$ is the exact solution of (1.1), we define the error function $\mathcal{E}_{N,\alpha}(x)$ as

$$\mathcal{E}_{N,\alpha}(x) = Y(x) - Y_{N,\alpha}(x). \quad (4.4)$$

Putting (4.4) into (1.1) and (1.2) while exploiting (4.2)-(4.3), we arrive at the error differential equation with the homogeneous boundary conditions

$$\mathcal{E}_{N,\alpha}''(x) + \mathcal{D}_\star^{(\gamma)}\mathcal{E}_{N,\alpha}(x) = -\mathcal{R}_{N,\alpha}(x), \quad \mathcal{E}_{N,\alpha}(0) = 0, \quad \mathcal{E}_{N,\alpha}(1) = 0. \quad (4.5)$$

Now, we solve the error differential equation (4.5) by means of the Chebyshev-collocation scheme, already described in the last section, to get the approximation

$$\widetilde{\mathcal{E}}_{N,M,\alpha}(x) = \sum_{m=0}^M e_m \mathcal{T}_m^\alpha(x), \quad (4.6)$$

for the error function $\mathcal{E}_{N,\alpha}(x)$ for $M > N$. Once the approximate solution $\widetilde{\mathcal{E}}_{N,M,\alpha}(x)$ is obtained, the corrected solution $Y_{N,M,\alpha}(x)$ defined in (4.1) will be known. Moreover, we also compute the error function as well as the residual error function for the corrected approximate solution as

$$\mathcal{E}_{N,M,\alpha}(x) = Y(x) - Y_{N,M,\alpha}(x), \quad (4.7a)$$

$$\mathcal{R}_{N,M,\alpha}(x) = Y_{N,M,\alpha}''(x) + \mathcal{D}_\star^{(\gamma)}Y_{N,M,\alpha}(x) - f(x), \quad (4.7b)$$

for the purpose of comparison.

5 Illustrative Examples

In this section, to describe the efficiency and accuracy of the proposed Chebyshev collocation method, some numerical examples are given and the comparisons are made with the results of the other methods. All numerical computations have been done using MATLAB R2017a.

Example 3. As the first example, we consider the linear fractional boundary value problem (1.1) with

$$f(x) = 2 + \frac{2}{\Gamma(3-\gamma)}x^{2-\gamma} - \frac{1}{\Gamma(2-\gamma)}x^{1-\gamma}, \quad 0 < \gamma \leq 1,$$

and $\beta_0 = \beta_1 = 0$. This problem with $\gamma = 1/2$ is considered in [28]. It can be easily verified that the exact solution of this FBVPs is $Y(x) = x^2 - x$ for any $0 < \gamma \leq 1$.

In all examples below, we take $L = 1$. By employing $N = 2$, we are looking for an approximate solution in the form $Y_{2,\alpha}(x) = \sum_{n=0}^2 a_n \mathcal{T}_n^\alpha(x)$. To this end, we calculate the unknown coefficients a_0, a_1 , and a_2 . For this example we set $\alpha = 1$ and therefore the following spectral collocation points are used

$$\left\{ x_0 = \frac{195}{2911}, x_1 = \frac{1}{2}, x_3 = \frac{2716}{2911} \right\}.$$

Using $\gamma = 1/2$, the corresponding matrices and vectors in the fundamental matrix equation (3.8) become

$$\mathbb{D}^T = \begin{bmatrix} 1 & 0 & 0 \\ 1 & -2 & 0 \\ 1 & -8 & 8 \end{bmatrix}, \quad \mathbf{B}^{(1/2)} = \begin{bmatrix} 0 & 481/1647 & 92/3527 \\ 0 & 679/851 & 1383/2600 \\ 0 & 1418/1301 & 1162/857 \end{bmatrix}, \quad \ddot{\mathbf{B}} = \begin{bmatrix} 0 & 0 & 2 \\ 0 & 0 & 2 \\ 0 & 0 & 2 \end{bmatrix},$$

$$\mathbf{F} = \begin{bmatrix} 4590/2647 \\ 4590/2647 \\ 5998/2647 \end{bmatrix}, [\widehat{\mathbf{W}}; \widehat{\mathbf{F}}] = \begin{bmatrix} 1 & 1 & 1 & ; & 0 \\ 0 & -1358/851 & 9017/650 & ; & 4590/2647 \\ 1 & -1 & 1 & ; & 0 \end{bmatrix}.$$

Solving the system corresponding to $[\widehat{\mathbf{W}}; \widehat{\mathbf{F}}]$, the coefficients matrix is found as

$$\mathbb{A} = [-1/8 \quad 0 \quad 1/8]^t.$$

Hence, inserting the determined coefficients into $Y_{2,1}(x)$ we get the approximate solution

$$Y_{2,1}(x) = [1 \quad 1 - 2x \quad 8x^2 - 8x + 1] \mathbb{A} = x^2 - x,$$

which is the desired exact solution. The numerical solutions, which are obtained using the Chebyshev-collocation scheme, at some points $x \in [0, 1]$ for Example (3), are presented in Table 1. The corresponding exact solutions along with the absolute errors and the results obtained via residual error functions (4.2) are further reported in this table. In addition, in order to justify our results, the solutions are also compared with the numerical solutions computed using the sinc-Galerkin method (SGM). Obviously, our numerical solutions are in excellent agreement with the exact solutions compared to the SGM.

Table 1. The comparison of the numerical solutions and the absolute/residual errors in Example 3 for $\gamma = 1/2, \alpha = 1$, and $N = 2$ for various $x \in [0, 1]$.

x	Exact	Chebyshev	$ \mathcal{E}_{2,1}(x) $	$ \mathcal{R}_{2,1}(x) $	SGM	Absolute Errors
0.0	0.0	0.0	0.0	1.28×10^{-16}	0.0	0
0.1	-0.09	-0.09	5.76×10^{-18}	1.08×10^{-16}	-0.0899988	1.15×10^{-6}
0.2	-0.16	-0.16	1.02×10^{-17}	1.04×10^{-16}	-0.159998	1.50×10^{-6}
0.3	-0.21	-0.21	1.34×10^{-17}	1.04×10^{-16}	-0.209998	1.85×10^{-6}
0.4	-0.24	-0.24	1.54×10^{-17}	1.07×10^{-16}	-0.239999	1.43×10^{-6}
0.5	-0.25	-0.25	1.60×10^{-17}	1.11×10^{-16}	-0.249999	1.04×10^{-6}
0.6	-0.24	-0.24	1.54×10^{-17}	1.17×10^{-16}	-0.239999	1.27×10^{-6}
0.7	-0.21	-0.21	1.34×10^{-17}	1.24×10^{-16}	-0.209999	5.20×10^{-7}
0.8	-0.16	-0.16	1.02×10^{-17}	1.32×10^{-16}	-0.16000015	1.59×10^{-7}
0.9	-0.09	-0.09	5.76×10^{-18}	1.42×10^{-16}	-0.0900004	3.50×10^{-7}
1.0	0.0	0.0	0.0	1.52×10^{-16}	0.0	0

Example 4. Consider the boundary value problem (1.1) with the right-hand side $f(x)$ taken as

$$f(x) = 20x^3 - 12x^2 + \frac{120}{\Gamma(6 - \gamma)}x^{5-\gamma} - \frac{24}{\Gamma(5 - \gamma)}x^{4-\gamma}, \quad 0 < \gamma \leq 1,$$

and also zero boundary conditions. In this case, the exact solution is $Y(x) = x^4(x - 1)$ for any $0 < \gamma \leq 1$. This FBVPs is taken from [35] and [1].

We first take $\gamma = 3/10$ in the second example and set $N = 5$ as the number of basis functions. The parameter $\alpha = 1$ is also sufficient to get the desired approximation. The approximate solutions $Y_{5,1}(x)$ of this model problem using the Chebyshev basis functions

in the interval $0 \leq x \leq 1$ are obtained as follows:

$$Y_{5,1}(x) = 0.9999999999999999 x^5 - 0.9999999999999998 x^4 - 1.2253730 \times 10^{-15} x^3 + 3.5162677643 \times 10^{-16} x^2 - 7.0610181123 \times 10^{-17} x + 3.5373746402 \times 10^{-74}.$$

The corresponding residual error function $\mathcal{R}_{5,1}(x)$ takes the form

$$\begin{aligned} \mathcal{R}_{5,1}(x) &= 3.163714295 \times 10^{-15} x^2 - 1.280874739 \times 10^{-15} x - 2.371724879 \times 10^{-15} x^3 \\ &- 9.248187761 \times 10^{-18} x^{\frac{7}{10}} + 9.947106210 \times 10^{-17} x^{\frac{17}{10}} - 3.071162029 \times 10^{-16} x^{\frac{27}{10}} \\ &+ 4.100356309 \times 10^{-16} x^{\frac{37}{10}} - 1.962058927 \times 10^{-16} x^{\frac{47}{10}} + 1.536515417 \times 10^{-16} \end{aligned}$$

The above approximation solution and its related residual error function are visualized in Fig. 1. To validate our results, we also plot the exact solution, which is represented by a solid line. Obviously, our approximated solution is matching up to the machine epsilon.

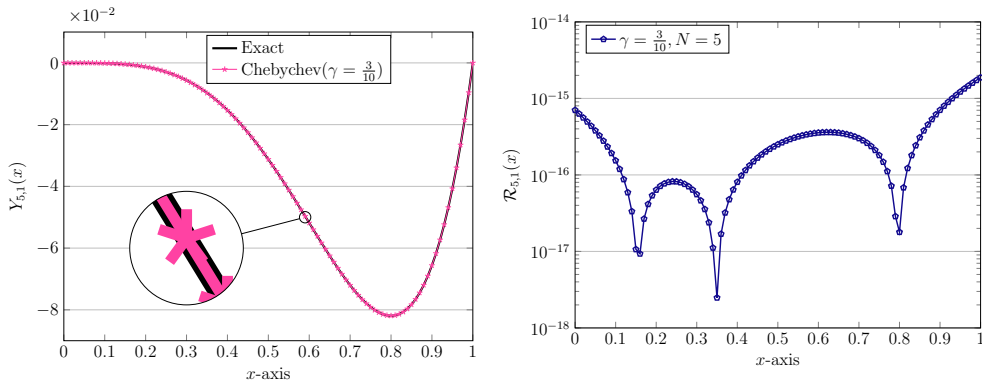


Figure 1. The comparison of the approximated and the exact solutions using the Chebyshev functions (left) and the corresponding residual error function (right) for Example 4 with $\gamma = 3/10$, $\alpha = 1$, and $N = 5$.

In Table 2, we report the numerical results as well as the absolute errors correspond to $N = 5$ obtained by the Chebyshev-collocation procedure using $\gamma = 3/10$ and $\alpha = 1$ at some points $x \in [0, 1]$. A comparison in this table is also made with the exponential spline approach from [1]. As one can see in Table 2, the results obtained by our proposed scheme, are superior in terms of accuracy. The impact of utilizing the various values of the fractional orders $\gamma = 0, 0.25, 0.5, 0.75$, and $\gamma = 1$ are depicted in Fig. 2. From Fig. 2 it can be inferred that the same accuracies are achieved using different γ in the range $[0, 1]$.

In the last experiment, we show the benefits of using the fractional version of the Chebyshev polynomials. For this purpose, we construct an example that has a fractional solution.

Example 5. Let us consider (1.1) with the function $f(x)$ defined as

$$f(x) = \frac{15}{4}\sqrt{x} - \frac{35}{4}\sqrt[3]{x^2} + \frac{\Gamma(7/2)}{\Gamma(7/2 - \gamma)}x^{5/2-\gamma} - \frac{\Gamma(9/2)}{\Gamma(9/2 - \gamma)}x^{7/2-\gamma}, \quad 0 < \gamma \leq 1.$$

Using the zero boundary conditions, it is not difficult to show that the exact solution of this problem satisfies $Y(x) = \sqrt{x^5} - \sqrt{x^7}$.

Table 2. The comparison of the numerical solutions and the absolute errors in Example 4 with $\gamma = 3/10, \alpha = 1$, and $N = 5$ for various $x \in [0, 1]$.

x	Chebyshev	$ \mathcal{E}_{5,1}(x) $	Exp-Spline	Max. Abs. Errors
0.000	0.0000000000000000	7.03×10^{-16}	0	0
0.125	-0.000213623046875	7.29×10^{-17}	0.0026	2.8×10^{-3}
0.250	-0.002929687500000	8.17×10^{-17}	0.0028	5.7×10^{-3}
0.375	-0.012359619140625	3.99×10^{-17}	-0.0040	8.4×10^{-3}
0.500	-0.031250000000000	2.50×10^{-16}	-0.0211	1.0×10^{-2}
0.625	-0.057220458984375	3.61×10^{-16}	-0.0471	1.0×10^{-2}
0.750	-0.079101562500000	1.81×10^{-16}	-0.0710	8.1×10^{-3}
0.875	-0.073272705078125	4.93×10^{-16}	-0.0689	4.4×10^{-3}
1.000	0.000000000000000	1.87×10^{-15}	0	0

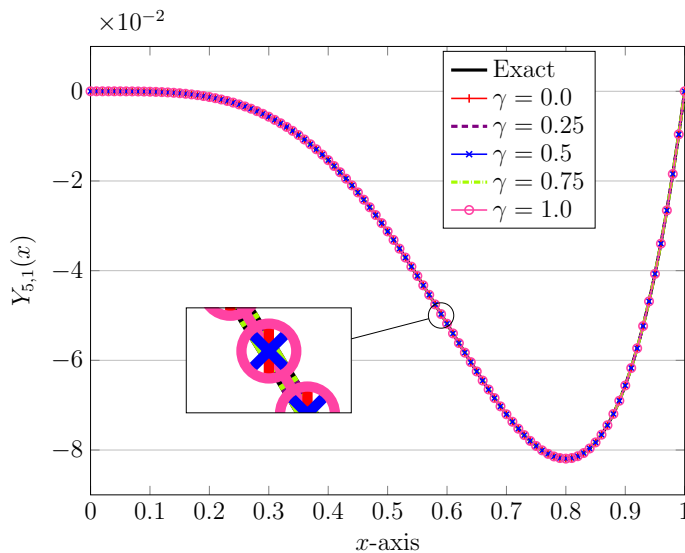


Figure 2. The approximated Chebyshev series solutions $Y_{N,\alpha}(x)$ for Example 4 using $N = 5, \alpha = 1$ for different $\gamma = 0, 0.25, 0.5, 0.75$, and $\gamma = 1.0$.

For this example, we fix $N = 7$ and use two values of $\alpha = 1$ and $\alpha = 1/2$, which indicate the difference between the fractional and non-fractional Chebyshev basis functions respectively. Setting $\gamma = 1/2$, the approximate solutions $Y_{7,1}(x)$ and $Y_{7,1/2}(x)$ obtained via (3.9) of the model (1.1) in the interval $[0, 1]$ are as follows

$$\begin{aligned}
 Y_{7,1}(x) = & 0.176260724015854 x^7 - 0.792821466676062 x^6 + 1.58262835557799 x^5 \\
 & - 2.23737888512802 x^4 + 1.01020023333265 x^3 + 0.268398536500592 x^2 \\
 & - 0.00728749762300631 x,
 \end{aligned}$$

and

$$\begin{aligned}
 Y_{7, \frac{1}{2}}(x) = & -1.7687 \times 10^{-74} - 3.7183 \times 10^{-13} x - 7.5367 \times 10^{-14} x^2 \\
 & - 3.6789 \times 10^{-14} x^3 + 1.7053 \times 10^{-13} x^{\frac{1}{2}} + 2.0876 \times 10^{-13} x^{\frac{3}{2}} \\
 & + 1.000000000000011 x^{\frac{5}{2}} - 1.0 x^{\frac{7}{2}}.
 \end{aligned}$$

Evidently, using the generalized Chebyshev basis functions leads to a considerably more accurate solution than usual ones. This fact can be further confirmed in the next two Figs. 3-4, in which we plot these approximations with the corresponding residual error functions $\mathcal{R}_{7, \alpha}(x)$ for $\alpha = 1, 1/2$.

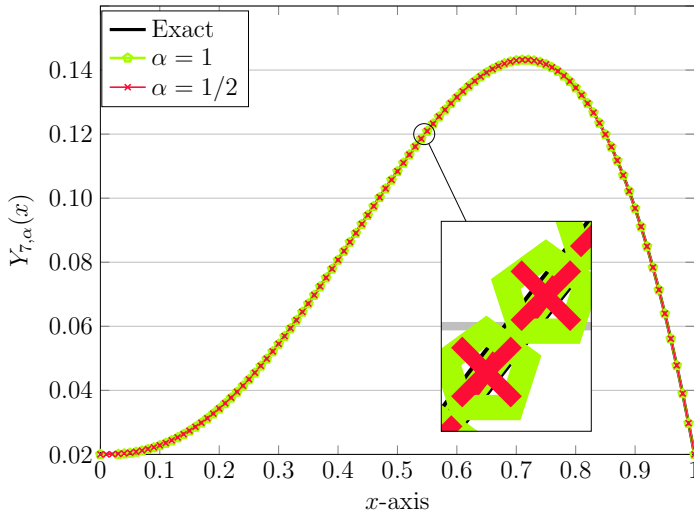


Figure 3. The approximated Chebyshev series solutions $Y_{7, \alpha}(x)$ for Example 5 using $\gamma = 1/2$ for two different $\alpha = 1$ and $\alpha = 1/2$.

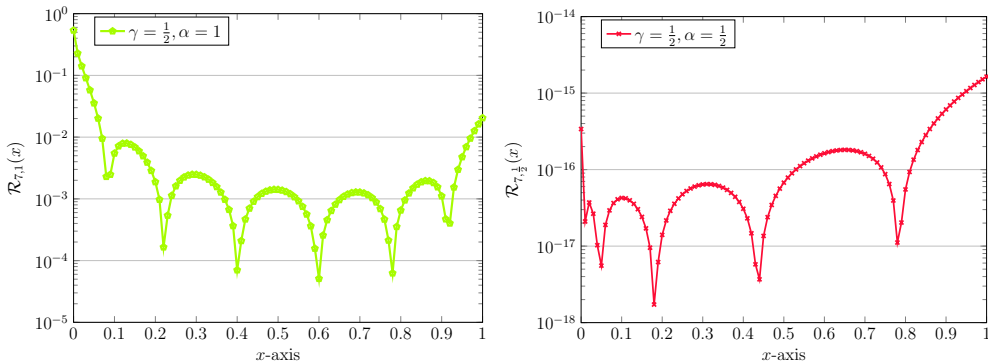


Figure 4. The comparison of the residual error functions using $\alpha = 1$ (left) and $\alpha = 1/2$ (right) for Example 5 with $\gamma = 1/2$ and $N = 7$.

Our next goal is to improve the current obtained solution $Y_{N, \alpha}(x)$ for Example 5 to get a solution of the form $Y_{N, M, \alpha}(x)$, where $N = 7$ and $\alpha = 1/2$. To this end, we solve the error problem (4.5) for $\mathcal{E}_{N, \alpha}(x)$. Choosing $M = 8$ and using the Chebyshev-collocation

procedure, the coefficient matrix of the error problem is calculated. These coefficients e_0, e_1, \dots, e_8 are approximately expressed as

$$\begin{aligned} e_0 &= -8.1044 \times 10^{-15}, & e_1 &= -6.8377 \times 10^{-15}, & e_2 &= 8.226 \times 10^{-15}, \\ e_3 &= 6.8944 \times 10^{-15}, & e_4 &= -1.4792 \times 10^{-16}, & e_5 &= -5.6145 \times 10^{-17}, \\ e_6 &= 2.6377 \times 10^{-17}, & e_7 &= -6.01 \times 10^{-19}, & e_8 &= -4.0568 \times 10^{-33}. \end{aligned}$$

By inserting the coefficient matrix into (4.6) and simplifying, we get the error function approximately as

$$\begin{aligned} \widetilde{\mathcal{E}}_{7,8,\frac{1}{2}}(x) &= -6.2836 \times 10^{-87} + 3.7183 \times 10^{-13} x + 7.5367 \times 10^{-14} x^2 \\ &+ 3.6789 \times 10^{-14} x^3 - 1.3293 \times 10^{-28} x^4 - 1.7053 \times 10^{-13} x^{1/2} \\ &- 2.0876 \times 10^{-13} x^{3/2} - 1.0962 \times 10^{-13} x^{5/2} + 4.9234 \times 10^{-15} x^{7/2}. \end{aligned}$$

Finally, we substitute the error function $\widetilde{\mathcal{E}}_{7,8,\frac{1}{2}}(x)$ into (4.1), the corrected approximate solution $Y_{7,8,\frac{1}{2}}(x)$ for $(N, M) = (7, 8)$ is calculated as

$$\begin{aligned} Y_{7,8,\frac{1}{2}}(x) &= -1.7687 \times 10^{-74} + 7.2131 \times 10^{-27} x - 2.3010 \times 10^{-28} x^2 \\ &+ 1.4667 \times 10^{-27} x^3 - 1.3293 \times 10^{-28} x^4 + 5.1996 \times 10^{-28} x^{1/2} \\ &- 7.0356 \times 10^{-27} x^{3/2} + 1.0 x^{5/2} - 1.0 x^{7/2}. \end{aligned}$$

Table 3 reports the comparison of the Chebyshev approximate solution $Y_{7,\frac{1}{2}}(x)$ and the corrected Chebyshev approximate solution $Y_{7,8,\frac{1}{2}}(x)$ with the exact solution $Y(x)$ at some points $x \in [0, 1]$ in Example 5. The excellent agreement between the exact and corrected approximate solutions is evident in this table. Note that we have only shown the numerical results up to 15 digits. In fact, using $M = N + 1$, the contribution of the correction term is a considerable achievement to the accuracy of the solutions compared to non-corrected results. To highlight the advantage of applying the correction technique, we also present the results obtained by the error functions defined in (4.4), (4.7a) and the residual error functions in (4.2), (4.7b). These results are shown in Table 4.

6 Conclusions

In this work, an accurate approximation algorithm based on the generalized Chebyshev functions is developed to solve the fractional-order differential equation under the boundary conditions. Utilizing the (fractional) Chebyshev functions together with the collocation points, the differential equations is transformed into an algebraic system of linear equations. Illustrative examples are given to demonstrate the efficiency and accuracy of the proposed method and a comparison between the method and other existing schemes is done. Moreover, the performance of fractional and non-fractional basis functions has been assessed and the reliability of the proposed technique is checked through defining the error as well as the residual error functions. The approximate solutions are further improved through these error functions.

It can be seen from Figures and Tables that the proposed scheme is not only a simple but also an accurate and powerful tool for obtaining the approximate solutions of FBVPs. From comparisons, it is observed that our results are more accurate than the numerical results of other existing well-known computational methods. The method can be easily extended to the solutions of higher-order FBVPs and systems appearing in the modelling of many problems in the science and engineering fields.

x	$Y(x)$ (Exact)	$Y_{7,\frac{1}{2}}(x)$	$Y_{7,8,\frac{1}{2}}(x)$
0.0	0.0000000000000000	$-17.686873200833 \times 10^{-75}$	$-17.686873200840 \times 10^{-75}$
0.1	0.002846049894152	$2.84604989417444 \times 10^{-03}$	$2.84604989415154 \times 10^{-03}$
0.2	0.014310835055999	$14.3108350560179 \times 10^{-03}$	$14.3108350559987 \times 10^{-03}$
0.3	0.034506521122826	$34.5065211228392 \times 10^{-03}$	$34.5065211228255 \times 10^{-03}$
0.4	0.060715731075233	$60.7157310752413 \times 10^{-03}$	$60.7157310752329 \times 10^{-03}$
0.5	0.088388347648318	$88.3883476483224 \times 10^{-03}$	$88.3883476483184 \times 10^{-03}$
0.6	0.111541920370774	$111.541920370774 \times 10^{-03}$	$111.541920370774 \times 10^{-03}$
0.7	0.122989023900509	$122.989023900508 \times 10^{-03}$	$122.989023900509 \times 10^{-03}$
0.8	0.114486680447989	$114.486680447987 \times 10^{-03}$	$114.486680447989 \times 10^{-03}$
0.9	0.076843347142092	$76.8433471420900 \times 10^{-03}$	$76.8433471420916 \times 10^{-03}$
1.0	0.0000000000000000	$24.7616224811668 \times 10^{-72}$	$24.3127412678843 \times 10^{-72}$

Table 3. The comparison of the numerical solutions in the Chebyshev and the corrected Chebyshev collocation methods in Example 5 for $(N, M) = (7, 8)$, $\gamma, \alpha = 1/2$.

x	Chebyshev		Corrected Chebyshev	
	$ \mathcal{E}_{7,\frac{1}{2}}(x) $	$ \mathcal{R}_{7,\frac{1}{2}}(x) $	$ \mathcal{E}_{7,8,\frac{1}{2}}(x) $	$ \mathcal{R}_{7,8,\frac{1}{2}}(x) $
0.0	$1.7686873 \times 10^{-74}$	$3.9527851 \times 10^{-16}$	$1.7686873 \times 10^{-74}$	$1.5352514 \times 10^{-31}$
0.1	$2.2899936 \times 10^{-14}$	$4.5204731 \times 10^{-17}$	$6.5569279 \times 10^{-28}$	$4.5813764 \times 10^{-30}$
0.2	$1.9204119 \times 10^{-14}$	$1.5524563 \times 10^{-17}$	$1.0108576 \times 10^{-27}$	$3.4952039 \times 10^{-30}$
0.3	$1.3711741 \times 10^{-14}$	$6.5574364 \times 10^{-17}$	$1.2093598 \times 10^{-27}$	$4.9166546 \times 10^{-30}$
0.4	$8.4135756 \times 10^{-15}$	$2.9473773 \times 10^{-17}$	$1.2839077 \times 10^{-27}$	$1.6561716 \times 10^{-29}$
0.5	$3.9783696 \times 10^{-15}$	$7.0097562 \times 10^{-17}$	$1.2542846 \times 10^{-27}$	$2.5916463 \times 10^{-29}$
0.6	$6.8238175 \times 10^{-16}$	$1.6365969 \times 10^{-16}$	$1.1354044 \times 10^{-27}$	$2.7219049 \times 10^{-29}$
0.7	$1.3641080 \times 10^{-15}$	$1.5692961 \times 10^{-16}$	$9.3978665 \times 10^{-28}$	$1.4805308 \times 10^{-29}$
0.8	$2.1366920 \times 10^{-15}$	$5.8523449 \times 10^{-17}$	$6.7858449 \times 10^{-28}$	$1.6783724 \times 10^{-29}$
0.9	$1.6619505 \times 10^{-15}$	$5.9956544 \times 10^{-16}$	$3.6208852 \times 10^{-28}$	$7.2771193 \times 10^{-29}$
1.0	$2.4743936 \times 10^{-71}$	$1.5881998 \times 10^{-15}$	$2.4312741 \times 10^{-71}$	$1.5814277 \times 10^{-28}$

Table 4. The comparison of the error and residual error functions in the Chebyshev and the corrected Chebyshev collocation methods in Example 5 for $(N, M) = (7, 8)$, $\gamma, \alpha = 1/2$.

References

- [1] G. Akram, H. Tariq, An exponential spline technique for solving fractional boundary value problem, *Calcolo* **53**(4) (2016), 545–558 .
- [2] Z. Bai, H. Lu, Positive solutions for boundary value problem of nonlinear fractional differential equations, *J. Math. Anal. Appl.* **311** (2005), 495–505.
- [3] A.H. Bhrawy, T.M. Taha, J.A.T. Machado, A review of operational matrices and spectral techniques for fractional calculus, *Nonlinear Dyn.* **81**(3) (2015), 1023–1052.
- [4] I. Celik, Collocation method and residual correction using Chebyshev series, *Appl. Math. Comput.* **174**(2) (2006), 910–920.
- [5] C.F. Chen, C.H. Hsiao, A state-space approach to Walsh series solution of linear systems, *Int. J. Systems Sci.* **6**(9) (1975), 833–858.

- [6] K. Diethelm, N. J. Ford, and A. D. Freed, A predictor-corrector approach for the numerical solution of fractional differential equations, *Nonlinear Dyn.* **29**(1) (2002), 3–22.
- [7] L. Fox, I.B. Parker, “Chebyshev Polynomials in Numerical Analysis”, London, Oxford University Press, 1968.
- [8] M. Izadi, Fractional polynomial approximations to the solution of fractional Riccati equation, *Punjab Univ. J. Math.* **51**(11) (2019), 123–141.
- [9] M. Izadi, Approximate solutions for solving fractional-order Painlevé equations, *Contemporary Mathematics* **1**(1) (2019), 12–24.
- [10] M. Izadi, Application of LDG scheme to solve semi-differential equations, *J. Appl. Math. Comput. Mech.* **18**(4) (2019), 29–37.
- [11] M. Izadi, Comparison of various fractional basis functions for solving fractional-order logistic population model, *Facta Univ. Ser. Math. Inform.* University of Niš: Niš, Serbia, (2020).
- [12] M. Izadi, A comparative study of two Legendre-collocation schemes applied to fractional logistic equation, *Int. J. Appl. Comput. Math.* **6**(3), (2020), 71.
- [13] M. Izadi, M.R. Negar, Local discontinuous Galerkin approximations to fractional Bagley-Torvik equation, *Math. Meth. Appl. Sci.* **43**(7) (2020), 4978–4813.
- [14] M. Izadi, C. Cattani, Generalized Bessel polynomial for multi-order fractional differential equations, *Symmetry* **12**(8) (2020), 1260.
- [15] M. Izadi, M. Afshar, Solving the Basset equation via Chebyshev collocation and LDG methods, *J. Math. Model.* (2020), DOI:10.22124/jmm.2020.17135.1489.
- [16] H. Jafari, V. Daftardar-Gejji, Positive Solutions of Nonlinear Fractional Boundary Value Problems Using Adomian Decomposition Method, *Appl. Math. Comput.* **180** (2006), 700–706.
- [17] A. A. Kilbas, H. M. Srivastava, J. J. Trujillo, “Theory and Applications of Fractional Differential Equations”, Elsevier B. V., Amsterdam, 2006.
- [18] C. Lubich, Discretized fractional calculus, *SIAM J. Math. Anal.* **17**(3) (1986), 704–719.
- [19] Z. Odibat, S. Momani, Application of variational iteration method to nonlinear differential equations of fractional order. *Int. J. Nonlinear Sci. Numer. Simul.* **7**(1) (2006), 15–27.
- [20] Z. M. Odibat, N. T. Shawagfeh, Generalized Taylor’s formula, *Appl. Math. Comput.* **186** (2007), 286–293.
- [21] K.B. Oldham and J. Spanier, “The Fractional Calculus”, Academic Press, New York, 1974.
- [22] F.A. Oliveira, Collocation and residual correction, *Numer. Math.* **36** (1980), 27–31.
- [23] A. Ouahab, Some results for fractional boundary value problem of differential inclusions, *Nonlinear Anal.* **69** (2008), 3877–3896.
- [24] K. Parand, M. Delkhosh, Solving Volterra’s population growth model of arbitrary order using the generalized fractional order of the Chebyshev functions, *Ricerche Mat.* **65** (2016), 307–328.
- [25] P.N. Paraskevopoulos, P.D. Sparis, S.G. Mouroutsos, The Fourier series operational matrix of integration, *Int. J. Syst. Sci.* **16** (1985) 171–176.
- [26] I. Podlubny, “Fractional Differential Equations”, Academic Press, New York, 1999.
- [27] G. P. Rao, “Piecewise Constant Orthogonal Functions and Their Application to Systems and Control”, Springer, New York, 1983.
- [28] A. Secer, S. Alkan, M. A. Akinlar, M. Bayram, Sinc-Galerkin method for approximate solutions of fractional order boundary value problems, *Boundary Value Problems* **2013**, (2013), 281.

- [29] N. T. Shawagfeh, Analytical approximate solutions for nonlinear fractional differential equations, *Appl. Math. Comput.* **131** (2002), 517–529.
- [30] S. Shahmorad, Numerical solution of general form linear Fredholm Volterra integro-differential equations by the tau method with an error estimation, *Appl. Math. Comput.* **167** (2005), 1418–1429.
- [31] P.D. Sparis, S.G. Mouroutsos, A comparative study of the operational matrices of integration and differentiation for orthogonal polynomial series, *Int. J. Control* **42** (1985), 621–638.
- [32] X. Su, S. Zhang, Solution to boundary value problem for nonlinear differential equations of fractional order, *Electr. J. Differ. Equ.* **26** (2009), 1–15.
- [33] F. I. Taukenova, M. Kh. Shkhanukov-Lafishev, Difference methods for solving boundary value problems for fractional differential equations, *Comput. Math. Math. Phys.* **46** (2006), 1785–1795.
- [34] Ş. Yüzbaşı, An exponential method to solve linear Fredholm-Volterra integro-differential equations and residual improvement, *Turk. J. Math.* **42** (2018), 2546–2562.
- [35] W.K. Zahra, S.M. Elkholy, Quadratic spline solution for boundary value problem of fractional order, *Numer. Algor.* **59** (2012), 373–391.
- [36] S.Q. Zhang, Existence of solution for a boundary value problem of fractional order, *Acta Math. Sci.* **26B**(2) (2006), 220–228.

Recent developments on gracefulness of graphs. A survey complemented with chessboard representations

Katarína Kotuľová

*Faculty of Natural Sciences, M Bel University,
Tajovského 40, 974 01 Banská Bystrica, Slovakia
kvasekova29@gmail.com*

Miroslav Haviar*

*Faculty of Natural Sciences, M Bel University,
Tajovského 40, 974 01 Banská Bystrica, Slovakia
miroslav.haviar@umb.sk*

Abstract

We present a survey of selected new results about graceful labellings of graphs which were published during the last seven years. Among them a proof of famous Ringel-Kotzig Conjecture from the 1960s, which for “large” trees was announced in February 2020, has a prominent role. Many of the new results are complemented by our own representations of the discovered graceful labellings of graphs via their graph chessboards and labelling tables. The aim of creating these representations has been to provide an extra value of visualization, in particular to allow seeing better a pattern of the graceful labelling in graph chessboards or in labelling sequences.

Received June 24, 2020

Accepted in final form October 20, 2020

Communicated with Ján Karabáš.

Keywords simple graph, graceful labelling, graph chessboard, labelling sequence, labelling relation.

MSC(2010) Primary 05C78; Secondary 05C05.

1 Introduction

The study of graph labellings started in the late 1960s. Since then a lot of methods and techniques on graph labellings have been studied in almost 3000 research papers, surveys and theses. The best source of information on results concerning the graph labellings is the electronic book *Dynamic Survey of Graph Labeling* by Gallian [10]. Our survey is mainly, though not entirely, based on the information provided in this book.

The history of the study of graph labellings began with a problem on decompositions of a complete graph into trees. In 1963 Ringel conjectured at a conference in Smolenice, Slovakia [40] that for any tree of size m the complete graph K_{2m+1} can be decomposed into $2m + 1$ copies of the given tree. Kotzig conjectured (as far as we know at the same conference) that this decomposition can be cyclic. A proof of the Ringel-Kotzig Conjecture has recently been announced in [32] for *large* trees. (By “large” is meant that the size of the tree is comparable with the size of the complete graph.)

*The second author acknowledges the (honorary) position of a Visiting Professor at University of Johannesburg since June 1, 2020.

With the aim to give a better insight to the Ringel-Kotzig Conjecture, in 1965 Rosa in his dissertation [42], and two years later in his seminal paper [43], defined four new labellings of graphs: $\alpha, \beta, \sigma, \rho$. Here α is the strongest and ρ is the weakest labelling. A graph with m edges has a β -labelling if its vertices can be assigned different labels from the set $\{0, 1, \dots, m\}$ such that the absolute values of the differences in the vertex labels between adjacent vertices form exactly the set $\{1, \dots, m\}$. Later on Golomb [12] called β -labellings *graceful labellings* and the graphs possessing graceful labellings are called *graceful graphs*. The famous *Graceful Tree Conjecture* stated by Rosa in [42] and [43], which implies the Ringel-Kotzig Conjecture, says that *every tree is graceful*, that is, every tree can be gracefully labelled. The conjecture, due to its close relationship with the Ringel-Kotzig Conjecture, which we explain later on, is known also as the Ringel-Kotzig-Rosa Conjecture (see also [32, Conjecture 8.1]).

In this survey of recent developments on gracefulness of graphs we mapped selected new results on gracefully labelled graphs over the last seven years. We divided these results into four sections. The first section relates to the mentioned recent proof of the Ringel-Kotzig Conjecture for *large* trees and explains some background related to it. The second section informs about selected new results on gracefulness of certain trees, among them specific trees of diameter six, spider graphs, symmetrical trees and specific caterpillars and lobsters. The third section focuses on recent results on graceful cyclic graphs such as linear cyclic snakes, certain cycle related graphs, unicyclic graphs and *corona* product of an aster flower graph. The last section is about recent results on graceful subdivisions of selected graphs such as complete bipartite graphs and wheels. We finalize our survey with so-called shell and bow graphs.

Most of the presented results are complemented by our own representations of the given graceful labelling of a graph by its simple chessboard, labelling relation and labelling sequence. They have been created in order to provide the extra value of visualization and to allow seeing better a certain pattern in the graceful labelling. These representations have not been done in each case, only when the corresponding simple chessboards to the graceful graphs have *reasonable* sizes enabling their presentations (considering up to 45 vertices). The diagrams of the presented gracefully labelled graphs were taken from the original papers or created, by applying the formulas for the graceful labellings provided in the papers, with the help of a *Graph processor* – a computer program which was developed by and is presented in Haviar and Ivaška [17, Chapter 7].

2 Preliminaries

We note that all basic concepts and facts in this chapter concerning graphs are taken from [17] and [29].

By a graph in this paper we mean what is called a *simple graph*, that is, an undirected finite graph without loops and multiple edges. To denote the vertex set of some known graph G , we use the symbol V_G and to denote the edge set of some known graph G , we use the symbol E_G .

The *order* of a graph G is the number of vertices in G . The *size* of a graph G is the number of edges in G .

Definition 2.1. ([17, Definition 1.2.1]) A **vertex labelling** f of a graph G is a mapping of its vertex set V_G into the set of non-negative integers (which are called **vertex labels**).

Throughout our survey by a *labelling* we mean a *vertex labelling*. If $f(u), f(v)$ are the labels of vertices u, v respectively, then the number $|f(u) - f(v)|$ will be called an *induced label* of the edge uv in the labelling f . Assigning to every edge $uv \in E_G$ the

induced label of the edge uv in the labelling f naturally yields the usual understanding of the labelling f as acting also on the set E_G of the edges of G .

The following two labellings play an important role with respect to the Ringel-Kotzig Conjecture and the Graceful Tree Conjecture.

Definition 2.2. ([17, Definition 1.2.5]) Let G be a graph of size $|E_G| = m$ and let f be its one-to-one labelling. Then f is called a ρ -labelling if

1. $f(V_G) \subseteq \{0, 1, \dots, 2m\}$, and
2. $f(E_G) = \{x_1, x_2, \dots, x_m\}$, where $x_i = i$ or $x_i = 2m + 1 - i$, for all $i \in \{0, 1, \dots, m\}$.

Definition 2.3. ([17, Definition 1.2.3]) Let G be a graph of size m and let f be its one-to-one labelling. Then f is called a **graceful labelling** (in the old terminology a β -labelling) if

1. $f(V_G) \subseteq \{0, 1, \dots, m\}$, and
2. $f(E_G) = \{1, 2, \dots, m\}$.

The Ringel-Kotzig Conjecture ([40], [43]) says:

Conjecture 2.4. (Ringel-Kotzig Conjecture): For any tree of size m the complete graph K_{2m+1} has a cyclic decomposition into $2m + 1$ copies of the given tree.

It is important to note that Rosa showed ([42], [43]) that the Ringel-Kotzig Conjecture is equivalent to the existence of the ρ -labelling of every tree.

The *Graceful Tree Conjecture*, which is due to Rosa ([42], [43]) says:

Conjecture 2.5. (Graceful Tree Conjecture): All trees are graceful.

In Figure 1 we see an example of a graph with its graceful labelling.

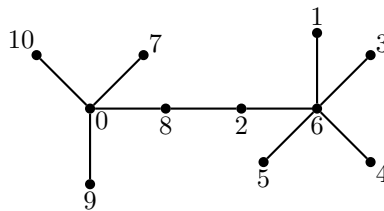


Figure 1. An example of a gracefully labelled graph

Since the ρ -labelling is weaker than the graceful labelling, it follows immediately that the Ringel-Kotzig Conjecture is weaker than the Graceful Tree Conjecture.

In 2016 the authors of [2] proved that the Graceful Tree Conjecture holds asymptotically for trees of maximum degree at most $\frac{n}{\log n}$. Almost all studies on the graph labellings since the 1960s have been devoted to the graceful labellings and to the Graceful Tree Conjecture, and its elder *cousin*, the Ringel-Kotzig Conjecture, and the corresponding ρ -labellings of trees, have received much less attention. However, recent progress has been mainly made on the Ringel-Kotzig Conjecture as we shall see in Section 3.

In [17] the second author of this survey together with his former student Ivaška described the idea that every labelled graph of order n can be visualized by a *simple chessboard* (called also a *graph chessboard* or just a *chessboard*). It is a table with n rows and n columns, in which every edge uv is represented by a pair of dots with coordinates

$[u, v]$ and $[v, u]$. (In Figure 2 we see a graph and its corresponding chessboard.) One can also obtain such a graph chessboard using the adjacency matrix of a graph by placing dots to the cells corresponding to “ones” in the matrix.

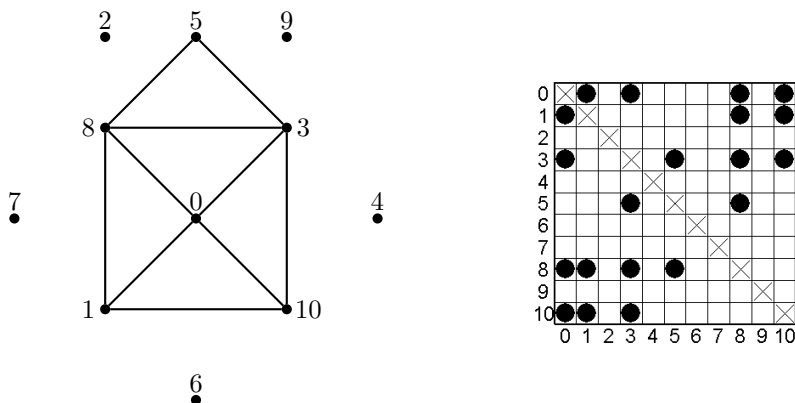


Figure 2. A graph and its corresponding chessboard

Let G be a graph whose vertices are labelled by distinct numbers from the set $\{0, 1, 2, \dots, n - 1\}$. Consider a chessboard of size n , i.e. table with n rows and n columns. Let the r -th diagonal (or the diagonal with value r) be the set of all cells with the coordinates $[i, j]$ where $i - j = r$ and $i \geq j$. The 0-th diagonal is called the *main diagonal* of the chessboard and the other diagonals are called *associate diagonals*. We do not need to consider the diagonals “above” the main diagonal, since the chessboard is *symmetric* with respect to the main diagonal.

A simple chessboard will be called *graceful* if there is exactly one dot on each of its associate diagonals.

Example 2.6. In Figure 3 we see a graceful labelling of a graph G and its corresponding chessboard. We can clearly see the gracefulness of the graph because on each of the associate diagonals there is exactly one dot.

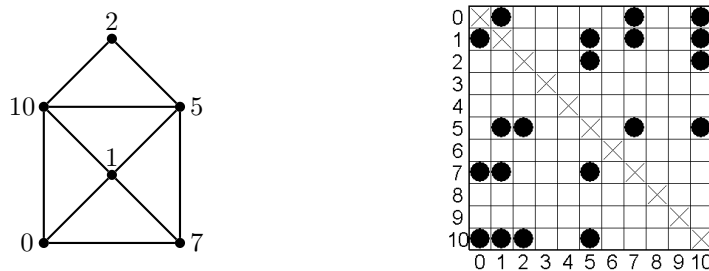


Figure 3. Graceful labelling of graph G and its graceful chessboard

Each gracefully labelled graph can be represented by *labelling sequence*, whose concept was introduced by Sheppard in [55]. He proved there that there is unique correspondence between gracefully labelled graphs and labelling sequences. In [17] Haviar and Ivaška

introduced and studied the graph chessboards and *labelling relations*, and showed a one-to-one correspondence between these two concepts and the labelling sequences. Let us now give more details on this.

Definition 2.7. ([55], [17, Definition 3.1.1]) For a positive integer m , the sequence of integers (j_1, j_2, \dots, j_m) , denoted (j_i) , is a **labelling sequence** if

$$0 \leq j_i \leq m - i \quad \text{for all } i \in \{1, 2, \dots, m\}. \tag{LS}$$

The labelling sequences can be understood as a tool to encode graceful labellings of graphs. The correspondence between gracefully labelled graphs (without isolated vertices) and the labelling sequences is described in the following theorem.

Theorem 2.8. ([55], [17, Theorem 3.1.2]) There is a one-to-one correspondence between graphs with m edges having a graceful labelling f and between labelling sequences (j_i) of m terms (entries). The correspondence is given by

$$j_i = \min\{f(u), f(v)\}, \quad i \in \{1, 2, \dots, m\},$$

where u, v are the end-vertices of the edge labelled i .

Since the graceful simple chessboards also encode gracefully labelled graphs, it is natural that also the following result holds:

Proposition 2.9. ([17, Proposition 3.1.3]) There is a one-to-one correspondence between all graceful simple chessboards and all labelling sequences.

Now we turn to the concept of a labelling relation which is the third main tool of [17] to encode gracefully labelled graphs.

1	2	3	4	5	6	7	8	9	10
0	5	2	1	5	1	0	2	1	0
1	7	5	5	10	7	7	10	10	10

Figure 4. The labelling table of graph G above

Definition 2.10. ([17, Definition 3.5.1]) Let $L = (j_1, j_2, \dots, j_m)$ be a labelling sequence. Then the relation $A(L) = \{[j_i, j_i + i], i \in \{1, 2, \dots, m\}\}$ is called a **labelling relation** assigned to the labelling sequence L .

From the book [17] we also use the concept of a *labelling table* to visualize a labelling relation (for particular case see Figure 4 above and for a general case see Figure 5 below).

1	2	3	...	m
j_1	j_2	j_3	...	j_m
$j_1 + 1$	$j_2 + 2$	$j_3 + 3$...	$j_m + m$

Figure 5. Displaying a labelling relation in a table (taken from [17, Figure 3.3])

The table header contains the numbers $1, 2, \dots, m$. The numbers from the labelling sequence are situated in the first row and the sums of numbers from the heading and the first row are in the second row. The pairs from first and second row in each column are then the elements of the labelling relation (and also the edges of the graph).

3 Proof of Ringel's Conjecture for large trees

As we mentioned, the history of the study of graph labellings began with a problem on decompositions of the complete graph into trees. This led to the Ringel's Conjecture that for any tree of size n the complete graph K_{2n+1} can be decomposed into $2n + 1$ copies of the given tree [40]. As also mentioned, Kotzig strengthened the conjecture by claiming that this decomposition can be *cyclic*.

In the area of the conjecture only some partial general results have been achieved for almost six decades. As already mentioned, Rosa (cf. [42], [43]) showed that the Ringel-Kotzig Conjecture is equivalent to the existence of the ρ -labelling for any tree. Hence the existence of the stronger graceful labelling for any tree, thus the *Graceful Tree Conjecture*, implies the Ringel-Kotzig Conjecture.

In February 2020, Montgomery, Pokrovskiy and Sudakov published in arXiv a proof of the Ringel-Kotzig Conjecture [32] for *large* trees, where the size of the tree is comparable with the size of the complete graph. In their proof they used a language of *rainbow subgraphs*, which describe the ρ -labellings.

Definition 3.1. ([32, page 2]) A **rainbow copy** of a graph H in an edge-coloured graph G is a subgraph of G isomorphic to H whose edges have different colours.

The Ringel-Kotzig Conjecture is implied by the existence of a rainbow copy of every tree T of size n in a so-called *near distance colouring* of the complete graph K_{2n+1} :

Definition 3.2. ([32, page 2]) Let $\{0, 1, \dots, 2n\}$ be the vertex set of K_{2n+1} . Colour the edge ij by colour k , where $k \in \{1, \dots, n\}$, if either $i = j + k$ or $j = i + k$ with addition modulo $2n + 1$. This is called **the near distance (ND) colouring**.

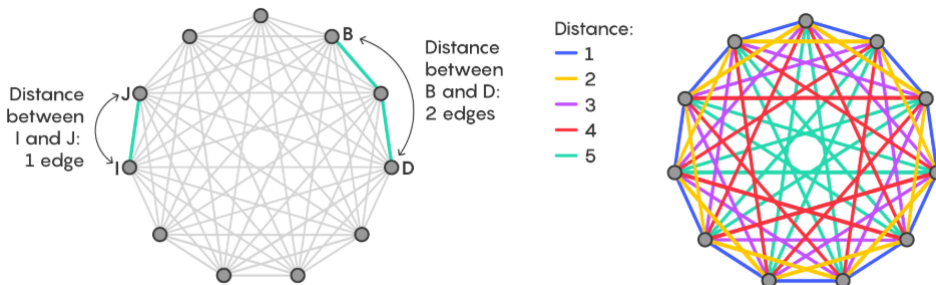


Figure 6. Left is a distance and right the ND-colouring of K_{11} (taken from [16])

Example 3.3. ([16]) Let us consider the complete graph K_{11} of order 11. We color the edges the way that edges of the same distance have the same colour. The distance is defined as the number of edges of circuit we need to move from one vertex to another. No shortcuts through the inside of the circle are allowed (see Figure 6). We always have two options, but we choose the shorter one. Now color the edges of the graph considering distance. All edges connecting vertices of distance 1 paint, say, by blue. All edges connecting vertices of distance 2 paint, say, by yellow. Etc. (See Figure 6.) On the complete graph of order $2n + 1$ we need n different colors to paint the whole graph.

Kotzig realized that this colouring can be helpful to place a given tree over the complete graph. By a placement of a *rainbow copy* of the tree is meant to position the tree so that every edge of the tree has different colour (see Figure 7).

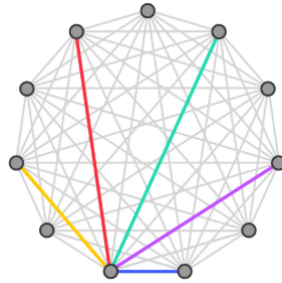


Figure 7. A rainbow copy of a tree (taken from [16])

If the ND-colouring of K_{2n+1} contains a rainbow copy of a tree T , then K_{2n+1} can be decomposed into copies of T by taking $2n + 1$ cyclic shifts of the original rainbow copy. This idea and Ringel’s Conjecture motivated Kotzig to conjecture that the ND-colouring of K_{2n+1} contains a rainbow copy of every tree of size n . It is important to note that a rainbow copy of a tree T with vertex set $\{0, 1, \dots, n\}$ in the ND-colouring of K_{2n+1} is equivalent to a graceful labelling of the tree T .

Montgomery, Pokrovskiy, and Sudakov already in 2019 [33] gave a new approach to embedding *large* trees (with no degree restrictions) into edge-colourings of complete graphs, and used this to prove the Ringel’s Conjecture asymptotically. In [32] they further developed and refined their approach, combining it with several critical new ideas to prove Ringel’s Conjecture for large complete graphs:

Theorem 3.4. ([32, Theorem 1.2]) For every sufficiently large n the complete graph K_{2n+1} can be decomposed into copies of any tree with n edges.

In [32] the authors, instead of working directly with tree decompositions or studying graceful labellings, proved for large n that every ND-coloured complete graph K_{2n+1} contains a rainbow copy of every tree of size n :

Theorem 3.5. ([32, Theorem 2.1]) For sufficiently large n , every ND-coloured K_{2n+1} has a rainbow copy of every n -edge tree.

Then they obtain a decomposition of the complete graph by rotating one copy of a given tree. Hence this gives a proof of the whole Ringel-Kotzig Conjecture for *large* n .

The proof approach of the authors of [32] builds on ideas from the previous research on both graph decompositions and graceful labellings. From the work on graph decompositions, their approach is inspired by *randomized* decompositions and so-called *absorption technique*. The rough idea of the method of “absorption” is as follows (cf. [32]):

- (1) Before the embedding of a tree T prepare a *template* which has some useful properties.
- (2) Find a partial embedding of the tree T with some vertices removed such that it does not use the edges of the template.
- (3) Use the template to embed the remaining vertices extensively since then.

This idea was introduced by Rödl, Rucinski and Szemerédi [41]. Also the proof of Ringel’s Conjecture for *bounded degree* trees is based on this method [23].

From the work on graceful labellings, the proof approach of [32], when dealing with trees with very high degree vertices, is based on a completely deterministic approach for finding a rainbow copy of the tree. This approach heavily relies on features of the ND-colouring and produces something very close to a graceful labelling of the tree. Their theorem is the first general result giving a perfect decomposition of a graph into subgraphs with arbitrary degrees. All previous comparable results placed a bound on the maximum degree of the subgraphs into which they decomposed the complete graph. Hence all these techniques encounter some barrier when dealing with trees with arbitrarily large degrees. Having overcome this “bounded degree barrier” for Ringel’s Conjecture, the authors of [32] hope that further development of their techniques can help overcome the “bounded degree barrier” also in other problems (cf. [32, page 3]).

The authors of [32] in their concluding remarks return to two other conjectures, the first one is the Graceful Tree Conjecture. They mention that this conjecture was proved for many isolated classes of trees, among them caterpillars, trees with at most 4 leaves, firecrackers, all trees with diameter at most 5, symmetrical trees, trees with at most 35 vertices, and olive trees (see [10]). They also mention that the Graceful Tree Conjecture is known to hold asymptotically for trees of maximum degree at most $\frac{n}{\log n}$ [2]. But as they emphasize, solving the Graceful Tree Conjecture for general trees, even asymptotically, is still wide open.

The second conjecture the authors of [32] mention in their concluding remarks is the *Tree Packing Conjecture* ([13], [32, Conjecture 8.2]):

Conjecture 3.6. (Tree Packing Conjecture) Let T_1, \dots, T_n be trees with $|T_i| = i$ for each $i \in \{1, \dots, n\}$. The edges of K_n can be decomposed into n trees which are isomorphic to T_1, \dots, T_n respectively.

In 2018 this conjecture was proved for bounded degree trees by Joos, Kim, Kühn and Osthus [23], but in general it is also wide open. The authors of [32] remark that it would be interesting to see if any of their techniques could be used here to make further progress on the Tree Packing Conjecture.

4 Recent results on graceful trees

4.1 Diameter six trees

In [19] Hrnčiar and Haviar proved that all trees of diameter five are graceful, which is still the best result on gracefulness of all trees with a bounded diameter. Mishra and Panigrahi in [30] and [31] gave a new class of graceful lobsters obtained from diameter four trees. Based on their techniques, in 2015-2017 Mishra and Panda [36] found graceful labellings for some new classes of diameter six trees [34], [35] and [36]. We briefly present the main results of [36].

Definition 4.1. ([36, Definition 1.2]) A **diameter six tree** can be represented as $(a_0; a_1, a_2, \dots, a_m; b_1, b_2, \dots, b_n; c_1, c_2, \dots, c_r)$, where a_0 is the center of the tree; a_i for $i = 1, 2, \dots, m$; b_j for $j = 1, 2, \dots, n$, and c_k for $k = 1, 2, \dots, r$ are the vertices of the trees adjacent to a_0 such that each a_i is a central vertex of some diameter three tree, each b_j is the central vertex of some star, and each c_k is some pendant vertex.

We note that in the above definition the authors mistakenly wrote in [36] that “each a_i is the center of some diameter four tree” while above we correctly write “each a_i is a central vertex of some diameter three tree” (meaning by a_i that of the two central vertices that is adjacent to a_0). Also the authors mistakenly wrote in [36] the following:

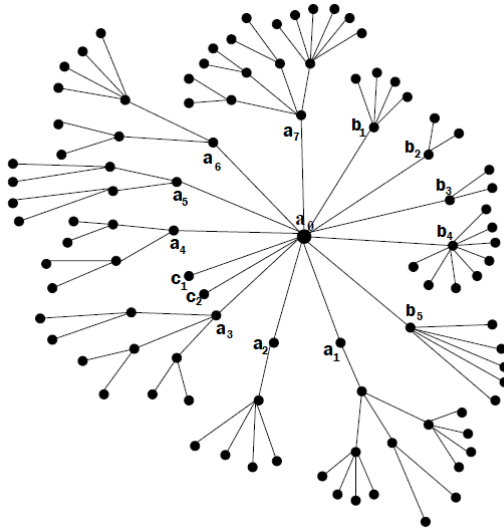


Figure 8. A diameter six tree (a corrected figure from [36])

“It is readily observed that for a diameter six tree with the above representation there are at least two neighbours of a_0 which are the centers of diameter four trees.” It should be corrected such that “there are at least two neighbours of a_0 which are central vertices of diameter three trees”.

In summary, in [36] graceful labellings were given for new classes of diameter six trees in which the diameter three trees adjacent with the center a_0 consist of six different combinations of odd, even, and pendant branches.

Example 4.2. In Figure 9 we see a diameter six tree D_6 with its graceful labelling found by Mishra and Panda in [34]. The size of the graph is 90, the degree of a_0 is 11.

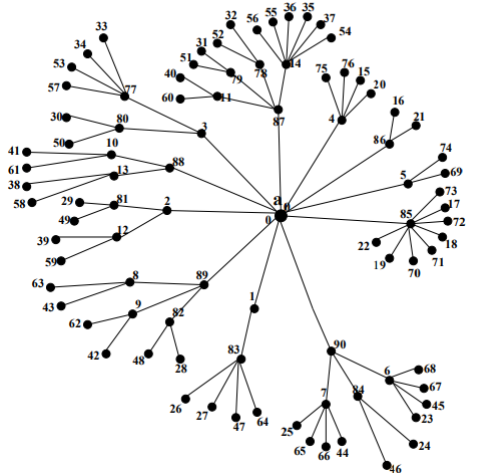


Figure 9. D_6 of order 91 (taken from [34, Figure 2(b)])

4.2 Spider graphs

In the early 1980s graceful labellings were found for all *spider graphs* with three or four legs [20]. Ten years ago it was proved in [5] that a spider graph for which the lengths of all legs (paths from the center to a leaf) differ by at most one is graceful. In 2014 in [21] some other classes of spiders were shown to be graceful, too.

Definition 4.3. A tree with at most one vertex of degree greater than two is called a **spider**, and this vertex is called a **branch vertex**. A path from the branch vertex to a leaf is called a **leg** of the spider.

Let us denote by $S_n(m_1, m_2, \dots, m_k)$ the spider with n legs such that $n \geq k$ and the legs have lengths one except for k legs of the lengths m_1, m_2, \dots, m_k , where $m_i \geq 2$ for all $i = 1, 2, \dots, k$.

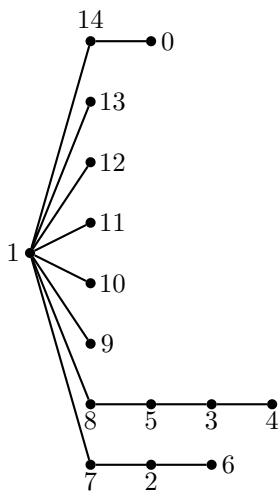
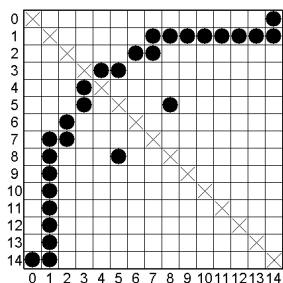


Figure 10. A graceful labelling of a spider $S_8(2, 4, 3)$

In 2016 in [37] graceful labellings were found for all spiders with at most four legs of lengths greater than one.



1	2	3	4	5	6	7	8	9	10	11	12	13	14
3	3	5	2	2	1	1	1	1	1	1	1	1	0
4	5	8	6	7	7	8	9	10	11	12	13	14	14

Figure 11. The representations of the gracefully labelled spider $S_8(2, 4, 3)$

Example 4.4. In Figure 10 we see a gracefully labelled spider graph $S_8(2, 4, 3)$ of order 15 with 8 legs with lengths 2,1,1,1,1,4,3. The branch vertex has label 1. Below the graph we added in Figure 11 also the simple chessboard and the labelling relation of this gracefully labelled graph. We see that the labelling sequence is $(3, 3, 5, 2, 2, 1, 1, 1, 1, 1, 1, 1, 0)$.

4.3 Symmetrical trees

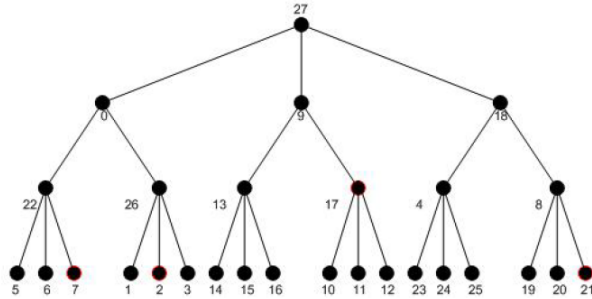
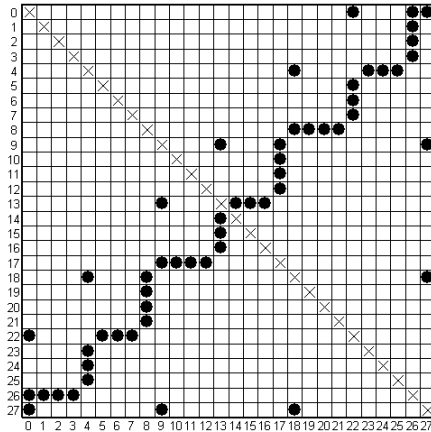


Figure 12. A symmetrical tree (taken from [45, Figure 3])

A **rooted tree** is known as a tree with a countable number of vertices, in which a particular vertex is distinguished from the others and called the **root**.



1	2	3	4	5	6	7	8	9	10	11	12	13	14
13	13	13	9	12	11	10	9	18	8	8	8	8	4
14	15	16	13	17	17	17	17	27	18	19	20	21	18

15	16	17	18	19	20	21	22	23	24	25	26	27
7	6	5	9	4	4	4	0	3	2	1	0	0
22	22	22	27	23	24	25	22	26	26	26	26	27

Figure 13. The representations of the symmetrical tree

For a given vertex, a number of vertices in the path from the root to this vertex is

called the **level** of the vertex. A **symmetrical tree** is a rooted tree with k levels, where every level contains vertices of the same degree.

In [38] an algorithm for graceful labelling of symmetrical trees was given. In 2018 Sandy, Rizal, Manurung, and Sugeng [45] gave an alternative construction of graceful symmetrical trees.

Example 4.5. In Figure 12 we see a symmetrical tree with graceful labelling. Again, below the graph we added in Figure 13 the simple chessboard and the labelling relation of this gracefully labelled graph. One can see that the labelling sequence is $(13, 13, 13, 9, 12, 11, 10, 9, 18, 8, 8, 8, 8, 4, 7, 6, 5, 9, 4, 4, 4, 0, 3, 2, 1, 0, 0)$. Here we very well see that creating the graph chessboard provides an extra value of visualization to the graceful labelling, and enables us seeing better a certain pattern of the graceful labelling in the graph chessboard.

4.4 Caterpillars and lobsters

Definition 4.6. ([17, page 72]) A **caterpillar** is a tree with the property that the removal of its vertices of degree one leaves a path.

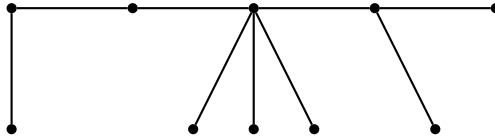


Figure 14. Example of a caterpillar

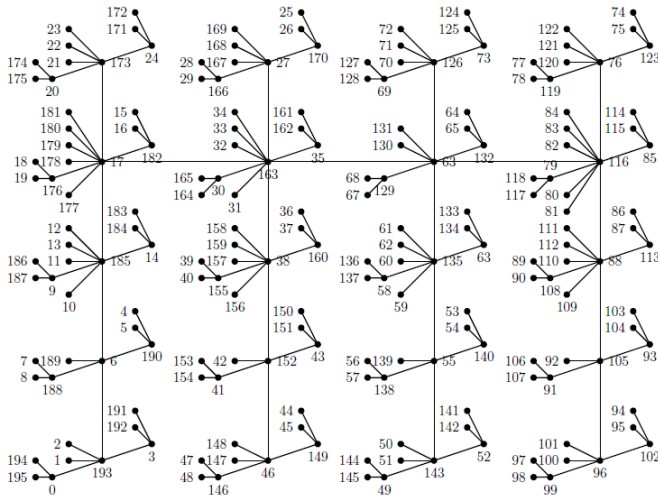


Figure 15. A graceful labelling of a tree (taken from [58, Figure 9])

By combining known graceful trees one can construct larger graceful trees. This idea was used by Sethuraman and Murugan [58] in 2016 and they constructed graceful trees from caterpillars in a specific way. An example of a gracefully labelled tree obtained from caterpillars by their method is seen in Figure 15. Also in this case the representations by

the simple chessboard, the labelling relation and the labelling sequence would be possible, but we do not provide them here due to the enormous size of the graph.

Definition 4.7. ([47, Definition 1.2]) For each vertex v of a graph G , take a new vertex v' and join v' to all vertices of G adjacent to v . The graph thus obtained is called the **splitting graph** of G and denoted $S'(G)$.

Sekar in [48] found graceful labellings of $S'(P_n)$ for all n (where P_n is a path) and $S'(C_n)$ for $n \equiv 0, 1 \pmod{4}$ (where C_n is a cycle). A gracefulness of the splitting graph of a bistar and a star was proved in [57]. Latest result from 2017 is proved in [47] and it says that the splitting graphs of caterpillars are graceful.

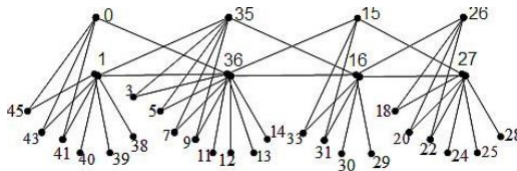


Figure 16. A graceful labelling of a splitting graph (taken from [47, Figure 3])

Example 4.8. In Figure 16 we see an illustration of a splitting graph constructed to a caterpillar by the above definition and its graceful labelling according to [47].

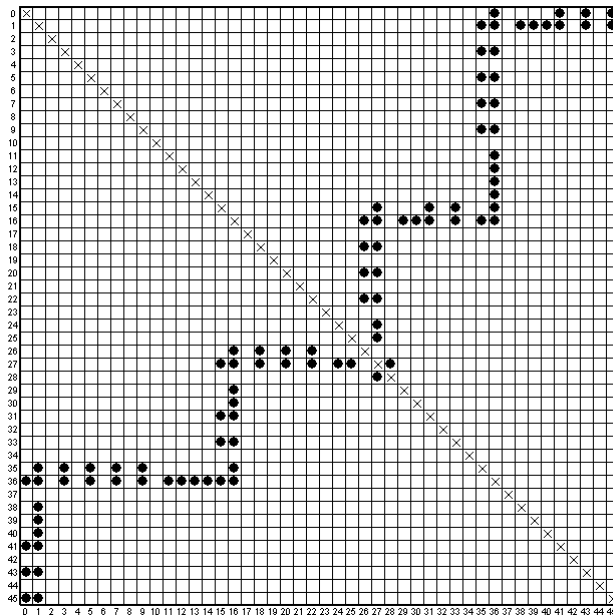


Figure 17. The chessboard of the splitting graph

And in Figures 17 and 18 we added its representations by the simple chessboard and the labelling relation, respectively. The labelling sequence of this gracefully labelled

splitting graph ('split' according to the labelling table below) is

(27, 25, 24, 22, 22, 20, 20, 18, 18, 16, 16, 15, 16, 16, 16,
 15, 16, 15, 16, 16, 15, 14, 13, 12, 11, 9, 9, 7, 7, 5, 5, 3, 3,
 1, 1, 0, 1, 1, 1, 1, 0, 1, 0, 1, 0).

1	2	3	4	5	6	7	8	9	10	11	12	13	14	15
27	25	24	22	22	20	20	18	18	16	16	15	16	16	16
28	27	27	26	27	26	27	26	27	26	27	27	29	30	31

16	17	18	19	20	21	22	23	24	25	26	27	28	29	30
15	16	15	16	16	15	14	13	12	11	9	9	7	7	5
31	33	33	35	36	36	36	36	36	36	35	36	35	36	35

31	32	33	34	35	36	37	38	39	40	41	42	43	44	45
5	3	3	1	1	0	1	1	1	1	0	1	0	1	0
36	35	36	35	36	36	38	39	40	41	41	43	43	45	45

Figure 18. The chessboard of the splitting graph

Definition 4.9. ([10]) A **lobster** is a tree with the property that the removal of the vertices of degree 1 leaves a caterpillar.

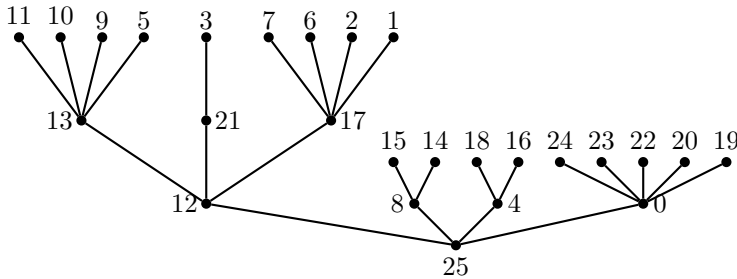
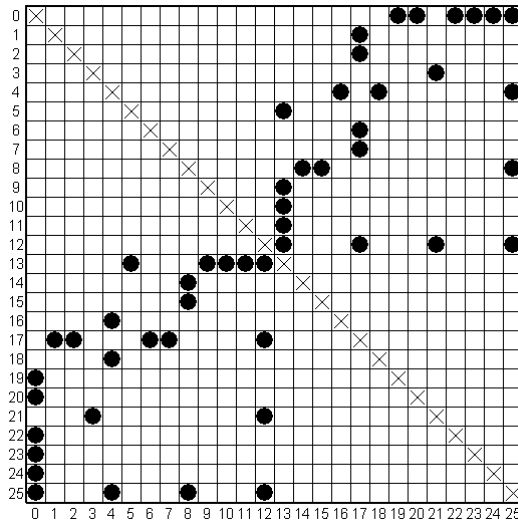


Figure 19. A graceful labelling of a lobster (taken from [11, Figure 18])

Bermond in [7] conjectured that all lobsters are graceful. Then Ghosh in [11] gave some methods how to join graceful graphs and graphs with the α -labelling. He defined three special classes of gracefully labelled lobsters. In 2015 Krop in [27] showed graceful-ness of each lobster that has a *perfect matching* that covers all but one vertex. Some new constructions of graceful classes of caterpillars and lobsters were given in 2018 in [56] by Suparta and Ariawan.

Example 4.10. In Figure 19 we see an example of a gracefully labelled lobster. We added its representations by the simple chessboard and the labelling relation that are seen in Figure 20. The labelling sequence representing this gracefully labelled graph is (12, 11, 10, 9, 12, 8, 8, 5, 12, 7, 6, 4, 12, 4, 2, 1, 8, 3, 0, 0, 4, 0, 0, 0, 0).



1	2	3	4	5	6	7	8	9	10	11	12
12	11	10	9	12	8	8	5	12	7	6	4
13	13	13	13	17	14	15	13	21	17	17	16

13	14	15	16	17	18	19	20	21	22	23	24	25
12	4	2	1	8	3	0	0	4	0	0	0	0
25	18	17	17	25	21	19	20	25	22	23	24	25

Figure 20. The representations of the gracefully labelled lobster

5 Recent results on graceful cyclic graphs

5.1 Linear cyclic snakes

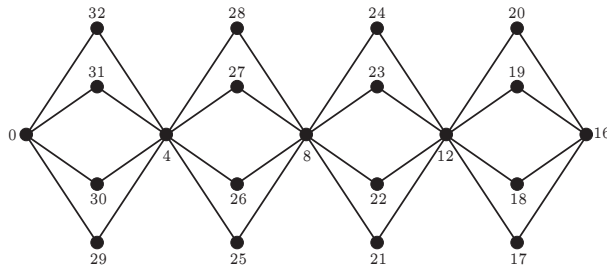
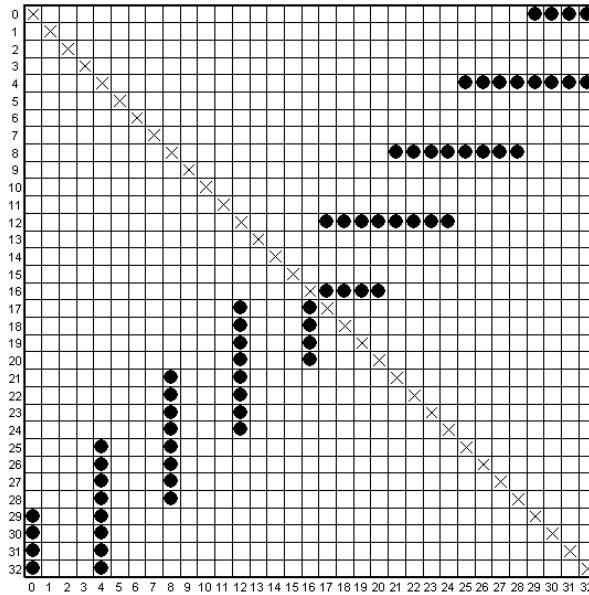


Figure 21. The graceful labelling of $(2, 4)C_4$ (taken from [3, Figure 3] and corrected)

Recalling briefly a history of *linear cyclic snakes*, we start with Barrientos who in [6] gave graceful labelings of *cyclic snakes*. Rosa in [44] glued together triangles in a special way and called it a *triangular snake*.

In 2015 Badr proved gracefulness of linear cyclic snakes $(1, k)C_4$, $(2, k)C_4$, $(1, k)C_8$ and $(2, k)C_8$ and showed that every linear cyclic snake of type $(m, k)C_n$ for $m \equiv 0$

(mod 4) and $m \equiv 3 \pmod{4}$ is graceful [3].



1	2	3	4	5	6	7	8	9	10	11	12	13	14	15	16
16	16	16	16	12	12	12	12	12	12	12	12	8	8	8	8
17	18	19	20	17	18	19	20	21	22	23	24	21	22	23	24

17	18	19	20	21	22	23	24	25	26	27	28	29	30	31	32
8	8	8	8	4	4	4	4	4	4	4	4	0	0	0	0
25	26	27	28	25	26	27	28	29	30	31	32	29	30	31	32

Figure 22. The representations of the gracefully labelled linear cyclic snake

We notice that the way Badr in [3] defined his “linear cyclic snakes” is rather badly written and hardly understandable. That is why we do not present his definition and try to explain the notation $(m, k)C_n$ in our own words via the example below.

Example 5.1. In Figure 21 we see a linear cyclic snake $(2, 4)C_4$ obtained by joining 4 copies of C_4 graphs in such a way that each of them contains inside an another copy of C_4 .

This graph is gracefully labelled. We added its representations by the simple chessboard and the labelling relation which can be seen in Figure 22. The labelling sequence representing this gracefully labelled graph is

$$(16, 16, 16, 16, 12, 12, 12, 12, 12, 12, 12, 12, 8, 8, 8, 8, 8, 8, 8, 8, 4, 4, 4, 4, 4, 4, 4, 4, 0, 0, 0, 0).$$

This is an excellent example where one can see that creating the graph chessboard provides the mentioned extra value of visualization to the graceful labelling, and allows to see, very clearly in this case in the graph chessboard, the pattern of the graceful labelling.

5.2 Cycle related graphs

Let C_n be a cycle of length n .

Definition 5.2. ([59, Definition 1.1]) A **chord** of the cycle is an edge connecting two non-neighbouring vertices of the cycle.

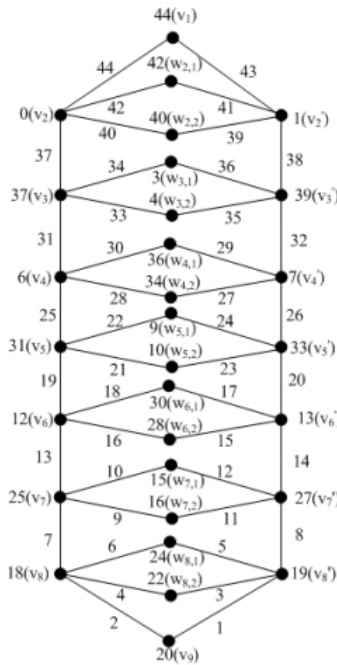


Figure 23. Graceful labelling of $C_{16,4}^+$ (taken from [59, Figure 4])

Recalling briefly a history of *cycle related graphs*, we start with Rosa, who in [43] showed that a cycle C_n is graceful if and only if $n \equiv 0$ or $3 \pmod{4}$. Later the authors of [8] proved gracefulness of a cycle with a chord. The authors of [25] proved that each cycle with P_3 -chord is graceful and conjectured that, more generally, each cycle with P_k -chord is graceful. (We recall that a cycle with a P_k -chord is a cycle with the path P_k joining two nonconsecutive vertices of the cycle.)

The mentioned conjecture was proved in [39] for all $k \geq 4$. In [49] the authors defined a graph obtained from a cycle C_n ($n \geq 6$) so that disjoint paths P_k (where $k \geq 3$ is fixed) are added between each pair of non-adjacent vertices of C_n and they call it a *cycle with parallel P_k chords*. They verified that each cycle C_n (where $n \geq 6$) with parallel P_k chords is graceful in cases $k = 3, 4, 6, 8$ and 10 .

Definition 5.3. ([59, Definition 1.2]) A graph acquired from the cycle C_n by adding the cycle C_k between every non-adjacent vertices is called a **cycle with C_k -chord** and denoted $C_{n,k}$.

Definition 5.4. ([59, Definition 1.3]) A graph acquired from the cycle C_n by adding the cycle C_k between every pair of non-neighbouring vertices $(v_2, v_n), (v_3, v_{n-1}), \dots, (v_a, v_b)$ where $a = \lfloor \frac{n}{2} \rfloor, b = \lfloor \frac{n}{2} \rfloor + 2$ if n is even, and $a = \lfloor \frac{n}{2} \rfloor, b = \lfloor \frac{n}{2} \rfloor + 3$ if n is odd, is called a **parallel cycle with C_k -chord** and denoted $C_{n,k}^+$.

Latest result in this direction was proved in 2017 by Venkatesh and Sivagurunathan

in [59]. It says that graphs $C_{n,4}$ and $C_{n,4}^+$ for each $n \equiv 0 \pmod{4}$ and $C_{n,6}$ for each odd $n \geq 5$ are graceful.

Example 5.5. In Figure 23 we see a gracefully labelled parallel cycle C_{16} with C_4 -chord.

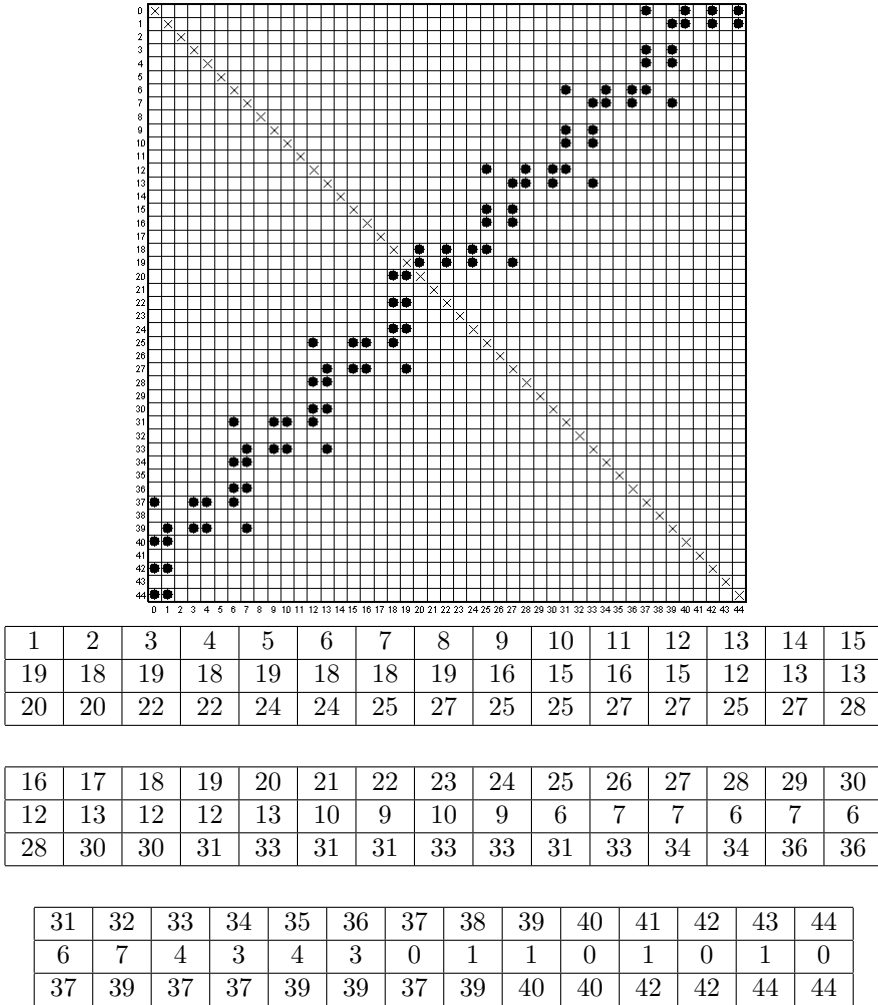


Figure 24. The representations of the gracefully labelled of $C_{16,4}^+$

We added its representations by the simple chessboard and the labelling relation that are seen in Figure 24. The labelling sequence representing this gracefully labelled graph is

$$(19, 18, 19, 18, 19, 18, 18, 19, 16, 15, 16, 15, 12, 13, 13, 12, 13, 12, 12, 13, 10, 9, 10, 9, 6, 7, 7, 6, 7, 6, 6, 7, 4, 3, 4, 3, 0, 1, 1, 0, 1, 0, 1, 0).$$

5.3 Corona product of aster flower graph

Definition 5.6. ([24, Definition 1]) An **aster flower graph** $(A_{(m,n)})$ is a graph which is generated from a cycle graph C_m ($m \geq 3$) by connecting path graphs P_{n+1} ($n \geq 1$) at

two adjacent vertices. A **corona product** $(A_{(m,n)} \odot \bar{K}_r)$ of aster flower graph is a graph which is generated from an aster graph $(A_{(m,n)})$ ($m \geq 3, n \geq 1$) by adding r leaf vertices on each vertex.

In [14] the gracefulness was proved for *corona product* of two graphs. Later in [9] it was proved that any cycle with a leaf connected at each vertex is graceful. In 2018 in [24] Khairunnisa and Sugeng found graceful labelling for each corona product $(A_{(3,1)} \odot \bar{K}_r)$ of aster flower graph (for $r \geq 1$).

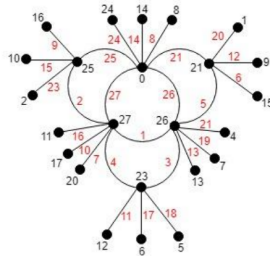
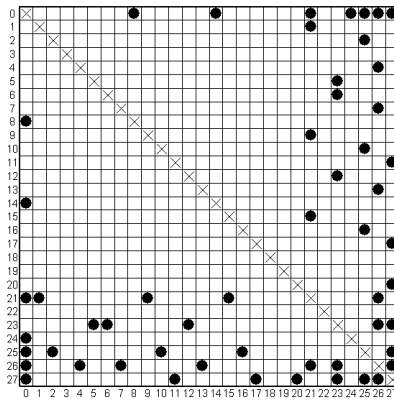


Figure 25. A corona product $(A_{(3,1)} \odot \bar{K}_3)$ (taken from [24, Figure 4])

Example 5.7. In Figure 25 we see a gracefully labelled corona product $(A_{(3,1)} \odot \bar{K}_3)$ of aster flower graph. We added its representations by the simple chessboard and the labelling relation which can be seen in Figure 26. The labelling sequence representing this gracefully labelled graph is

$$(26, 25, 23, 23, 21, 15, 20, 0, 16, 17, 12, 9, 13, 0, 10, 11, 6, 5, 7, 1, 0, 4, 2, 0, 0, 0, 0).$$



1	2	3	4	5	6	7	8	9	10	11	12	13	14
26	25	23	23	21	15	20	0	16	17	12	9	13	0
27	27	26	27	26	21	27	8	25	27	23	21	26	14

15	16	17	18	19	20	21	22	23	24	25	26	27
10	11	6	5	7	1	0	4	2	0	0	0	0
25	27	23	23	26	21	21	26	25	24	25	26	27

Figure 26. The representations of the gracefully labelled $(A_{(3,1)} \odot \bar{K}_3)$

5.4 Unicyclic graphs

Definition 5.8. ([15, page 41]) A graph is **unicyclic** if it contains just one cycle and is connected.

In Figure 27 we see an example of unicyclic graph.

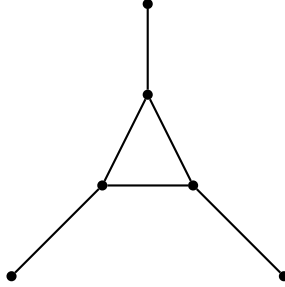


Figure 27. An example of unicyclic graph

Recalling briefly a history of embedding graphs into graceful graphs (see [53, page 11]), we start with Acharya who in [1] proved that each connected graph can be embedded in a graceful graph. Later, the authors of [50] generalized this result and showed that any set of graphs can be “packed” into a graceful graph.

In 2015 Bagga, Fotso, Max, and Arumugam in [4] explored the gracefulness of graphs with only one cycle with some pendant caterpillars at two neighbouring vertices of cycle and pendant edges at some other vertices of the cycle. A cycle with a pendant caterpillar is obtained by identifying a vertex of the cycle with a leaf of caterpillar.

In 2016 Sethuraman in [51] showed that every tree can be embedded in a graceful tree. This inspired Sethuraman and Murugan who proved in 2019 in [53] that any acyclic graph can be embedded in a unicyclic graceful graph. The authors found an algorithm that from any acyclic graph constructs a graceful unicyclic graph.

Also in 2019 Sethuraman and Murugan [52] presented a construction of graceful labeling of a graph G from a graceful tree T in case the number of vertices of G is equal to number of vertices of T . The constructed graph is unicyclic.

6 Recent results on graceful subdivisions of graphs

6.1 Complete bipartite graphs

Definition 6.1. ([46]) If in a graph G an edge uv is replaced by the path $P : uww$, where w is the new vertex, then the edge uv is called **subdivided**. A **subdivision** of a graph G is the graph obtained by subdividing each edge of the graph G and it is denoted by $S(G)$.

In 2016 Sankar and Sethuraman in [46] proved that each subdivision of the complete bipartite graph $K_{2,n}$ is graceful for every $n \geq 1$.

Example 6.2. In Figure 28 we see the subdivision graph $S(K_{2,4})$ and its graceful labeling. Its representations by the simple chessboard and the labelling relation can be seen in Figure 29. The labelling sequence representing this gracefully labelled graph is $(8, 8, 8, 8, 7, 5, 3, 1, 7, 5, 3, 1, 0, 0, 0, 0)$. This is another excellent example where one can see that creating the graph chessboard allows to see very clearly the pattern of the graceful labelling.

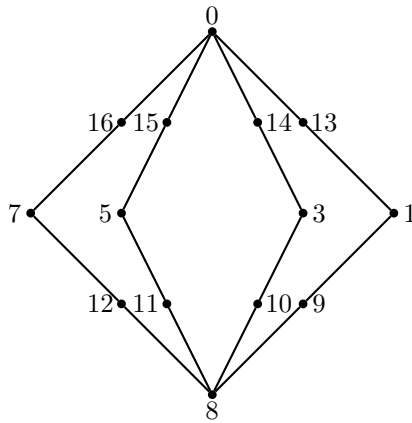
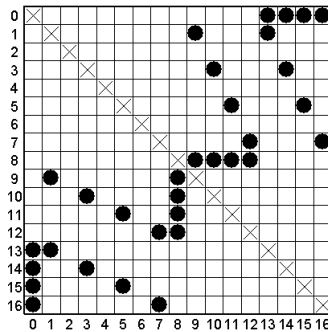


Figure 28. A graceful labeling of $S(K_{2,4})$



1	2	3	4	5	6	7	8	9	10	11	12	13	14	15	16
8	8	8	8	7	5	3	1	7	5	3	1	0	0	0	0
9	10	11	12	12	11	10	9	16	15	14	13	13	14	15	16

Figure 29. The representations of the gracefully labelled $S(K_{2,4})$

6.2 Wheels

Definition 6.3. ([54]) A **wheel** is a graph obtained by connecting a single vertex K_1 to all vertices of a cycle C_n . A wheel W_n is the graph $C_n + K_1$ for $n \geq 3$.

Some authors use the symbol W_n to denote the wheel with n vertices.

In [18] it was proved that all wheels for $n \geq 3$ are graceful. In [28] graceful labellings of directed wheels were presented. In 2015 in [54] Sethuraman and Sankar proved that the subdivision $S(W_n)$ of the wheel W_n is graceful for even numbers $n \geq 4$.

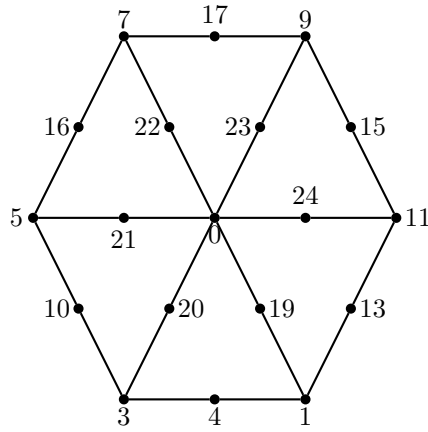


Figure 30. Gracefully labeled wheel $S(W_6)$

Example 6.4. In Figure 30 we see a gracefully labelled subdivision $S(W_6)$ of order 19 and size 24.

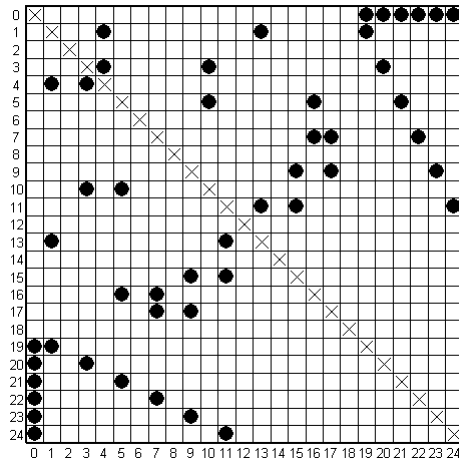


Figure 31. The chessboard of the gracefully labelled $S(W_6)$

We added its representations by the simple chessboard in Figure 31 and the labelling table which can be seen in Figure 32. The labelling sequence representing this gracefully labelled graph is $(3, 11, 1, 11, 5, 9, 3, 9, 7, 7, 5, 1, 11, 9, 7, 5, 3, 1, 0, 0, 0, 0, 0, 0)$.

1	2	3	4	5	6	7	8	9	10	11	12
3	11	1	11	5	9	3	9	7	7	5	1
4	13	4	15	10	15	10	17	16	17	16	13

13	14	15	16	17	18	19	20	21	22	23	24
11	9	7	5	3	1	0	0	0	0	0	0
24	23	22	21	20	19	19	20	21	22	23	24

Figure 32. The labelling table of the gracefully labelled $S(W_6)$

6.3 Shell and bow graphs

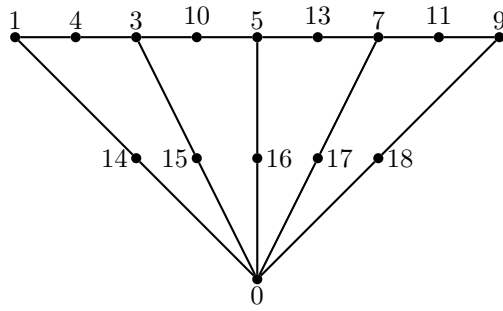


Figure 33. The graph $S(C(6, 3))$

Definition 6.5. ([46]) A **shell graph** is a cycle $C_n(v_0, v_1, v_2, \dots, v_{n-1})$ with $(n-3)$ chords connecting vertex v_0 , we denote it $C(n; n-3)$. The vertex v_0 is called *apex* of the shell graph.

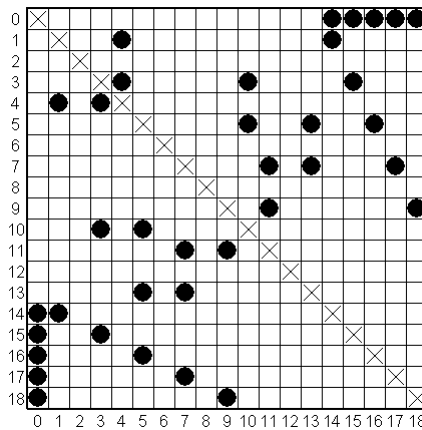


Figure 34. The chessboard of the gracefully labelled $S(C(6, 3))$

1	2	3	4	5	6	7	8	9	10	11	12	13	14	15	16	17	18
3	9	1	7	5	7	3	5	9	7	5	3	1	0	0	0	0	0
4	11	4	11	10	13	10	13	18	17	16	15	14	14	15	16	17	18

Figure 35. The labelling table of the gracefully labelled $S(C(6, 3))$

Example 6.6. In Figure 33 we see a gracefully labelled subdivision of the shell graph $C(6, 3)$. The graph $S(C(6, 3))$ is of size 18. Its representations by the simple chessboard can be seen in Figure 34 and the labelling table can be seen in Figure 35. The labelling sequence representing this gracefully labelled graph is

$$(3, 9, 1, 7, 5, 7, 3, 5, 9, 7, 5, 3, 1, 0, 0, 0, 0, 0).$$

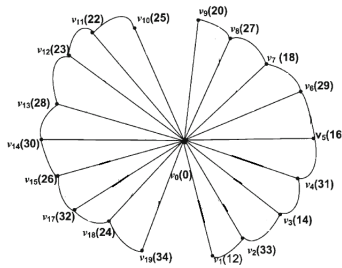


Figure 36. A uniform bow graph (taken from [22, Figure 2])

Definition 6.7. ([22]) A **bow graph** is a graph consisting of two shells of any orders. If each shell has the same order, we call it a **uniform bow graph**. A special case of a bow graph is a **shell butterfly graph**. This is a bow graph with two special edges from the apex.

In 2015 Jesintha and Hilda in [22] proved gracefulness of all uniform bow graphs. In Figure 36 we see a gracefully labelled uniform bow graph of size 34.

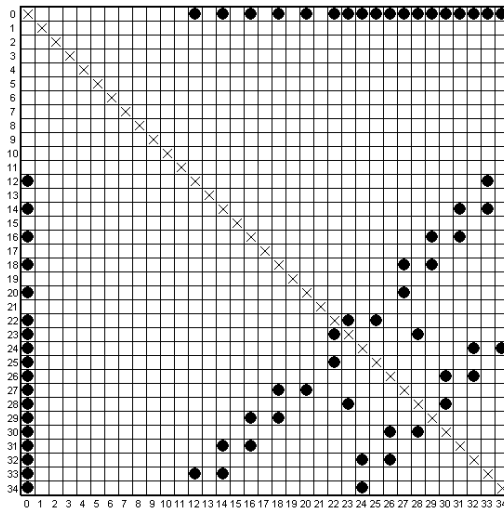


Figure 37. The chessboard of the gracefully labelled uniform bow graph

- [14] F. Harary and R. Frucht: On the Corona of Two Graphs. *Aequationes mathematicae* **4** (1970), 322–325.
- [15] F. Harary: “Graph Theory”. Addison Wesley, Reading, MA, 1969.
- [16] K. Hartnett: Rainbow Proof Shows Graphs Have Uniform Parts. *Quanta magazine*, February 2020. Available at <https://www.quantamagazine.org/mathematicians-prove-ringels-graph-theory-conjecture-20200219/>.
- [17] M. Haviar and M. Ivaška: “Vertex Labellings of Simple Graphs”. Research and Exposition in Mathematics, Vol. 34, Heldermann-Verlag, Lemgo, Germany, 2015.
- [18] C. Hoede and H. Kuiper: All wheels are graceful. *Util. Math.* **14** (1987), 311.
- [19] P. Hrnčiar and A. Haviar: All trees of diameter five are graceful. *Discrete Mathematics* **233** (2001), 133–150.
- [20] C. Huang, A. Kotzig and A. Rosa: Further results on tree labellings. *Utilitas Mathematica* **21** (1982), 31–48.
- [21] P. Jampachon, K. Nakprasit and T. Poomsa-ard: Graceful labeling of some classes of spider graphs with three legs greater than one. *Thai J. Math.* **12** (2014), 621–630.
- [22] J. Jeba Jesintha and K. Ezhilarasi Hilda: All uniform bow graphs are graceful. *Math. Comput. Sci.* **9** (2015), 185–191.
- [23] F. Joos, J. Kim, D. Kühn and D. Osthus: Optimal packings of bounded degree trees. *J. European Math. Soc.*, to appear, 2018.
- [24] E. Khairunnisa and K.A. Sugeng: Graceful labelling of corona product of aster ower graph. *Adv. Intel. Systems Res. (AISR)* **157** (2018), 68–71.
- [25] K.M. Koh and K.Y. Yap: Graceful numberings of cycles with a P3 chord. *Bull. Inst. Math. Acad. Sinica* **12** (1985), 41–48.
- [26] K. Kotul'ová: “Recent research on graceful labellings of simple graphs”. Bc. thesis, M. Bel University, Banská Bystrica, 2020.
- [27] E. Krop: Lobsters with an almost perfect matching are graceful. *Bull. Inst. Combin. Appl.* **74** (2015), 21–24.
- [28] A.M. Marr: Graceful labelings of directed graphs. *J. Combin. Math. Combin. Comput.* **66** (2008), 97–103.
- [29] J. Matoušek and J. Nešetřil: “Invitation to Discrete Mathematics”. Oxford University Press, 2008.
- [30] D. Mishra and P. Panigrahi: Some graceful lobsters with all three types of branches incident on the vertices of the central path. *Computers and Mathematics with Applications* **56**, (2008), 1382–1394.
- [31] D. Mishra and P. Panigrahi: New class of graceful lobsters obtained from diameter four trees. *Utilitas Mathematica* **80** (2009), 183–209.
- [32] R. Montgomery, A. Pokrovskiy and B. Sudakov: A proof of Ringel’s Conjecture. *arXiv:2001.02665v2*, February 2020.
- [33] R. Montgomery, A. Pokrovskiy and B. Sudakov: Embedding rainbow trees with applications to graph labelling and decomposition. *J. European Math. Soc.*, to appear, 2019.
- [34] A.C. Panda and D. Mishra: Some new classes of graceful diameter six trees. *Turkic World Math. Soc. J. Appl. Engin. Math.* **5** (2015), 269–275.
- [35] A.C. Panda, D. Mishra and R. B. Dash: A class of diameter six trees exhibiting graceful labeling. *J. Discrete Math. Sci. Cryptogr.* **19** (2016), 947–963.
- [36] A.C. Panda and D. Mishra: A family of graceful diameter six trees generated by component moving techniques. *British J. Math. Comput. Sci.* **21** (2017), 1–15.

- [37] A. Panpa and T. Poomsa-ard: On graceful spider graphs with at most four legs of lengths greater than one. *J. Appl. Math.* **3** (2016), 1–5.
- [38] S. Poljak and M. Sura: An algorithm for graceful labeling of a class of symmetrical trees. *Ars Combin.* **14** (1982), 57–66.
- [39] N. Punnim and N. Pabhapote: On graceful graphs: cycles with a P_k chord, $k \geq 4$. *Ars Combinatoria* **23A** (1987), 225–228.
- [40] G. Ringel: Problem 25. *Theory of Graphs and its Application*. Proc. Sympos. Smolenice 1963, Nakl. CSAV, Prague, 1964.
- [41] V. Rödl, A. Rucinski and E. Szemerédi: A dirac-type theorem for 3-uniform hypergraphs. *Combin. Probab. Comput.* **15** (2006), 229–251.
- [42] A. Rosa: “O cyklických rozkladoch kompletného grafu”. PhD thesis (in Slovak). Československá akadémia vied, Bratislava, 1965.
- [43] A. Rosa: On certain valuations of the vertices of a graph. *Theory of Graphs* (Internat. Symposium, Rome, July 1966), Gordon and Breach, N. Y. and Dunod Paris, 1967, 349–355.
- [44] A. Rosa: Cyclic Steiner Triple Systems and Labeling of Triangular Cacti. *Scientia* **5** (1967), 87–95.
- [45] I.P. Sandy, A. Rizal, E.N. Manurung and K. A. Sugeng: Alternative construction of graceful symmetric trees. *J. Phys.: Conf. Ser.* **1008** (2018), 012031.
- [46] K. Sankar and G. Sethuraman: Graceful and cordial labeling of subdivision of graphs. *Electronic Notes Disc. Math.* **53** (2016), 123–131.
- [47] G. Sathiamoorthy, C. Natarajan, S.K. Ayyaswamy and T.N. Janakiraman: Graceful labeling of splitting graph of a caterpillar. *Internat. J. Mech. Engin. Tech.* (IJMET) **8** (2017), 663–667.
- [48] C. Sekar: “Studies in Graph Theory”. Ph. D. Thesis, Madurai Kamaraj University, 2002.
- [49] G. Sethuraman and A.Elumalai: Gracefulness of a cycle with parallel P_k chords. *Australian Journal of Combinatorics* **32** (2005), 205–211.
- [50] G. Sethuraman and A. Elumalai: Packing of any set of graphs into a graceful/ harmonious/elegant graph. *Ars Combin.* **76** (2005), 297–301.
- [51] G. Sethuraman and V. Murugan: Generating graceful trees from caterpillars by recursive attachment. *Electronic Notes Discrete Math.* **53** (2016), 133–147.
- [52] G. Sethuraman and V. Murugan: Generating graceful unicyclic graph from a given graceful tree. *Ars. Combin.*, to appear, 2019.
- [53] G. Sethuraman and V. Murugan: Generating graceful unicyclic graphs from a given forest. *AKCE Internat. J. Graphs Combin.*, to appear.
- [54] G. Sethuraman and K. Sankar: Subdivision of wheel is graceful and cordial. *Internat. J. Math. Anal.* **17** (2015), 817–822.
- [55] D.A. Sheppard: The factorial representation of major balanced labelled graphs. *Discrete Math.* **15** (1976), 379–388.
- [56] N. Suparta and D.M.A. Ariawan: Some methods for constructing some classes of graceful uniform trees. *Indonesian J. Combin.* **2** (2018), 123–135.
- [57] S.K. Vaidya and N.H.A. Shah: Graceful and odd graceful labeling of some graphs. *Internat. J. Mathematics Soft Comput.* **3** (2013), 61–68.
- [58] M. Varadhan and S. Guruswamy: Generating graceful trees from caterpillars by recursive attachment. *Electronic Notes Disc. Math.* **53** (2016), 133–147.
- [59] S. Venkatesh and S. Sivagurunathan: On the gracefulness of cycle related graphs. *Int. J. Pure Appl. Math.* (IJPAM) **117** (2017), 589–598.

New descriptions of certain classes of graceful graphs

Samuel Kurtulík

Faculty of Natural Sciences, Matej Bel University,

Tajovského 40, 974 01 Banská Bystrica, Slovakia

kurtuliksamuel@gmail.com

Abstract

The aim of this paper is to bring new descriptions and characterizations of graceful labellings of certain graphs by using methods and tools such as graph chessboard, labelling sequence and labelling relation. These methods and tools bring new insights to the study of graceful graphs, among them the extra value of visualization. By their application new descriptions of graceful labellings of sunlet graphs and wheels are presented. These classes of graphs are known to be graceful, however the results presented in this paper bring their new characterisations.

Received May 15, 2020

Accepted in final form June 14, 2020

Communicated with Miroslav Haviar.

Keywords sunlet graph, wheel graph, graceful labelling, graph chessboard, labelling sequence, labelling relation.

MSC(2010) Primary 05C78; Secondary 05C38.

1 Introduction

The basis of the study of graph labellings was laid out in the late 1960s. Interest in graph labellings began with a Kotzig-Ringel conjecture and a paper by Rosa [10]. The most extensive source of regularly updated information on graph labellings is “Dynamic Survey of Graph Labeling” by Galian [2], where one can find a huge number of results, methods and techniques on graph labellings.

The subject of study in this text are β -labellings, which were introduced together with other types of graph labellings by Rosa [9] in 1965. Later Golomb [4] named β -labelling as *graceful labelling*. A graph with m edges has a graceful labelling and it is said to be graceful, when its vertices can be assigned the labels from the set $\{0, 1, \dots, m\}$ such that the absolute values of the differences in vertex labels of edges form the set $\{1, \dots, m\}$.

This paper brings new results in the area of graceful labellings of graphs which have been achieved by tools such as graph chessboard, labelling sequence and labelling relation. The main source of inspiration for this text has been the book “Vertex Labellings of Simple Graphs” by the authors Haviar and Ivaška [5], where the mentioned tools are described. The labelling sequences were introduced in 1976 by Sheppard in [11] while the graph chessboards and labelling relations were introduced and studied in [5]. We also used a computer program called *Graph processor* from [6], which turned out to be very helpful for finding and describing graceful labellings of graphs during our investigations.

The basic terms from graph theory needed in the paper are introduced in Section 2. Here we also present the basic facts on the graph labellings and especially graceful labellings. Then we introduce the tools that we used to achieve our results, namely the graph chessboards, labelling sequences and labelling relations.

In this text we focus on two classes of graphs: *sunlet graphs* and *wheel graphs*. In both cases the graceful labellings of these graphs have been known since 1979 due to Frucht [1]. It might sound interesting this time that the author in his paper called the sunlet graphs by *coronas*. When studying the sunlet graphs by our tools and our methods, we distinguish four subclasses according to the length of the cycle of these graphs: $n \equiv 0 \pmod{4}$, $n \equiv 1 \pmod{4}$, $n \equiv 2 \pmod{4}$ and $n \equiv 3 \pmod{4}$. As we shall see in Section 3, all four cases have something in common, yet they are different in details. For the wheel graphs we will similarly distinguish two subcases, for even and odd lengths of their cycle. In both classes of graphs the pattern which represents the graceful labellings of these graphs is very well indicated in the graph chessboard, where one can immediately recognize that the corresponding graph labelling is graceful. For the sunlet graphs we show and prove formulas for the labelling sequence and the labelling relation. For the wheel graphs we define specific labelling sequences, which correspond to the graceful labellings of these graphs. Our methods are frequently illustrated by figures and examples.

2 Preliminaries

Here we mention certain terms from graph theory. We present graph labellings, especially graceful labellings (called in the original terminology β -labellings), which we use in our paper. Moreover we introduce labelling sequences, labelling relations and simple chessboard as our tools to describe graceful graphs. These basic preliminaries, concepts and definitions are taken primarily from [5].

Simple graphs are in graph theory well-known as finite undirected graphs without loops and multiple edges. In this work we use only these graphs. As usual, for the number of vertices of a graph G we use the term *order* of G , and for the number of edges in G we use the term *size* of G .

2.1 Graph labellings

Definition 2.1. A **vertex labelling** (or only labelling) f of a graph $G = (V, E)$ is a one-to-one mapping of its vertex set $V(G)$ into the set of non-negative integers assigning to the vertices so-called **vertex labels**.

Definition 2.2. By the **label of an edge** uv in the labelling f we mean the number $|f(u) - f(v)|$, where $f(u), f(v)$ are the labels of the vertices u, v , respectively.

In this text we will denote $f(V_G)$ the set of all vertex labels and $f(E_G)$ the set of all edge labels in the labelling f of the graph G .

We know several types of graph labellings, e.g. $\alpha, \beta, \sigma, \rho$ defined by Rosa in his seminal paper [10] in 1967, and further γ, δ, p, q introduced also by Rosa in his dissertation thesis [9] in 1965. There exists a hierarchy of labellings $\alpha, \beta, \sigma, \rho$:

α -labelling
 β -labelling
 σ -labelling
 ρ -labelling.

Each labelling of a given graph is at the same time also the next lower labelling. For instance, every σ -labelling is also ρ -labelling, but a σ -labelling need not be β -labelling or α -labelling.

For this hierarchy of labellings we shall be using the term *Rosa hierarchy* as in [5]. In this text we study only β -labelling, which is called **graceful labelling**, therefore we will present only definition of this labelling.

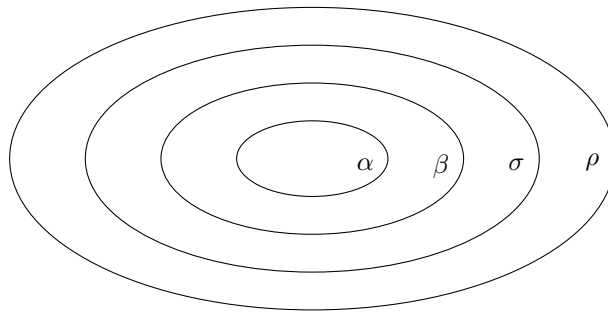


Figure 1. Visualization of a Rosa hierarchy

Definition 2.3. A **graceful labelling** (or β -labelling) of a graph $G = (V, E)$ of size m is a vertex labelling with the following properties:

1. $f(V_G) \subseteq \{0, 1, \dots, m\}$, and
2. $f(E_G) = \{1, 2, \dots, m\}$.

Hence a graceful labelling of a graph of size m has vertex labels among the numbers $0, 1, \dots, m$ such that the induced edge labels are different and cover all values $1, 2, \dots, m$. When a graph has a graceful labelling then we say that graph is *graceful*. While the concept of a β -labelling was introduced by Rosa [10] in 1967, in 1972 Golomb [4] called such labelling “graceful” and this term was popularized by mathematician Martin Gardner [3]. In Figure 2 we can see some graceful graphs.

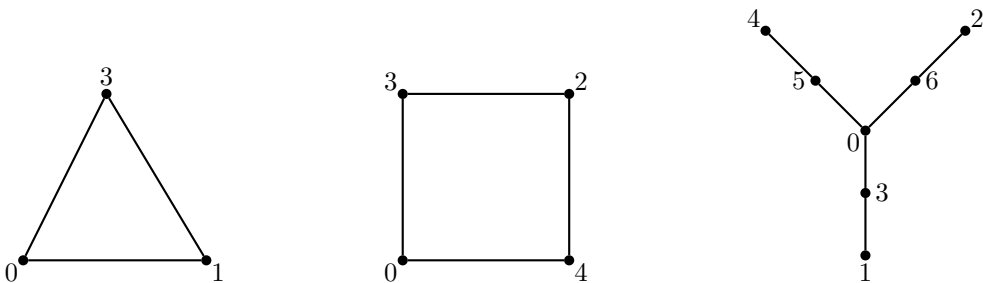


Figure 2. Some graceful graphs

2.2 Labelling sequences and relations

Each graceful graph can be represented by a sequence of non-negative integers. It was shown by Sheppard in his article [11], where he introduced a new concept of a *labelling sequence* as follows:

Definition 2.4. ([11], [5]) For a positive integer m , a **labelling sequence** is the sequence of non-negative integers (j_1, j_2, \dots, j_m) , denoted (j_i) , where

$$0 \leq j_i \leq m - i \quad \text{for all } i \in \{1, 2, \dots, m\}. \tag{LS}$$

Sheppard also proved that there is a one-to-one correspondence between graceful labellings of graphs (without isolated vertices) and labelling sequences. Therefore we can understand labelling sequences as a tool to encode graceful labellings of graphs. The connection is described in the following theorem.

Theorem 2.5. ([11], [5]) There exists a one-to-one correspondence between graphs of size m having a graceful labelling f and between labelling sequences (j_i) of m terms. The correspondence is given by

$$j_i = \min\{f(u), f(v)\}, \quad i \in \{1, 2, \dots, m\},$$

where u, v are the end-vertices of the edge labelled i .

Now we introduce definition of a labelling relation. It is another tool to describe gracefully labelled graphs, which is closely related to term of labelling sequence. The concept of a *labelling relation* was introduced and studied by Haviar and Ivaška in [5]:

Definition 2.6. ([5]) Let $L = (j_1, j_2, \dots, j_m)$ be a labelling sequence. Then the relation $A(L) = \{[j_i, j_i + i], i \in \{1, 2, \dots, m\}\}$ will be called a **labelling relation** assigned to the labelling sequence L .

To visualize a labelling relation and also a labelling sequence we shall use a *labelling table* (see Figure 3). A table is formed by heading with the numbers $1, 2, \dots, m$ and two rows. The first row contains the numbers from the labelling sequence and the second row contains the sums of numbers from the heading and the first row. The pairs from first and second row in each column are then the elements of the labelling relation (and also edges of the graph).

1	2	3	...	m
j_1	j_2	j_3	...	j_m
$j_1 + 1$	$j_2 + 2$	$j_3 + 3$...	$j_m + m$

Figure 3. Displaying a labelling table

Example 2.7. In Figure 4 we can see the labelling table assigned to the labelling sequence $(5, 4, 3, 2, 1, 0)$ and its corresponding graceful graph whose edges are the elements of the labelling relation.

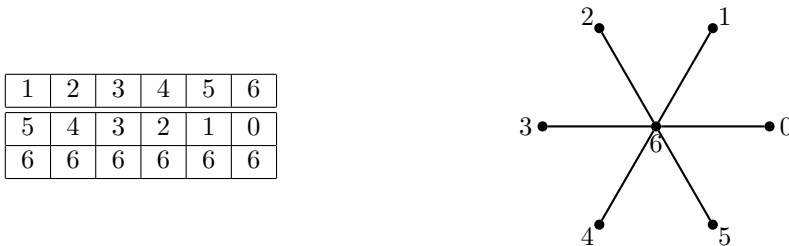


Figure 4. Example of a labelling table and its corresponding graceful graph

2.3 Simple graph chessboards

Every labelled simple graph with n vertices can be represented by a *chessboard*, i.e. a table with n rows and n columns, where every edge of graph uv is represented by a pair of dots with coordinates (u, v) or (v, u) . This idea of visualization of vertex labellings of graphs by chessboard and also other independent discoveries of similar ideas are described in [5].

There exist several types of graph chessboards like simple chessboard, double chessboard, M-chessboard, dual chessboard and twin chessboard, which were discovered by Haviar and Ivaška and presented in [5]. In this text we use only the idea of a simple chessboard, which is a useful tool in visualization of labelled graphs. Consider a graph G

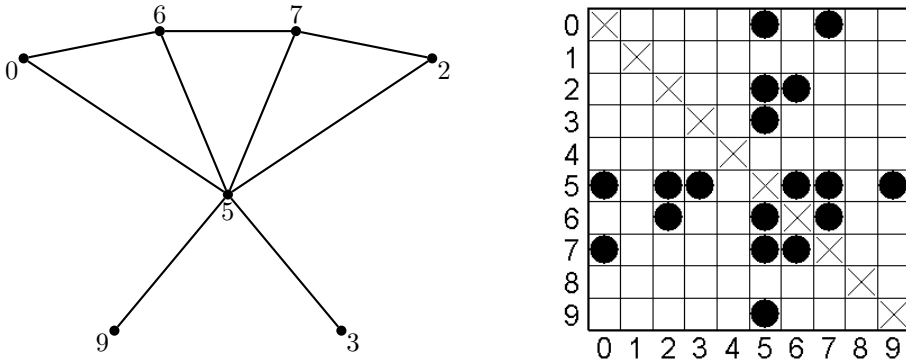


Figure 5. Example of a graph and its corresponding simple chessboard

of size m whose vertices are labelled by different numbers from the set $\{0, 1, 2, \dots, m\}$ and consider a table with $m + 1$ rows and $m + 1$ columns. Rows are numbered by $0, 1, \dots, m$ from the top to the bottom and columns are numbered by $0, 1, \dots, m$ from the left to the right as we can see in Figure 5. The cell with coordinates $[i, j]$ of the table will mean the cell in the i -th row and the j -th column. The r -th diagonal in the table is the set of all cells with coordinates $[i, j]$ where $i - j = r$ and $i \geq j$. The main diagonal is 0-th diagonal in the table and other diagonals are associated. A simple chessboard of size m is

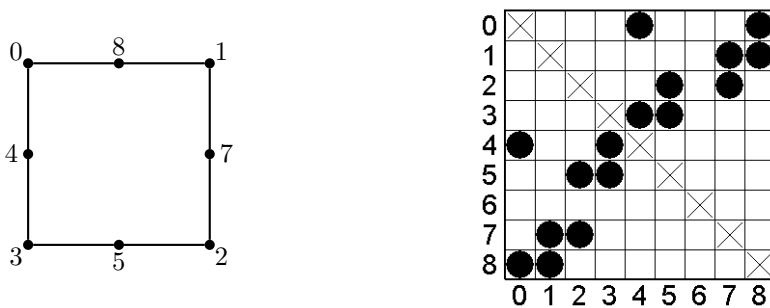


Figure 6. Gracefully labelled graph and its graceful simple chessboard

a table, which is assigned to a labelled graph of size m in the following way: every edge uv in the graph is represented by a pair of dots in the cells with coordinates $[u, v]$ and $[v, u]$. It follows that the simple chessboards are symmetric about the main diagonal. An illustration of the simple chessboard of a graph is in Figure 5.

If there is exactly one dot on each of the associate diagonals, then a simple chessboard will be called *graceful* as it clearly encodes a graceful graph. We can see a gracefully labelled graph and its graceful simple chessboard in Figure 6.

3 Sunlet graphs

Here we present new characterizations of sunlet graphs. We describe their graceful labellings via labelling sequences, labelling relations and simple graph chessboards. Our method is similar to that used in [5, Chapter 4].

Definition 3.1. ([7]) The **sunlet graph** is the graph on $2n$ vertices obtained by attaching n pendant edges to a cycle graph C_n . We will denote it by SG_n .

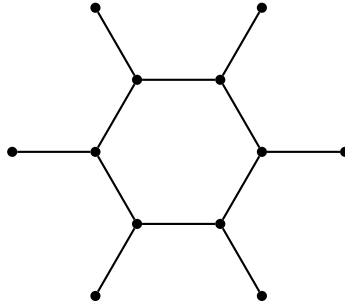


Figure 7. The sunlet graph SG_6

In Figure 7 we see the sunlet graph SG_6 . These graphs are known to be graceful since 1979 due to Roberto Frucht [1]. In this paper the author called these graphs as *coronas*, in the book [2] they are also called *crown graphs*. We will use the name *sunlet graphs*. We shall describe graceful labellings of these graphs via labelling sequences, labelling relations and simple chessboards. We distinguish four subclasses of sunlet graphs according to the length of their cycle: $n \equiv 0 \pmod{4}$, $n \equiv 1 \pmod{4}$, $n \equiv 2 \pmod{4}$ and $n \equiv 3 \pmod{4}$. All four cases have something in common, yet they are different in details.

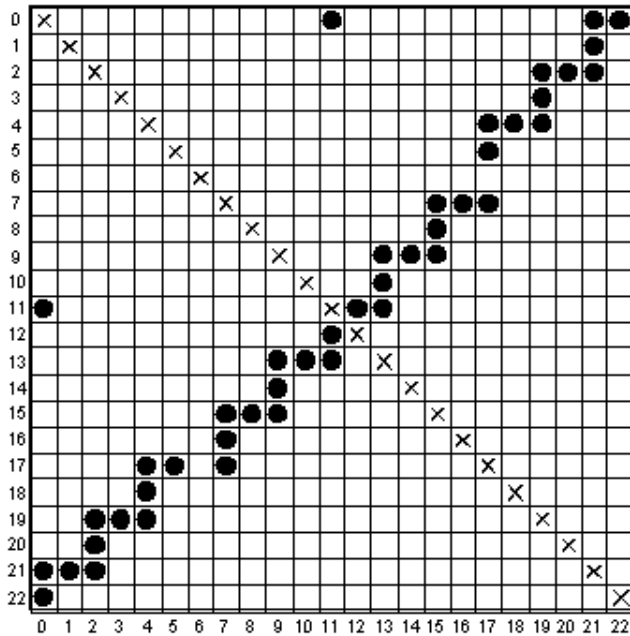
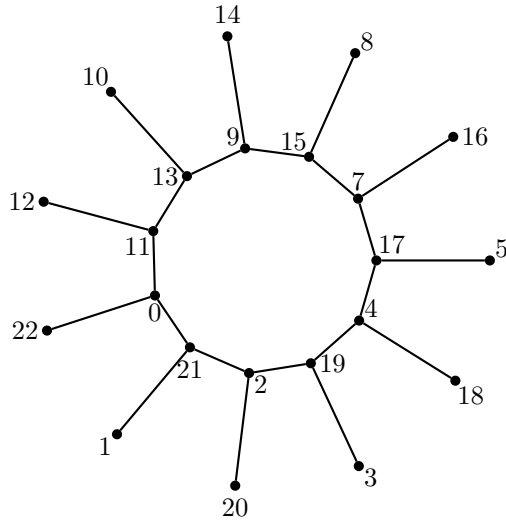
Before presenting our descriptions of sunlet graphs via simple chessboards, labelling sequences and labelling relations, we illustrate these descriptions on an example.

Example 3.2. The sequence $(11, 11, 10, 9, 9, 9, 8, 7, 7, 7, 0, 5, 4, 4, 4, 3, 2, 2, 2, 1, 0, 0)$ is a labelling sequence of the sunlet fan graph SG_n of size m where we have $n = 11$ and $m = 22$. Corresponding graph diagram, labelling relation and graph chessboard are in Figure 8. We can divide this labelling sequence into three parts: the first cascade of the labelling sequence (from the number n to the number $\lfloor \frac{n}{2} \rfloor + 2$), number 0 and the second cascade (from the number $\lfloor \frac{n}{2} \rfloor$ to the number 0). So number zero is between two decreasing cascades of numbers.

As we see in Figure 8 in the simple chessboard below its main diagonal, these cascade parts of the labelling sequence (or these parts in the labelling relation) are represented by two decreasing cascade roads of dots in the chessboard (the beginning of the first one is on the first diagonal and the end of the second one is on the m -th diagonal). The number zero in the labelling sequence is represented by the isolated dot in the position $[n, 0]$ below its main diagonal in the graph chessboard.

Definition 3.3. The graph chessboard described in Example 3.2 will be called a **cascade graph chessboard of type 3**.

We see an example of a cascade graph chessboard of type 3 also in Figure 9 together with the corresponding graph diagram and the labelling relation. The corresponding labelling sequence is $(7, 7, 6, 5, 5, 5, 0, 3, 2, 2, 2, 1, 0, 0)$.



1	2	3	4	5	6	7	8	9	10	11
11	11	10	9	9	9	8	7	7	7	0
12	13	13	13	14	15	15	15	16	17	11
12	13	14	15	16	17	18	19	20	21	22
5	4	4	4	3	2	2	2	1	0	0
17	17	18	19	19	19	20	21	21	21	22

Figure 8. The representations of the sunlet graph SG_{11}

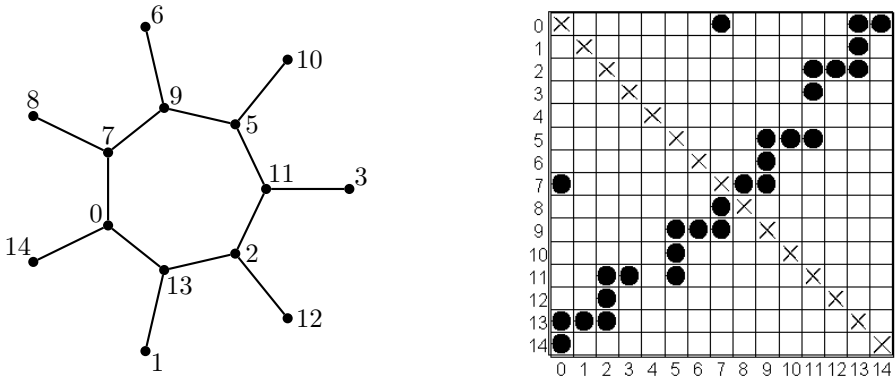


Figure 9. The representations of the sunlet graph SG_7

We prove our results only in the case $n \equiv 3 \pmod{4}$ that follows. In all other three cases we only formulate the results, their proofs can be done analogously. We illustrate each case on an example.

Theorem 3.4. Let G be a graph of size $m = 2n$ for $n \equiv 3 \pmod{4}$. Then the following are equivalent:

- (1) G is the sunlet graph SG_n .
- (2) There is a graceful labelling of G with a cascade graph chessboard of type 3.
- (3) There exists a labelling sequence $L = (j_1, j_2, \dots, j_m)$ of G such that

$$j_i = \begin{cases} n - 2 \lfloor \frac{i+1}{4} \rfloor, & \text{if } i \leq n - 1 \wedge i \equiv 0, 1, 2 \pmod{4}, \\ n + 1 - \lceil \frac{i}{2} \rceil, & \text{if } i \leq n - 1 \wedge i \equiv 3 \pmod{4}, \\ 0, & \text{if } i = n, \\ 2 \lceil \frac{i-2}{4} \rceil - (i \bmod n), & \text{if } i \geq n + 1 \wedge i \equiv 0, 1, 3 \pmod{4}, \\ n - \frac{i}{2}, & \text{if } i \geq n + 1 \wedge i \equiv 2 \pmod{4}. \end{cases} \quad (LSSG3)$$

- (4) There exists a labelling sequence L of G with labelling relation $A(L)$ of the form

$$\begin{aligned} & \{[n - 2 \lfloor \frac{i+1}{4} \rfloor, n - 2 \lfloor \frac{i+1}{4} \rfloor + i] \mid i \leq n - 1 \wedge i \equiv 0, 1, 2 \pmod{4}\} \cup \\ & \{[n + 1 - \lceil \frac{i}{2} \rceil, n + 1 - \lceil \frac{i}{2} \rceil + i] \mid i \leq n - 1 \wedge i \equiv 3 \pmod{4}\} \cup \\ & \{[0, n]\} \cup \{[2 \lceil \frac{i-2}{4} \rceil - i \pmod{n}, 2 \lceil \frac{i-2}{4} \rceil - i \pmod{n} + i] \mid \\ & i \geq n + 1 \wedge i \equiv 0, 1, 3 \pmod{4}\} \cup \\ & \{[n - \frac{i}{2}, n + \frac{i}{2}] \mid i \geq n + 1 \wedge i \equiv 2 \pmod{4}\}. \end{aligned}$$

Proof. (1) \Rightarrow (2) Let G be the sunlet fan graph SG_n of size $m = 2n$ for $n \equiv 3 \pmod{4}$. We label graph according to Frucht [1] and then we construct to G a simple graph chessboard of size m as a cascade graph chessboard of type 3. (We have seen an illustration of such cascade graph chessboard of type 3 for $n = 11$ in Figure 8 and for $n = 7$ in Figure 9.) The first cascade road of our constructed graph chessboard represents the part of the sunlet graph from the edge $\{m, 0\}$ anticlockwise to the edge $\{m - \lfloor \frac{n}{2} \rfloor, \lfloor \frac{n}{2} \rfloor\}$, where the dots of the road in which the direction is changing represent the edges in the cycle and the dots between these dots represent the pendant edges. In the same way this pattern is valid for the second cascade road, which represents the part of the sunlet graph from the edge $\{m - \lfloor \frac{n}{2} \rfloor, \lfloor \frac{n}{2} \rfloor + 2\}$ anticlockwise to the edge $\{n + 1, n\}$. The isolated dot, which represents the edge $\{n, 0\}$ in the cycle, connects these two cascade roads.

Hence we have been able to represent the edges of the given sunlet fan graph SG_n as the dots in a simple graph chessboard in the way that every diagonal of the chessboard contains exactly one dot. This determines a graceful labelling of the graph. We have showed (2).

(2) \Rightarrow (3) Assume we have a graceful labelling of G with a cascade graph chessboard of type 3. The first road in the chessboard starting on the first diagonal is represented in the corresponding labelling sequence by the members described in the first two cases of the formula (LSSG3). More specifically, the vertical columns of the dots of this road correspond to the integers j_i from the labelling sequence, which have the form $n - 2 \lfloor \frac{i+1}{4} \rfloor$ and the single dots connecting these vertical columns correspond to the integers j_i from the labelling sequence, which have the form $n + 1 - \lfloor \frac{i}{2} \rfloor$. The isolated dot corresponds to number 0 for $i = n$ in the labelling sequence. The second road then corresponds to the members described in the last two cases of the formula (LSSG3). More precisely, the vertical columns of the dots of this road correspond to the integers j_i from the labelling sequence, which have the form $2 \lfloor \frac{i-2}{4} \rfloor - (i \bmod n)$ and the single dots connecting these vertical columns correspond to the integers j_i from the labelling sequence, which have the form $n - \frac{i}{2}$.

Therefore the labelling sequence corresponding to the cascade graph chessboard of type 3 of G is given by the formula (LSSG3).

(3) \Rightarrow (4) Assume we have a labelling sequence of G which satisfies the formula (LSSG3). It can be seen that when we make the corresponding labelling relation $A(L)$, it has the form described in (4). Indeed, the non-negative integers j_i from the labelling sequence are gradually paired in the labelling relation $A(L)$ with the sums of the integers j_i with the numbers $1, 2, 3, \dots, 2n$. It follows that the integers j_i from the labelling sequence of the form $n - 2 \lfloor \frac{i+1}{4} \rfloor$ correspond to the pairs $\{[n - 2 \lfloor \frac{i+1}{4} \rfloor, n - 2 \lfloor \frac{i+1}{4} \rfloor + i] \mid i \leq n - 1 \wedge i \equiv 0, 1, 2 \pmod{4}\}$ in $A(L)$. The next j_i from the labelling sequence, which have the form $n + 1 - \lfloor \frac{i}{2} \rfloor$ correspond to the pairs $\{[n + 1 - \lfloor \frac{i}{2} \rfloor, n + 1 - \lfloor \frac{i}{2} \rfloor + i] \mid i \leq n - 1 \wedge i \equiv 3 \pmod{4}\}$. The number 0 from the labelling sequence corresponds to the pair $\{[0, n]\}$. The integers j_i from the labelling sequence, which have the form $2 \lfloor \frac{i-2}{4} \rfloor - (i \bmod n)$ correspond to the pairs $\{[2 \lfloor \frac{i-2}{4} \rfloor - (i \bmod n), 2 \lfloor \frac{i-2}{4} \rfloor - (i \bmod n) + i] \mid i \geq n + 1 \wedge i \equiv 0, 1, 3 \pmod{4}\}$. Finally, the integers j_i from the labelling sequence, which have the form $n - \frac{i}{2}$ correspond to the pairs $\{[n - \frac{i}{2}, n - \frac{i}{2} + i] \mid i \geq n + 1 \wedge i \equiv 2 \pmod{4}\}$ in $A(L)$.

(4) \Rightarrow (1) Let L be a labelling sequence of G with the labelling relation $A(L)$ of the form as in (4). We know that the edges of G are the pairs in $A(L)$. We explain this implication with a help of Example 3.2, where we can see in Figure 8 the table of the labelling relation satisfying our statement in (4). We shall look on the pairs in the labelling relation $A(L)$ as the edges of the graph G . In the first part of $A(L)$ ($i = 1, 2, \dots, n - 1$) we can note that the pairs on the even positions ($i = 2, 4, 6, \dots, n - 1$) as edges of G form a path, and

the pairs on the odd positions ($i = 1, 3, 5, \dots, n - 2$) correspond to the pendant edges of this path (see the graph diagram in Fig. 8). It holds the other way round for the second part of the relation $A(L)$. So the pairs on the odd positions as edges of G form a path, while the pairs on the even positions correspond to the pendant edges of this path. The edge $\{0, n\}$ connects the edges $\{n, n + 1\}$ and $\{0, m\}$, so it connects these two parts of the graph G , each of which is formed by a path with the pendant edges. We can also note that these two parts of the graph G have a common vertex because the expression $n - 2 \lfloor \frac{i+1}{4} \rfloor + i$ for $i = n - 1$ is equivalent to the expression $n - \lfloor \frac{i}{2} \rfloor + i$ for $i = n + 1$. (In Figure 8 it is the number 17.) It means that the paths of both parts of G are connected, so they form a cycle of length n in G . In this cycle every vertex has a pendant edge. So we get that the graph G is a sunlet graph SG_n . \square

We now present our result and its illustration by an example in the case $n \equiv 0 \pmod{4}$.

Example 3.5. The sequence $(8, 7, 7, 7, 6, 5, 5, 5, 0, 3, 2, 2, 2, 1, 0, 0)$ is a labelling sequence of the sunlet fan graph SG_8 of size 16. Corresponding graph diagram, labelling relation and graph chessboard are in Figure 10. We can note that this labelling sequence has an analogous structure as the labelling sequence for the graph SG_{11} in Figure 8 and so it consists of two decreasing cascades of numbers and the number 0 between them. The structure of the labelling sequence is different only in small detail that the first cascade of numbers in this case starts by single n followed by the triplet of numbers $n - 1$, and it does not start by two occurrences of n as in the previous case $n \equiv 3 \pmod{4}$.

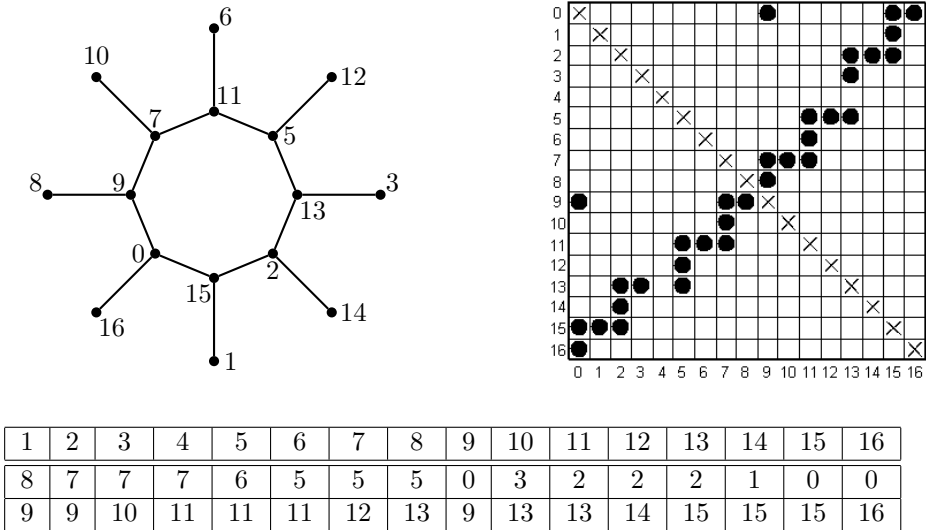


Figure 10. The representations of the sunlet graph SG_8

Definition 3.6. The graph chessboard with pattern as in Figure 10 will be called a **cascade graph chessboard of type 0**.

Theorem 3.7. Let G be a graph of size $m = 2n$ for $n \equiv 0 \pmod{4}$. Then the following are equivalent:

- (1) G is the sunlet graph SG_n .

- (2) There is a graceful labelling of G with a cascade graph chessboard of type 0.
- (3) There exists a labelling sequence $L = (j_1, j_2, \dots, j_m)$ of G such that

$$j_i = \begin{cases} n + 1 - 2 \lfloor \frac{i+3}{4} \rfloor, & \text{if } i \leq n \wedge i \equiv 0, 2, 3 \pmod{4}, \\ n - \lfloor \frac{i}{2} \rfloor, & \text{if } i \leq n \wedge i \equiv 1 \pmod{4}, \\ 0, & \text{if } i = n + 1, \\ 2 \lfloor \frac{i}{4} \rfloor - (i \bmod n) - 1, & \text{if } i \geq n + 2 \wedge i \equiv 1, 2, 3 \pmod{4}, \\ n - \frac{i}{2}, & \text{if } i \geq n + 2 \wedge i \equiv 0 \pmod{4}. \end{cases} \quad (LSSG0)$$

- (4) There exists a labelling sequence L of G with labelling relation $A(L)$ of the form

$$\begin{aligned} & \{[n + 1 - 2 \lfloor \frac{i+3}{4} \rfloor, n + 1 - 2 \lfloor \frac{i+3}{4} \rfloor + i] \mid i \leq n \wedge i \equiv 0, 2, 3 \pmod{4}\} \cup \\ & \{[n - \lfloor \frac{i}{2} \rfloor, n - \lfloor \frac{i}{2} \rfloor + i] \mid i \leq n \wedge i \equiv 1 \pmod{4}\} \cup \{[0, n + 1]\} \cup \\ & \{[2 \lfloor \frac{i}{4} \rfloor - i \pmod{n} - 1, 2 \lfloor \frac{i}{4} \rfloor - i \pmod{n} - 1 + i] \mid \\ & i \geq n + 2 \wedge i \equiv 1, 2, 3 \pmod{4}\} \cup \\ & \{[n - \frac{i}{2}, n + \frac{i}{2}] \mid i \geq n + 2 \wedge i \equiv 0 \pmod{4}\}. \end{aligned}$$

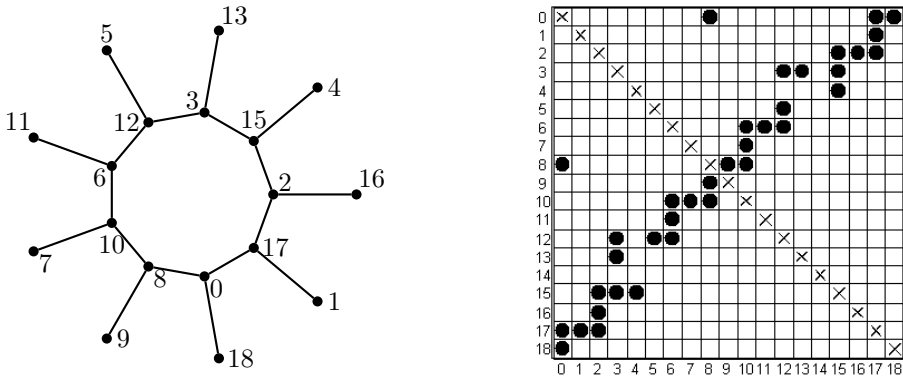
We now present our result and its illustration by an example in the case $n \equiv 1 \pmod{4}$.

Example 3.8. The sequence $(8, 8, 7, 6, 6, 6, 5, 0, 3, 3, 4, 3, 2, 2, 2, 1, 0, 0)$ is a labelling sequence of the sunlet fan graph SG_9 of size 18. Corresponding graph diagram, labelling relation and graph chessboard are in Figure 11. Unlike the first two cases, there is not only number 0 between two decreasing cascades of numbers, but there is also pair of integers, which are not part of two cascades. It is better seen in the chessboard. Therefore one more formula describing these two numbers is added in the third condition of Theorem 3.10. The structure of the labelling sequence is different compared to the previous case in small detail again. The first cascade of numbers starts by pair of integers $n - 1$ and ends by single integer $\lfloor \frac{n}{2} \rfloor$. The second cascade of numbers has the same form for all four cases.

Definition 3.9. The graph chessboard with pattern as in Figure 11 will be called a **cascade graph chessboard of type 1**.

Theorem 3.10. Let G be a graph of size $m = 2n$ for $n \equiv 1 \pmod{4}$. Then the following are equivalent:

- (1) G is the sunlet fan graph SG_n .
- (2) There is a graceful labelling of G with a cascade graph chessboard of type 1.



1	2	3	4	5	6	7	8	9	10	11	12	13	14	15	16	17	18
8	8	7	6	6	6	5	0	3	3	4	3	2	2	2	1	0	0
9	10	10	10	11	12	12	8	12	13	15	15	15	16	17	17	17	18

Figure 11. The representations of the sunlet graph SG_9

(3) There exists a labelling sequence $L = (j_1, j_2, \dots, j_m)$ of G such that

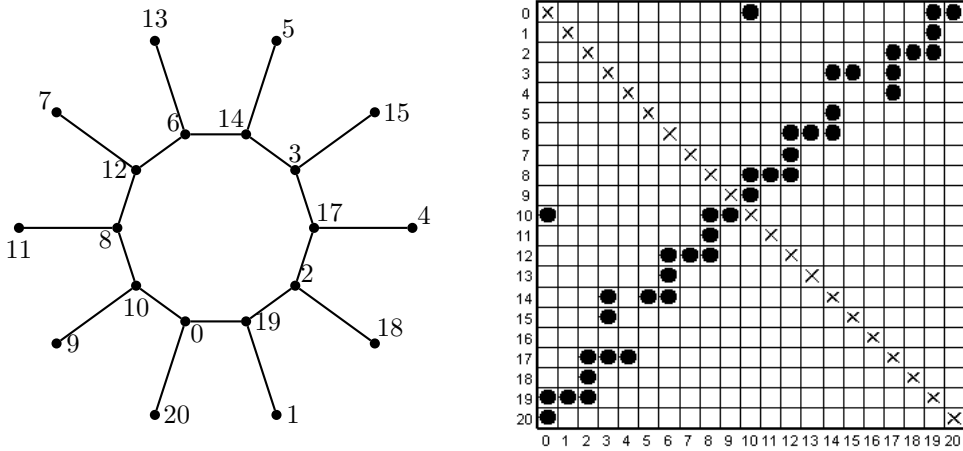
$$j_i = \begin{cases} n - 1 - 2 \lfloor \frac{i+1}{4} \rfloor, & \text{if } i \leq n - 2 \wedge i \equiv 0, 1, 2 \pmod{4}, \\ n - \lfloor \frac{i}{2} \rfloor, & \text{if } i \leq n - 2 \wedge i \equiv 3 \pmod{4}, \\ 0, & \text{if } i = n - 1, \\ n - 2 - 2 \lfloor \frac{i+1}{4} \rfloor, & \text{if } i = n, n + 1, \\ 2 \lfloor \frac{i-2}{4} \rfloor - (i \bmod n), & \text{if } i \geq n + 2 \wedge i \equiv 0, 1, 3 \pmod{4}, \\ n - \frac{i}{2}, & \text{if } i \geq n + 2 \wedge i \equiv 2 \pmod{4}. \end{cases} \quad (LSSG1)$$

(4) There exists a labelling sequence L of G with labelling relation $A(L)$ of the form

$$\begin{aligned} & \{ [n - 1 - 2 \lfloor \frac{i+1}{4} \rfloor, n - 1 - 2 \lfloor \frac{i+1}{4} \rfloor + i] \mid i \leq n - 2 \wedge i \equiv 0, 1, 2 \pmod{4} \} \cup \\ & \{ [n - \lfloor \frac{i}{2} \rfloor, n - \lfloor \frac{i}{2} \rfloor + i] \mid i \leq n - 2 \wedge i \equiv 3 \pmod{4} \} \cup \{ [0, n + 1] \} \cup \\ & \{ [n - 2 - 2 \lfloor \frac{i+1}{4} \rfloor, n - 2 - 2 \lfloor \frac{i+1}{4} \rfloor + i] \mid i = n, n + 1 \} \cup \\ & \{ [2 \lfloor \frac{i-2}{4} \rfloor - i \pmod{n}, 2 \lfloor \frac{i-2}{4} \rfloor - i \pmod{n} + i] \mid \\ & i \geq n + 2 \wedge i \equiv 0, 1, 3 \pmod{4} \} \cup \\ & \{ [n - \frac{i}{2}, n + \frac{i}{2}] \mid i \geq n + 2 \wedge i \equiv 2 \pmod{4} \}. \end{aligned}$$

Example 3.11. The sequence $(9, 8, 8, 8, 7, 6, 6, 6, 5, 0, 3, 3, 4, 3, 2, 2, 2, 1, 0, 0)$ is a labelling sequence of the sunlet fan graph SG_{10} of size 20. Corresponding graph diagram, labelling relation and graph chessboard are in Figure 12. A form of the labelling sequence for this case is very similar to the form of the labelling sequence in the previous case. They are

different only in the first cascade of numbers. Here it starts by a single integer followed by a triplet of the same integers.



1	2	3	4	5	6	7	8	9	10
9	8	8	8	7	6	6	6	5	0
10	10	11	12	12	12	13	14	14	10

11	12	13	14	15	16	17	18	19	20
3	3	4	3	2	2	2	1	0	0
14	15	17	17	17	18	19	19	19	20

Figure 12. The representations of the sunlet graph SG_{10}

Definition 3.12. The graph chessboard with pattern as in Figure 12 will be called a **cascade graph chessboard of type 2**.

Theorem 3.13. Let G be a graph of size $m = 2n$ for $n \equiv 2 \pmod{4}$. Then the following are equivalent:

- (1) G is the sunlet fan graph SG_n .
- (2) There is a graceful labelling of G with a cascade graph chessboard of type 2.
- (3) There exists a labelling sequence $L = (j_1, j_2, \dots, j_m)$ of G such that

$$j_i = \begin{cases} n - 2 \lfloor \frac{i+3}{4} \rfloor, & \text{if } i \leq n - 1 \wedge i \equiv 0, 2, 3 \pmod{4}, \\ n - \frac{i+1}{2}, & \text{if } i \leq n - 1 \wedge i \equiv 1 \pmod{4}, \\ 0, & \text{if } i = n, \\ n - 1 - 2 \lfloor \frac{i+3}{4} \rfloor, & \text{if } i = n + 1, n + 2, \\ 2 \lfloor \frac{i}{4} \rfloor - (i \bmod n) - 1, & \text{if } i \geq n + 3 \wedge i \equiv 1, 2, 3 \pmod{4}, \\ n - \frac{i}{2}, & \text{if } i \geq n + 3 \wedge i \equiv 0 \pmod{4}. \end{cases} \tag{LSSG2}$$

(4) There exists a labelling sequence L of G with labelling relation $A(L)$ of the form

$$\begin{aligned} & \{[n-2 \lfloor \frac{i+3}{4} \rfloor, n-2 \lfloor \frac{i+3}{4} \rfloor + i] \mid i \leq n-1 \wedge i \equiv 0, 2, 3 \pmod{4}\} \cup \\ & \{[n - \frac{i+1}{2}, n - \frac{i+1}{2} + i] \mid i \leq n-1 \wedge i \equiv 1 \pmod{4}\} \cup \{[0, n]\} \cup \\ & \{[n-1-2 \lfloor \frac{i+3}{4} \rfloor, n-1-2 \lfloor \frac{i+3}{4} \rfloor + i] \mid i = n+1, n+2\} \cup \\ & \{[2 \lceil \frac{i}{4} \rceil - (i \bmod n) - 1, 2 \lceil \frac{i}{4} \rceil - (i \bmod n) - 1 + i] \mid \\ & i \geq n+3 \wedge i \equiv 1, 2, 3 \pmod{4}\} \cup \\ & \{[n - \frac{i}{2}, n + \frac{i}{2}] \mid i \geq n+3 \wedge i \equiv 0 \pmod{4}\}. \end{aligned}$$

4 Wheels

In this section we shall show our method in class of graphs, which are called *wheels*.

Definition 4.1. A **wheel graph** (or shortly a **wheel**) is a graph obtained by connecting a single vertex to all vertices of a cycle. We will denote the wheel consisting of n vertices and $2(n-1)$ edges by W_n .

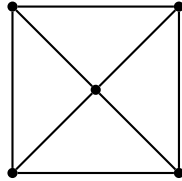


Figure 13. The wheel graph W_5

Some authors use the symbol W_n to denote the wheel with $n+1$ vertices, but we will use the above defined notation in this text. In Figure 13 we can see the wheel graph W_5 . We will distinguish two cases of wheels for even n and odd n . For both cases we describe graceful labelling via example and theorem. We use graceful labelling from Frucht [1] from 1979 for our methods. The proof of the theorem will be presented only for even n , because for odd n it can be done analogously.

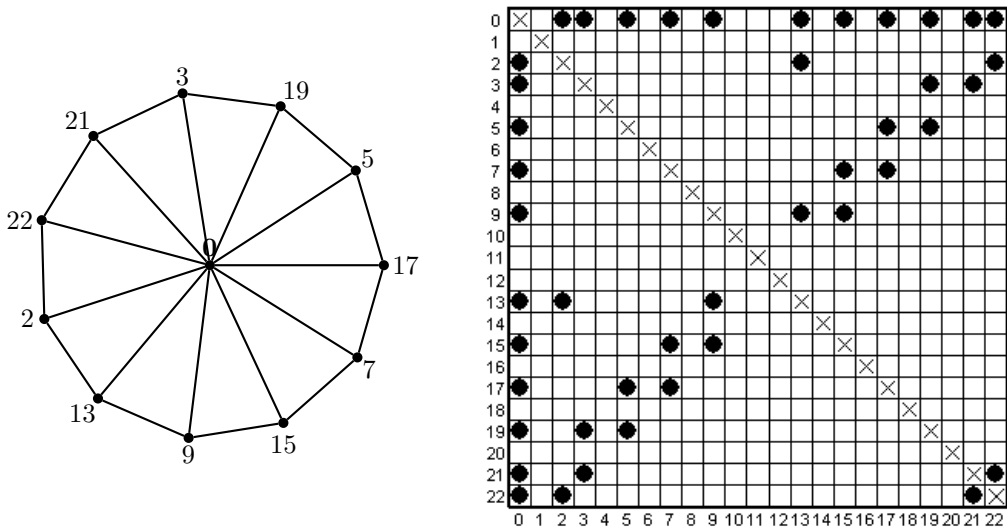
Now in an example we shall show and describe the labelling sequence for the wheel SG_{12} , which corresponds to graceful labelling of this graph. We explain here the pattern of graceful labelling for wheels with even n .

Example 4.2. The sequence $(21, 0, 0, 9, 0, 9, 0, 7, 0, 7, 2, 5, 0, 5, 0, 3, 0, 3, 0, 2, 0, 0)$ is a labelling sequence of the wheel graph SG_n of size m where we have $n = 12$ and $m = 22$.

Corresponding graph diagram, labelling relation and graph chessboard are in Figure 14.

We can divide this labelling sequence into three parts: the first triplet of numbers $(m-1, 0, 0)$, “regular sequence with exception”, and the last triplet of numbers $(2, 0, 0)$. The regular sequence with exception is the following sequence of numbers:

$$(n-3, 0, n-3, 0, n-1, 0, n-1, 0, \dots, 3, 0, 3, 0),$$



1	2	3	4	5	6	7	8	9	10	11
21	0	0	9	0	9	0	7	0	7	2
22	2	3	13	5	15	7	15	9	17	13

12	13	14	15	16	17	18	19	20	21	22
5	0	5	0	3	0	3	0	2	0	0
17	13	19	15	19	17	21	21	22	21	22

Figure 14. The representations of the wheel graph W_{12}

in our case

$$(9, 0, 9, 0, 7, 0, 7, 2, 5, 0, 5, 0, 3, 0, 3, 0),$$

where the exception is on the position $i = n - 1$ of the labelling sequence (the position $i = n - 4$ of the “regular sequence with exception”): here the number 0 would be expected by the pattern of this sequence, but we can see the number 2 instead 0 there.

As we see in Figure 14 in the simple chessboard below its main diagonal, the dots in the first column of the chessboard represent the $(n - 1)$ zeros in the labelling sequence. Numbers $(m - 1)$ and 2 from the first and the last triplet of numbers are represented by the dots in m -th row. Other dots in the chessboard are the dots “creating steps” which start on the position with coordinates $[m - 1, 3]$. They represent the regular sequence. The exception - number 2 - is represented by the dot, which is out of steps on the position with coordinates $[n + 1, 2]$.

In Figure 14 we can also note a pattern of the graceful labelling in the wheel graph W_{12} . The central vertex connected to all vertices of the cycle is always labelled by 0. Then let number 21 be on the first position in the cycle, number 3 on the second and we proceed clockwise using the following pattern: on the positions 1, 3, 5, 7, 9 are numbers 21, 19, 17, 15, 13 while on the positions 2, 4, 6, 8 are numbers 3, 5, 7, 9. The remaining vertices are labelled by m (in this case 22) and by 2.

Definition 4.3. The labelling sequence described in Example 4.2 will be called an **even wheel labelling sequence** and the graph chessboard described in Example 4.2 will be

called an **even wheel graph chessboard**.

Theorem 4.4. Let G be a graph of size $m = 2(n - 1)$ for even $n \geq 4$. Then the following are equivalent:

- (1) G is the wheel graph W_n .
- (2) There is a graceful labelling of G with an even wheel graph chessboard.
- (3) There exists an even wheel labelling sequence L of G with corresponding labelling relation $A(L)$.

Proof. (1) \Rightarrow (2) Let G be the wheel graph W_n . We shall label our graph according to labelling from Frucht [1], which is graceful and we construct an even wheel graph chessboard (see Figure 14). Let the central vertex of our graph with degree $n - 1$ be labelled by 0. The vertices of the cycle in our graph will be labelled in the following way. We start to label the graph with an arbitrary vertex of the cycle because the positions of all vertices of the cycle are equal. So we label any vertex of the cycle by $(m - 1)$. We will say that the vertex with labelling $(m - 1)$ is on the first position in the cycle and other vertices in the clockwise direction from this vertex have positions 2, 3, 4, ... up to $(n - 1)$. Then the vertices on the positions 3, 5, 7, ..., $n - 3$ are labelled gradually by numbers $m - 3, m - 5, m - 7, \dots, m - (n - 3)$. The vertices on the positions 2, 4, 6, ..., $n - 4$ are labelled gradually by numbers 3, 5, 7, ..., $n - 3$. Two unlabelled vertices remain. The vertex, which is adjacent to the vertex with labelling $m - 1$ will be labelled by m and the vertex, which is adjacent to the vertex with labelling $n - 3$ will be labelled by 2. Now our labelling is done and we shall show that the corresponding graph chessboard of this labelling is an even wheel graph chessboard.

There are $(n - 1)$ dots in the first column of the chessboard, which represent all edges connected to the central vertex. The dots creating the increasing steps in the chessboard together with the three dots out of the steps with coordinates $[n + 1, 2]$, $[m, 2]$, $[m, m - 1]$ represent the cycle in the graph. Hence we get an even wheel graph chessboard (see Figure 14). Since each diagonal of the chessboard contains exactly one dot, this confirms that the applied labelling is graceful.

(2) \Rightarrow (3) Assume we have a graceful labelling of the graph G with an even wheel graph chessboard. The dots which are on the positions with coordinates $[m, m - 1]$, $[2, 0]$, $[3, 0]$ are represented in the corresponding labelling sequence by numbers $(m - 1, 0, 0)$, what is the first triplet in the even wheel labelling sequence. The dots which create the increasing steps and start on the position with coordinates $[m - 1, 3]$, together with the dots in the first column of the chessboard excepting the first two and the last two dots of this column, and the dot with coordinates $[n + 1, 2]$ are represented in the labelling sequence by the sequence $(n - 3, 0, n - 3, 0, n - 1, 0, n - 1, 0, \dots, 3, 0, 3, 0)$, what is exactly the regular sequence with exception (see the description of the labelling sequence in Example 4.2). The last dots with coordinates $[m, 2]$, $[m - 1, 0]$, $[m, 0]$ are represented in the labelling sequence by the numbers $(2, 0, 0)$, what represents the last triplet in the even wheel labelling sequence.

(3) \Rightarrow (1) Let L be an even wheel labelling sequence with corresponding labelling relation $A(L)$. We shall verify that corresponding graph G to this labelling sequence is the wheel graph W_n . The wheel graph connects in a certain natural way a star S_{n-1} and a cycle with $(n - 1)$ edges. When we look at our labelling sequence L (for example in Fig. 14), we can find there exactly $(n - 1)$ zeros. It means that the pairs containing zero in the corresponding labelling relation represent the star S_{n-1} . Other pairs represent the cycle. Indeed, consider the pair $(m - 1, m)$ in $A(L)$. In the relation $A(L)$ there are also the

pairs $(m - 1, 3)$, $(3, m - 3)$, etc., and this way we get back to the pair $(m - 1, m)$. So we get in G the cycle with $(n - 1)$ edges. Every vertex in the cycle is also connected with the vertex labelled by zero. Hence we get the wheel graph W_n . \square

Now we present an example and the theorem for the wheels with odd n .

Example 4.5. The sequence $(0, 0, 0, 9, 0, 9, 0, 7, 0, 7, 2, 5, 0, 5, 0, 3, 0, 3, 0, 1, 0, 2, 1, 0)$ is the labelling sequence of the wheel graph W_n of size m where we have odd $n = 13$ and $m = 24$. Corresponding graph diagram, labelling relation and graph chessboard are in Figure 15. We can divide this labelling sequence also into three parts: the first triplet

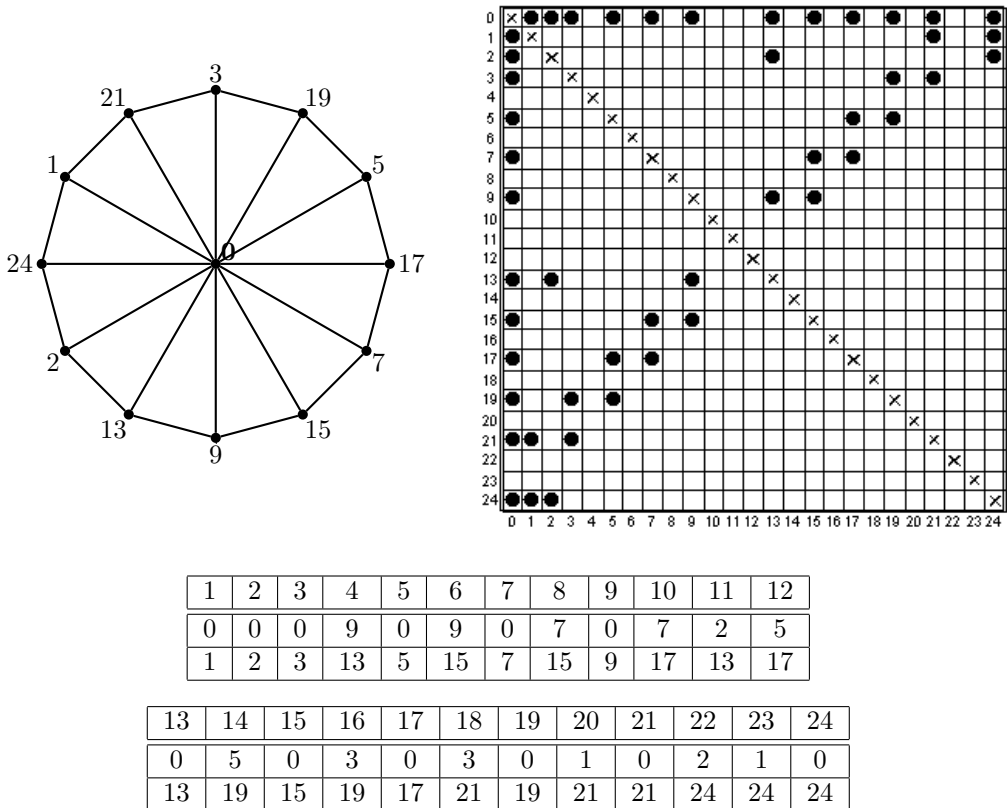


Figure 15. The representations of the wheel graph W_{13}

of zeros, regular sequence with exception and the last triplet of numbers $(2, 1, 0)$. The regular sequence with exception is the following sequence of numbers: $(m - 3, 0, m - 3, 0, m - 1, 0, m - 1, 0, \dots, 3, 0, 3, 0, 1, 0)$. So a small difference in the regular sequence with exception, compared to the previous case, is in adding the numbers 1 and 0 to the end of this sequence.

As we see in Figure 15 in the simple chessboard below its main diagonal, the zeros in the labelling sequence are represented by the dots in the first column of the chessboard. Numbers 1 and 2 from the last triplet of numbers are represented by the dots in the $(m + 1)$ -th row. Other dots in the chessboard are the dots in the “increasing steps”, which start on the position with coordinates $(m - 1, 3)$. They represent the regular

sequence. The exception - number 2 - is represented by the dot, which is out of the steps on the position $(n + 1, 2)$.

In Figure 15 we can also note the pattern of graceful labelling in the wheel graph W_{13} . The central vertex connected to all vertices of the cycle is always labelled by 0. Then let number 1 is on the first position in the cycle, number 21 on the second and we continue in the clockwise direction: so on the positions 1, 3, 5, 7, 9 are numbers 1, 3, 5, 7, 9 and on the positions 2, 4, 6, 8, 10 are numbers 21, 19, 17, 15, 13. Remaining vertices are labelled by m (in this case 24) and by 2.

Definition 4.6. The labelling sequence described in Example 4.5 will be called an **odd wheel labelling sequence** and the graph chessboard described in Example 4.5 will be called an **odd wheel graph chessboard**.

Theorem 4.7. Let G be a graph of size $m = 2(n - 1)$ for odd $n \geq 5$. Then the following are equivalent:

- (1) G is the wheel graph W_n .
- (2) There is a graceful labelling of G with an odd wheel graph chessboard.
- (3) There exists an odd labelling sequence L of G with corresponding labelling relation $A(L)$.

Proof. Analogous as the proof of Theorem 4.4. □

References

- [1] R. Frucht, Graceful numbering of wheels and related graphs, *Universidad Técnica Federico Santa María Casilla, 110-V*, Valparaíso, Chile, 1979.
- [2] J.A. Gallian, *A Dynamic Survey of Graph Labeling*, The Electronic Journal of Combinatorics DS6 (Twenty-first edition published December 21, 2018).
- [3] M. Gardner, *Mathematical Games: The graceful graphs of Solomon Golomb*, Sci. Am. **226** (1972), 108-112.
- [4] S.W. Golomb, How to number a graph. In: *R.C. Read (eds.) Graph Theory and Computing*. Academic Press, New York (1972), 23-37.
- [5] M. Haviar and M. Ivaška, *Vertex Labellings of Simple Graphs*, Research and Exposition in Mathematics, Vol. 34, Heldermann-Verlag, Lemgo, Germany (2015).
- [6] M. Ivaška, *Chessboard Representations and Computer Programs for Graceful Labelings of Trees*, Student Competition ŠVOČ, Matej Bel University, Banská Bystrica (2009).
- [7] Linfan MAO, *Mathematical combinatorics (International book series)*, The Madis of Chinese Academy of Sciences and Academy of Mathematical Combinatorics, USA (2016), 115-122.
- [8] J. Matoušek and J. Nešetřil, *Invitation to Discrete Mathematics*, Oxford University Press (2008).
- [9] A. Rosa, *O cyklických rozkladoch kompletneho grafu*, Kandidátska dizertačná práca, Československá akadémia vied, Bratislava (1965).
- [10] A. Rosa, On certain valuations of the vertices of a graph, *Theory of Graphs (Internat. Symposium, Rome, July 1966)*, Gordon and Breach, N. Y. and Dunod Paris (1967), 349-355.
- [11] D.A. Sheppard, The factorial representation of major balanced labelled graphs, *Discrete Math.* **15** (1976), 379-388.

A k -dimensional systems of fractional neutral functional differential equations involving ψ -Caputo fractional derivative

M. S. Shabna

Department of Mathematics, MES Mampad College, Malappuram, Kerala, India
shabnasaidh@gmail.com

M. C. Ranjini

Department of Mathematics, MES Mampad College, Malappuram, Kerala, India
ranjiniprasad@gmail.com

Abstract

This paper is devoted to the study of the initial value problem for a class of k -dimensional systems of fractional neutral functional differential equations involving ψ -Caputo fractional derivative with respect to another function. Existence and uniqueness results for the problem are established by means of some standard fixed point theorems. Finally, we give an example to demonstrate our results.

Received 09 November 2019

Accepted in final form March 24, 2020

Communicated with Víctor Jiménez López.

Keywords fractional neutral differential equations, ψ -Caputo fractional derivative, existence, bounded delay.

MSC(2010) 26A33, 34A08, 34A12.

1 Introduction

Fractional calculus is a branch of mathematics which deals with non-integer order integrals and derivatives. Though the fractional calculus developed as a pure mathematical idea, now it has tremendous applications. Viscoelasticity, electro magnetism, electrical circuits, sound propagation, lateral and longitudinal control, fluid mechanics, edge detection, cardiac tissue electrode interface, earth system dynamics are some of them [1, 2, 3, 4, 5, 6]. There are numerous definitions for fractional derivatives and integrals. Nowadays many studies are being done in generalised fractional operators [1, 2], [7, 8, 9, 10, 11]. Recently, Almeida [8] used the idea of the fractional derivative in the Caputo sense to propose a new generalized fractional differential operator called ψ -Caputo fractional derivative with respect to another function ψ . There are many studies on the existence and uniqueness of different fractional differential equations involving ψ -Caputo fractional differential and integral operators [8, 18, 19]. Neutral differential equations have importance in many areas of applied Mathematics [12, 13, 14, 15, 16, 17].

The aim of this paper is to investigate the existence and uniqueness of solutions of Initial Value Problem for a class of k -dimensional systems of fractional neutral functional differential equation with bounded delay involving the Caputo-type fractional derivative of a function x with respect to another function ψ .

$$\begin{cases} {}^C D_{t_0}^{\alpha_1, \psi}(x_1(t) - g_1(t, x_t)) &= f_1(t, x_t), \\ {}^C D_{t_0}^{\alpha_2, \psi}(x_2(t) - g_2(t, x_t)) &= f_2(t, x_t), \\ \vdots & \\ {}^C D_{t_0}^{\alpha_k, \psi}(x_k(t) - g_k(t, x_t)) &= f_k(t, x_t), \end{cases} \quad (1.1)$$

$$x_{1t_0} = \phi_1, \quad x_{2t_0} = \phi_2, \quad \dots, \quad x_{kt_0} = \phi_k,$$

where $a, r \in \mathbb{R}^+$, $t_0 \geq 0$ and $t \in (t_0, \infty)$, $0 < \alpha_i < 1$, for $i = 1, 2, \dots, k$. ${}^C D_{t_0}^{\alpha_i, \psi}$ is the Caputo-type fractional derivative of a function x_i with respect to another function ψ .

$f_i, g_i : ([t_0, \infty) \times C([-r, 0], \mathbb{R}^n) \times C([-r, 0], \mathbb{R}^n) \times \dots \times C([-r, 0], \mathbb{R}^n)) \rightarrow \mathbb{R}^n$, $i = 1, 2, \dots, k$ are \mathbb{R}^n -valued functions satisfying certain assumptions, which will be mentioned later. Consider $x_{it} = (x_{1t}, x_{2t}, \dots, x_{kt}) \in \mathbb{R}^n$ and $\phi_i \in C([-r, 0], \mathbb{R}^n)$ for $i = 1, 2, \dots, k$. If $x_i \in C([t_0 - r, t_0 + a], \mathbb{R}^n)$ define x_{it} by $x_{it}(\theta) = x_i(t + \theta)$ for $\theta \in [-r, 0]$, for any $t \in [t_0, t_0 + a]$. Let $\psi \in C^n[t_0, \infty)$ be a continuous increasing function such that $\psi'(x) \neq 0$, $\forall x \in [t_0, \infty)$.

In this paper, the first section deals with the introduction about the ψ -Caputo fractional differential equations and the problem is also given. In the second section we present essential definitions and results and in the third section we prove the existence and uniqueness results of the *IVP*(1.1) by means of Krasnoselskii's and Banach's fixed point theorems. In the last section, we give an example to demonstrate our results.

2 Preliminaries

Here we deal with fractional derivatives and fractional integrals with respect to another function.

Definition 1. [1] Let $\alpha > 0$, $I = [a, b]$ be a finite or infinite interval, f an integrable function defined on I and $\psi \in C^n(I)$ an increasing function such that $\psi'(t) \neq 0$, $\forall t \in I$. Fractional integrals and fractional derivatives of a function f with respect to another function ψ are defined as

$$I_a^{\alpha, \psi} f(t) = \frac{1}{\Gamma(\alpha)} \int_a^t \psi'(s) [\psi(t) - \psi(s)]^{\alpha-1} f(s) ds$$

and

$$\begin{aligned} D_a^{\alpha, \psi} f(t) &= \left[\frac{1}{\psi'(t)} \frac{d}{dt} \right]^n I_{a+}^{n-\alpha, \psi} f(t) \\ &= \frac{1}{\Gamma(n-\alpha)} \left[\frac{1}{\psi'(t)} \frac{d}{dt} \right]^n \int_a^t \psi'(s) [\psi(t) - \psi(s)]^{n-\alpha-1} f(s) ds \end{aligned}$$

where $n = [\alpha] + 1$.

For different choices of the function ψ , we get the Riemann-Liouville, the Hadamard and the Erdélyi-Kober fractional derivatives and fractional integrals, etc.

Definition 2. [8] Let $\alpha > 0$, $n \in \mathbb{N}$, I be the interval $-\infty \leq a < b \leq \infty$, $f, \psi \in C^{(n)}(I)$ be two functions such that ψ is increasing and $\psi'(t) \neq 0 \quad \forall x \in I$. Then the ψ -Caputo fractional derivative of f of order α is given by

$${}^C D_a^{\alpha, \psi} f(t) = I_a^{n-\alpha, \psi} \left[\frac{1}{\psi'(t)} \frac{d}{dt} \right]^n f(t)$$

where $n = [\alpha] + 1$ for $\alpha \notin \mathbb{N}$ and $n = \alpha$ for $\alpha \in \mathbb{N}$.

To simplify the notation, we are using the abbreviated symbol

$$f_{\psi}^{[n]} f(t) = \left[\frac{1}{\psi'(t)} \frac{d}{dt} \right]^n f(t)$$

From the definition it is clear that, given $\alpha = m \in \mathbb{N}$, ${}^C D_a^{\alpha, \psi} f(t) = f_{\psi}^{[m]}(t)$ and if $\alpha \notin \mathbb{N}$, then

$${}^C D_a^{\alpha, \psi} f(t) = \frac{1}{\Gamma(n - \alpha)} \int_a^t \psi'(s) [\psi(t) - \psi(s)]^{n-\alpha-1} f_{\psi}^{[n]}(s) ds$$

In particular, if $0 < \alpha < 1$

$${}^C D_a^{\alpha, \psi} f(t) = \frac{1}{\Gamma(1 - \alpha)} \int_a^t [\psi(t) - \psi(s)]^{-\alpha} f'(s) ds$$

Lemma 3. [8, 18, 19] Given a function $f \in C^n[a, b]$ and order $\alpha > 0$, we have for $n = [\alpha] + 1$:

$${}^C D_a^{\alpha, \psi} f(t) = D_a^{\alpha, \psi} \left[f(t) - \sum_{k=0}^{n-1} \frac{f_{\psi}^{[k]}(a)}{k!} [\psi(t) - \psi(a)]^k f_{\psi}^{[k]}(a) \right]$$

$$I_a^{\alpha, \psi} {}^C D_a^{\alpha, \psi} f(t) = f(t) - \sum_{k=0}^{n-1} \frac{f_{\psi}^{[k]}(a)}{k!} [\psi(x) - \psi(a)]^k$$

Also $I_a^{\alpha, \psi} {}^C D_a^{\alpha, \psi} f(t) = f(t) - f(a)$, if $0 < \alpha < 1$.

Lemma 4. (Krasnoselskii's Fixed Point Theorem)[20]

Let X be a Banach space, let E be a bounded closed convex subset of X and let S, U be maps of E into X such that $Sx + Uy \in E$ for every pair $x, y \in E$. If S is a contraction and U is completely continuous, then the equation $Sx + Ux = x$ has a solution on E .

Lemma 5. (Banach's Fixed Point Theorem)

Let (X, d) be a non-empty complete metric space with a contraction mapping $T : X \rightarrow X$. Then T admits a unique fixed point x^* in X .

Let $I \subset \mathbb{R}$ be any interval and $X = C(I, \mathbb{R}^n)$ with the norm $\|x\| = \sup_{t \in I} |x(t)|$, where $|\cdot|$ as a suitable complete norm on \mathbb{R}^n . Let $(X^k = \underbrace{X \times X \times \cdots \times X}_k, \|\cdot\|_*)$, where $\|(x_1, x_2, \dots, x_k)\|_* = \max\{\|x_1\|, \|x_2\|, \dots, \|x_k\|\}$ is the norm on the corresponding product Banach space X^k .

3 Main Results

Consider the Initial Value Problem (1.1). Let δ and $\gamma \in \mathbb{R}$ be positive constants, $I_0 = [t_0, t_0 + \delta]$ and

$$A(\delta, \gamma) = \{(x_1, x_2, \dots, x_k) : x_{i_{t_0}} = \phi_i \sup_{t_0 \leq t \leq t_0 + \delta} |x_i(t) - \phi_i(0)| \leq \gamma \quad \forall i = 1, 2, \dots, k\}, \quad (3.1)$$

where $x_i \in C([t_0 - r, t_0 + \delta], \mathbb{R}^n)$. Before starting and proving the main results, we assume the following hypotheses.

(H1) $f_i(t, \phi_1, \phi_2, \dots, \phi_k)$ is measurable with respect to t on I_0 , $\forall i = 1, 2, \dots, k$.

(H2) $f_i(t, \phi_1, \phi_2, \dots, \phi_k)$ is continuous with respect to ϕ_j on $C([-r, 0], \mathbb{R}^n)$,
 $\forall i, j = 1, 2, \dots, k$.

(H3) There exist $\alpha_{i_1} \in (0, \alpha_i)$ and a real valued function $m_i(t) \in L^{\frac{1}{\alpha_{i_1}}}(I_0)$, such that for any $(x_1, x_2, \dots, x_k) \in A(\delta, \gamma)$, $\forall i = 1, 2, \dots, k$

$$|f_i(t, x_t)| \leq m_i(t), \quad t \in I_0, \quad (3.2)$$

(H4) For any $(x_1, x_2, \dots, x_k) \in A(\delta, \gamma)$, $g_i(t, x_t) = g_{i_1}(t, x_t) + g_{i_2}(t, x_t)$.

(H5) g_{i_1} is continuous and $|g_{i_1}(t, x_t) - g_{i_1}(t, y_t)| \leq l_i \|x - y\|_*$,
 where $l_i \in (0, 1)$, $\forall x = (x_1, x_2, \dots, x_k), y = (y_1, y_2, \dots, y_k) \in A(\delta, \gamma), t \in I_0$,
 $i = 1, 2, \dots, k$.

(H6) g_{i_2} is completely continuous and for any bounded set $\Lambda \in A(\delta, \gamma)$ the set $\{t \rightarrow g_{i_2}(t, x_t) : (x_1, x_2, \dots, x_k) \in \Lambda\}$, is equicontinuous on $\underbrace{C(I_0, \mathbb{R}^n) \times C(I_0, \mathbb{R}^n) \times \dots \times C(I_0, \mathbb{R}^n)}_k \quad \forall i = 1, 2, \dots, k$.

(H7) $\psi \in C^1([t_0, \infty])$ is a continuous increasing function with $|\psi(t) - \psi(s)| \leq N|t - s|$, $N \in (0, 1)$ and $|\psi'(s)| < K$, K be any positive integer.

Lemma 6. *If there exist $\delta \in (0, a)$ and $\gamma \in (0, \infty)$ such that (H1) – (H3) are satisfied, then for $t \in (t_0, t_0 + \delta]$, IVP (1.1) is equivalent to the following equation:*

$$\begin{cases} x_i(t) = \phi_i(0) - g_i(t_0, \phi_1, \phi_2, \dots, \phi_k) + g_i(t, x_t) \\ \quad + \frac{1}{\Gamma(\alpha_i)} \int_{t_0}^t \psi'(s) [\psi(t) - \psi(s)]^{\alpha_i - 1} f_i(s, x_s) ds, \quad t \in I_0 \\ x_{i_{t_0}} = \phi_i \end{cases} \quad (3.3)$$

for $i = 1, 2, \dots, k$ and $t \in I_0$.

Proof. From the conditions (H1) and (H2), it is obvious that $f_i(t, x_t)$ is Lebesgue measurable on I_0 . A direct calculation using (H7) gives that

$$\left(\psi'(s) [\psi(t) - \psi(s)]^{\alpha_i - 1} \right) \in L^{\frac{1}{1 - \alpha_{i_1}}}(I_0) \quad t \in I_0$$

In the light of Holder's inequality and (H3), we obtain that

$\left(\psi'(s) [\psi(t) - \psi(s)]^{\alpha_i - 1} \right) f_i(s, x_s)$ is Lebesgue integrable with respect to $s \in [t_0, t]$
 $\forall t \in I_0$, $i = 1, 2, \dots, k$ and $(x_1, x_2, \dots, x_k) \in A(\delta, \gamma)$ and

$$\int_{t_0}^t \left(\psi'(s) [\psi(t) - \psi(s)]^{\alpha_i - 1} \right) f_i(s, x_s) ds \leq \left\| \psi'(s) [\psi(t) - \psi(s)]^{\alpha_i - 1} \right\|_{L^{\frac{1}{1 - \alpha_{i_1}}}(I_0)} \left\| m_i \right\|_{L^{\frac{1}{\alpha_{i_1}}}(I_0)}, \quad (3.4)$$

where

$$\|F\|_{L^p(J)} = \left(\int_J |f(t)|^p dt \right)^{\frac{1}{p}},$$

for any p integrable function $F : J \rightarrow \mathbb{R}$.

According to the definition of fractional integral of a function f with respect to another function ψ and Caputo derivative of order α_i , it is easy to see that if x_i is a solution of the IVP (1.1), then x_i is a solution of equation (3.3).

On the other hand, if equation (3.3) is satisfied then $\forall t \in (t_0, t_0 + \delta]$, we have:

$$\begin{aligned} & {}^C D_{t_0}^{\alpha_i, \psi} (x_i(t) - g_i(t, x_t)) = \\ & {}^C D_{t_0}^{\alpha_i, \psi} \left(\phi_i(0) - g_i(t_0, \phi_1, \phi_2, \dots, \phi_k) + \frac{1}{\Gamma(\alpha_i)} \int_{t_0}^t \psi'(s) [\psi(t) - \psi(s)]^{\alpha_i-1} f_i(s, x_s) ds \right) \\ & = {}^C D_{t_0}^{\alpha_i, \psi} \left(\frac{1}{\Gamma(\alpha_i)} \int_{t_0}^t \psi'(s) [\psi(t) - \psi(s)]^{\alpha_i-1} f_i(s, x_s) ds \right) \end{aligned}$$

$$\begin{aligned} & {}^C D_{t_0}^{\alpha_i, \psi} (x_i(t) - g_i(t, x_t)) = {}^C D_{t_0}^{\alpha_i, \psi} I_{t_0}^{\alpha_i, \psi} f_i(t, x_t) \\ & = D_{t_0}^{\alpha_i, \psi} \left[I_{t_0}^{\alpha_i, \psi} f_i(t, x_t) - \sum_{k=0}^{n-1} \frac{[I^{\alpha_i, \psi} f_i(t, x_t)]^{[k]}(t_0)}{k!} (\psi(t) - \psi(t_0))^k \right] \\ & = D_{t_0}^{\alpha_i, \psi} I_{t_0}^{\alpha_i, \psi} f_i(t, x_t) - \sum_{k=0}^{n-1} \frac{[I^{\alpha_i, \psi} f_i(t, x_t)]^{[k]}(t_0)}{\Gamma(k - \alpha_i + 1)} (\psi(t) - \psi(t_0))^{k-\alpha_i} \\ & = f_i(t, x_t) - [I^{\alpha_i, \psi} f_i(t, x_t)]_{t=t_0} \frac{(\psi(t) - \psi(t_0))^{-\alpha_i}}{\Gamma(1 - \alpha_i)} = f_i(t, x_t) \end{aligned}$$

since $[I^{\alpha_i, \psi} f_i(t, x_t)]_{t=t_0} = 0$.

Hence we get ${}^C D_{t_0}^{\alpha_i, \psi} (x_i(t) - g_i(t, x_t)) = f_i(t, x_t)$, $t \in (t_0, t_0 + \delta]$.
And this completes the proof. \square

Theorem 7. *If there are $\delta \in (0, a)$ and $\gamma \in (0, \infty)$ satisfying the assumptions (H1) – (H7), then IVP(1.1) has at least one solution on $[t_0, t_0 + \eta]$ for $\eta \in \mathbb{R}^+$.*

Proof. According to (H4), equation (3.3) is equivalent to the following equation:

$$\begin{cases} x_i(t) = \phi_i(0) - g_{i_1}(t_0, \phi_1, \phi_2, \dots, \phi_k) - g_{i_2}(t_0, \phi_1, \phi_2, \dots, \phi_k) \\ \quad + g_{i_1}(t, x_t) + g_{i_2}(t, x_t) \\ \quad + \frac{1}{\Gamma(\alpha_i)} \int_{t_0}^t \psi'(s) [\psi(t) - \psi(s)]^{\alpha_i-1} f_i(s, x_s) ds, \quad t \in I_0 \\ x_{i_{t_0}} = \phi_i \quad i = 1, 2, \dots, k \end{cases}$$

Let $(\tilde{\phi}_1, \tilde{\phi}_2, \dots, \tilde{\phi}_k) \in A(\delta, \gamma)$ be defined as

$$\tilde{\phi}_{i_{t_0}} = \phi_i, \quad \tilde{\phi}_i(t_0 + t) = \phi_i(0) \quad \forall t \in [0, \delta], \quad i = 1, 2, \dots, k.$$

If $x = (x_1, x_2, \dots, x_k)$ is a solution of the IVP(1.1), let $x_i(t_0 + t) = \tilde{\phi}_i(t_0 + t) + y_i(t)$, $t \in [-r, \delta]$, $i = 1, 2, \dots, k$.

Then we have, $x_{i_{t_0+t}} = \tilde{\phi}_{i_{t_0+t}} + y_{i_t}$, $t \in [0, \delta]$, $i = 1, 2, \dots, k$.

Thus

$$\begin{aligned}
 y_i(t) = & -g_{i_1}(t_0, \phi_1, \phi_2, \dots, \phi_k) - g_{i_2}(t_0, \phi_1, \phi_2, \dots, \phi_k) \\
 & + g_{i_1}(t_0 + t, y_{1_t} + \tilde{\phi}_{1_{t_0+t}}, y_{2_t} + \tilde{\phi}_{2_{t_0+t}}, \dots, y_{k_t} + \tilde{\phi}_{k_{t_0+t}}) \\
 & + g_{i_2}(t_0 + t, y_{1_t} + \tilde{\phi}_{1_{t_0+t}}, y_{2_t} + \tilde{\phi}_{2_{t_0+t}}, \dots, y_{k_t} + \tilde{\phi}_{k_{t_0+t}}) \\
 & + \frac{1}{\Gamma(\alpha_i)} \int_0^t \psi'(s + t_0) [\psi(t + t_0) - \psi(s + t_0)]^{\alpha_i - 1} \\
 & f_i(t_0 + s, y_{1_s} + \tilde{\phi}_{1_{t_0+s}}, y_{2_s} + \tilde{\phi}_{2_{t_0+s}}, \dots, y_{k_s} + \tilde{\phi}_{k_{t_0+s}}) ds,
 \end{aligned} \tag{3.5}$$

$$t \in [0, \delta], i = 1, 2, \dots, k.$$

Since g_{i_1}, g_{i_2} are continuous and x_{i_t} is continuous in t for all $i = 1, 2, \dots, k$, there exists $\delta' > 0$ such that:

$$|g_{i_1}(t_0 + t, y_{1_t} + \tilde{\phi}_{1_{t_0+t}}, y_{2_t} + \tilde{\phi}_{2_{t_0+t}}, \dots, y_{k_t} + \tilde{\phi}_{k_{t_0+t}}) - g_{i_1}(t_0, \phi_1, \phi_2, \dots, \phi_k)| < \frac{\gamma}{3} \tag{3.6}$$

$$|g_{i_2}(t_0 + t, y_{1_t} + \tilde{\phi}_{1_{t_0+t}}, y_{2_t} + \tilde{\phi}_{2_{t_0+t}}, \dots, y_{k_t} + \tilde{\phi}_{k_{t_0+t}}) - g_{i_2}(t_0, \phi_1, \phi_2, \dots, \phi_k)| < \frac{\gamma}{3} \tag{3.7}$$

for $0 < t < \delta'$ and $i = 1, 2, \dots, k$.

Choose

$$\eta = \min \left\{ \delta, \delta', \left(\frac{\gamma \Gamma(\alpha_i)(1 + \beta_i)^{(1 - \alpha_{i_1})}}{3M_i N K} \right)^{\frac{1}{(1 + \beta_i)(1 - \alpha_{i_1})}} \right\}, \tag{3.8}$$

where $\beta_i = \frac{\alpha_i - 1}{1 - \alpha_{i_1}} \in (-1, 0)$ and $M_i = \|m_i\|_{L^{\frac{1}{\alpha_{i_1}}}(I_0)}, i = 1, 2, \dots, k$

Define $E(\eta, \gamma)$ as follows:

$$\begin{aligned}
 E(\eta, \gamma) = \\
 \left\{ (y_1, y_2, \dots, y_k) : y_i \in C([-r, \eta], \mathbb{R}^n) / y_i(s) = 0 \text{ for } s \in [-r, 0], \|y_i\| \leq r, i = 1, 2, \dots, k \right\}.
 \end{aligned}$$

Then $E(\eta, \gamma)$ is a closed, bounded and convex subset of $C([-r, \eta], \mathbb{R}^n) \times C([-r, \eta], \mathbb{R}^n) \times \dots \times C([-r, \eta], \mathbb{R}^n)$.

On $E(\eta, \gamma)$, we define the operators S and U on $E(\eta, \gamma)$ by:

$$S(y_1, y_2, \dots, y_k)(t) = \begin{pmatrix} S_1(y_1, y_2, \dots, y_k)(t) \\ S_2(y_1, y_2, \dots, y_k)(t) \\ \vdots \\ S_k(y_1, y_2, \dots, y_k)(t) \end{pmatrix}$$

$$U(y_1, y_2, \dots, y_k)(t) = \begin{pmatrix} U_1(y_1, y_2, \dots, y_k)(t) \\ U_2(y_1, y_2, \dots, y_k)(t) \\ \vdots \\ U_k(y_1, y_2, \dots, y_k)(t) \end{pmatrix}$$

$$S_i(y_1, y_2, \dots, y_k)(t) = \begin{cases} 0 & t \in [-r, 0] \\ -g_{i_1}(t_0, \phi_1, \phi_2, \dots, \phi_k) \\ +g_{i_1}(t_0 + t, y_{1_t} + \tilde{\phi}_{1_{t_0+t}}, y_{2_t} + \tilde{\phi}_{2_{t_0+t}}, \dots, y_{k_t} + \tilde{\phi}_{k_{t_0+t}}) & t \in [0, \eta] \end{cases}$$

$$U_i(y_1, y_2, \dots, y_k)(t) = \begin{cases} 0 & t \in [-r, 0] \\ -g_{i_2}(t_0, \phi_1, \phi_2, \dots, \phi_k) \\ +g_{i_2}(t_0 + t, y_{1_t} + \tilde{\phi}_{1_{t_0+t}}, y_{2_t} + \tilde{\phi}_{2_{t_0+t}}, \dots, y_{k_t} + \tilde{\phi}_{k_{t_0+t}}) \\ + \frac{1}{\Gamma(\alpha_i)} \int_0^t \psi'(s + t_0) (\psi(t + t_0) - \psi(s + t_0))^{\alpha_i - 1} \\ f_i(t_0 + s, y_{1_s} + \tilde{\phi}_{1_{t_0+s}}, y_{2_s} + \tilde{\phi}_{2_{t_0+s}}, \dots, y_{k_s} + \tilde{\phi}_{k_{t_0+s}}) ds & t \in [0, \eta] \end{cases}$$

for $i = 1, 2, \dots, k$.

It is easy to see that if the operator equation $y = Sy + Uy$ has a solution $y = (y_1, y_2, \dots, y_k) \in E(\eta, \gamma)$ if and only if y_i is a solution of (3.5) $\forall i = 1, 2, \dots, k$. Thus $x_i(t_0 + t) = y_i(t) + \tilde{\phi}_i(t_0 + t)$ is a solution of equation (1.1) on $[0, \eta]$. Therefore the existence of a solution of the IVP(1.1) is equivalent to the existence of a fixed point for the operator $S+U$ on $E(\eta, \gamma)$. Hence it is sufficient to show that $S+U$ has a fixed point in $E(\eta, \gamma)$.

The proof is divided into three steps.

Step I: $Sz + Uy \in E(\eta, \gamma)$ for every pair $z = (z_1, z_2, \dots, z_k)$, $y = (y_1, y_2, \dots, y_k) \in E(\eta, \gamma)$.

In fact, for every pair $z, y \in E(\eta, \gamma)$, $S_i z + U_i y \in C([-r, \eta], \mathbb{R}^n)$, $i = 1, 2, \dots, k$, which implies $(Sz + Uy)(t) = 0$, $\forall t \in [-r, 0]$.

Now we have

$$\begin{aligned} & |S_i z(t) - U_i y(t)| \leq \\ & | -g_{i_1}(t_0, \phi_1, \phi_2, \dots, \phi_k) + g_{i_1}(t_0 + t, z_{1_t} + \tilde{\phi}_{1_{t_0+t}}, z_{2_t} + \tilde{\phi}_{2_{t_0+t}}, \dots, z_{k_t} + \tilde{\phi}_{k_{t_0+t}}) | \\ & + | -g_{i_2}(t_0, \phi_1, \phi_2, \dots, \phi_k) + g_{i_2}(t_0 + t, y_{1_t} + \tilde{\phi}_{1_{t_0+t}}, y_{2_t} + \tilde{\phi}_{2_{t_0+t}}, \dots, y_{k_t} + \tilde{\phi}_{k_{t_0+t}}) | \\ & + \frac{1}{\Gamma(\alpha_i)} \int_0^t |\psi'(s + t_0) [\psi(t + t_0) - \psi(s + t_0)]^{\alpha_i - 1} \\ & f_i(t_0 + s, y_{1_s} + \tilde{\phi}_{1_{t_0+s}}, y_{2_s} + \tilde{\phi}_{2_{t_0+s}}, \dots, y_{k_s} + \tilde{\phi}_{k_{t_0+s}}) | ds \end{aligned}$$

$$\begin{aligned}
&\leq \frac{2\gamma}{3} + \frac{1}{\Gamma(\alpha_i)} \left(\int_0^t |\psi'(s+t_0) [\psi(t+t_0) - \psi(s+t_0)]^{\alpha_i-1}|^{\frac{1}{1-\alpha_i}} ds \right)^{1-\alpha_i} \\
&\quad \left(\int_{t_0}^{t_0+t} (m_i(s))^{\frac{1}{\alpha_i}} ds \right)^{\alpha_i} \\
&\leq \frac{2\gamma}{3} + \frac{M_i K N^{\alpha_i-1} \eta^{(1+\beta_i)(1-\alpha_i)}}{\Gamma(\alpha_i) (1+\beta_i)^{1-\alpha_i}} \\
&\leq \gamma, \forall t \in [0, \eta] \text{ and } i = 1, 2, \dots, k
\end{aligned}$$

Therefore

$$\|S_i z + U_i y\| = \sup_{t \in [0, \eta]} |(S_i z)(t) + (U_i y)(t)| \leq \gamma, \forall i = 1, 2, \dots, k$$

which means that $Sz + Uy \in E(\eta, \gamma)$ for any $z, y \in E(\eta, \gamma)$.

Step II: To prove that S is a contraction on $E(\eta, \gamma)$.

Let $y' = (y'_1, y'_2, \dots, y'_k), y'' = (y''_1, y''_2, \dots, y''_k) \in E(\eta, \gamma)$,

then, $(y'_{1_t} + \tilde{\phi}_{1_{t_0+t}}, y'_{2_t} + \tilde{\phi}_{2_{t_0+t}}, \dots, y'_{k_t} + \tilde{\phi}_{k_{t_0+t}}) \in A(\delta, \gamma)$ and

$(y''_{1_t} + \tilde{\phi}_{1_{t_0+t}}, y''_{2_t} + \tilde{\phi}_{2_{t_0+t}}, \dots, y''_{k_t} + \tilde{\phi}_{k_{t_0+t}}) \in A(\delta, \gamma)$.

Also by (H5), we get that

$$\begin{aligned}
&|S_i y'(t) - S_i y''(t)| \\
&= |g_{i_1}(t_0+t, y'_{1_t} + \tilde{\phi}_{1_{t_0+t}}, y'_{2_t} + \tilde{\phi}_{2_{t_0+t}}, \dots, y'_{k_t} + \tilde{\phi}_{k_{t_0+t}}) \\
&\quad - g_{i_1}(t_0+t, y''_{1_t} + \tilde{\phi}_{1_{t_0+t}}, y''_{2_t} + \tilde{\phi}_{2_{t_0+t}}, \dots, y''_{k_t} + \tilde{\phi}_{k_{t_0+t}})| \\
&\leq l_i \|y' - y''\|_*
\end{aligned}$$

which implies $\|S y' - S y''\|_* \leq l \|y' - y''\|_*$ where $l = \max\{l_1, l_2, \dots, l_k\}$

Since $0 < l < 1$, S is a contraction on $E(\eta, \gamma)$.

Step III: Now we show that U is a completely continuous operator.

$$U_{i_1}(y_1, y_2, \dots, y_k)(t) = \begin{cases} 0 & t \in [-r, 0], \\ -g_{i_2}(t_0, \phi_1, \phi_2, \dots, \phi_k) \\ + g_{i_2}(t_0+t, y_{1_t} + \tilde{\phi}_{1_{t_0+t}}, y_{2_t} + \tilde{\phi}_{2_{t_0+t}}, \dots, y_{k_t} + \tilde{\phi}_{k_{t_0+t}}) & t \in [0, \eta]. \end{cases}$$

and

$$U_{i_2}(y_1, y_2, \dots, y_k)(t) = \begin{cases} 0 & t \in [-r, 0] \\ \frac{1}{\Gamma(\alpha_i)} \int_0^t \psi'(s + t_0) [\psi(t + t_0) - \psi(s + t_0)]^{\alpha_i - 1} \\ \quad \cdot f_i(t_0 + s, y_{1_s} + \tilde{\phi}_{1_{t_0+s}}, y_{2_s} + \tilde{\phi}_{2_{t_0+s}}, \dots, y_{k_s} + \tilde{\phi}_{k_{t_0+s}}) ds & t \in [0, \eta] \end{cases}$$

for $i = 1, 2, \dots, k$

Clearly $U = \begin{pmatrix} U_{11} + U_{12} \\ U_{21} + U_{22} \\ \vdots \\ U_{k1} + U_{k2} \end{pmatrix}$

Since g_{i_2} is completely continuous for all $i = 1, 2, \dots, k$, U_{i_1} is continuous and also $\{U_{i_1}(y) : y \in E(\eta, \gamma)\}$ is uniformly bounded. By using the condition (H6), it is easy to check that $\{U_{i_1}(y) : y \in E(\eta, \gamma)\}$ is a completely continuous operator.

On the other hand

$$\begin{aligned} |U_{i_2}y(t)| &\leq \frac{1}{\Gamma(\alpha_i)} \int_0^t |\psi'(s + t_0) [\psi(t + t_0) - \psi(s + t_0)]^{\alpha_i - 1} \\ &\quad \cdot f_i(t_0 + s, y_{1_s} + \tilde{\phi}_{1_{t_0+s}}, y_{2_s} + \tilde{\phi}_{2_{t_0+s}}, \dots, y_{k_s} + \tilde{\phi}_{k_{t_0+s}})| ds \\ &\leq \frac{1}{\Gamma(\alpha_i)} \left(\int_0^t |\psi'(s + t_0) [\psi(t + t_0) - \psi(s + t_0)]^{\alpha_i - 1}|^{\frac{1}{1-\alpha_{i_1}}} ds \right)^{1-\alpha_{i_1}} \\ &\quad \left(\int_0^t (m_i(s))^{\frac{1}{\alpha_{i_1}}} ds \right)^{\alpha_{i_1}} \\ &\leq \frac{1}{\Gamma(\alpha_i)} \frac{\eta^{(1+\beta_i)(1-\alpha_{i_1})} M_i K N^{\alpha_i - 1}}{(1 + \beta_i)^{1-\alpha_{i_1}} \Gamma(\alpha_i)}, \quad \forall t \in [0, \eta], \quad i = 1, 2, \dots, k \end{aligned}$$

Hence $\{U_{i_2}(y) : y \in E(\eta, \gamma)\}$ is uniformly bounded.

Now we will prove that $\{U_{i_2}y : y \in E(\eta, \gamma)\}$ is equicontinuous.

For any $0 \leq t_1 < t_2 \leq \eta$ and $y \in E(\eta, \gamma)$, we get that

$$\begin{aligned}
& |U_{i_2}y(t_2) - U_{i_2}y(t_1)| \\
& \leq \frac{1}{\Gamma(\alpha_i)} \int_0^{t_1} |\psi'(s+t_0) [(\psi(t_2+t_0) - \psi(s+t_0))^{\alpha_i-1} - (\psi(t_1+t_0) - \psi(s+t_0))^{\alpha_i-1}] \\
& \quad f_i(t_0+s, y_{1_s} + \tilde{\phi}_{1_{t_0+s}}, y_{2_s} + \tilde{\phi}_{2_{t_0+s}}, \dots, y_{k_s} + \tilde{\phi}_{k_{t_0+s}})| ds \\
& + \frac{1}{\Gamma(\alpha_i)} \int_{t_1}^{t_2} |\psi'(s+t_0) [\psi(t_2+t_0) - \psi(s+t_0)]^{\alpha_i-1} \\
& \quad f_i(t_0+s, y_{1_s} + \tilde{\phi}_{1_{t_0+s}}, y_{2_s} + \tilde{\phi}_{2_{t_0+s}}, \dots, y_{k_s} + \tilde{\phi}_{k_{t_0+s}})| ds \\
& \leq \frac{M_iKN^{\alpha_i-1}}{\Gamma(\alpha_i)} \left[\int_0^{t_1} (t_1-s)^{\beta_i} - (t_2-s)^{\beta_i} ds \right]^{\alpha_i-1} + \frac{M_iKN^{\alpha_i-1}}{\Gamma(\alpha_i)} \left[\int_{t_1}^{t_2} (t_2-s)^{\beta_i} ds \right]^{1-\alpha_{i_1}} \\
& \leq \frac{2M_iKN^{\alpha_i-1}}{\Gamma(\alpha_i)(\beta_i+1)^{1-\alpha_{i_1}}} (t_2-t_1)^{(1+\beta_i)(1-\alpha_{i_1})},
\end{aligned}$$

which means that $\{U_{i_2}y : y \in E(\eta, \gamma)\}$ is equicontinuous. Moreover, it is also clear that U_2 is continuous. So U_2 is a completely continuous operator. Then $U = U_1 + U_2$ is a completely continuous operator.

Therefore, Krasnoselskii's fixed point theorem shows that $S + U$ has a fixed point on $E(\eta, \gamma)$ and hence the IVP(1.1) has a solution $x = (x_1, x_2, \dots, x_k)$ where $x_i(t) = \phi_i(0) + y_i(t - t_0)$ for all $t \in [t_0, t_0 + \eta], i = 1, 2, \dots, k$. This completes the proof. \square

In the case where $g_{i_1} \equiv 0, \forall i = 1, 2, \dots, k$, we get the following result:

Corollary 8. [16] Assume that there exist $\delta \in (0, a)$ and $\gamma \in (0, \infty)$ such that (H1)–(H3) hold, g_{i_1} is continuous for all $i = 1, 2, \dots, k$ and

$$|g_i(t, x_t) - g_i(t, y_t)| \leq l_i \|x - y\|_*, \forall x = (x_1, x_2, \dots, x_k), y = (y_1, y_2, \dots, y_k) \in A(\delta, \gamma)$$

and $t \in I_0$ where $l_i \in (0, 1)$ is a constant for all $i = 1, 2, \dots, k$. Then IVP (1.1) has at least one solution on $[t_0, t_0 + \eta]$ for some positive number η .

In the case where $g_{i_2} \equiv 0, \forall i = 1, 2, \dots, k$, we have the following result:

Corollary 9. [16] Assume that there exist $\delta \in (0, a)$ and $\gamma \in (0, \infty)$ such that (H1)–(H3) hold, g_i is completely continuous for all $i = 1, 2, \dots, k$ and the family $\{t \rightarrow g_i(t, x_t) : (x_1, x_2, \dots, x_k) \in \Lambda\}$ is equicontinuous on $C(I_0, \mathbb{R}^n) \times C(I_0, \mathbb{R}^n) \times \dots \times C(I_0, \mathbb{R}^n)$ for all bounded sets Λ in $A(\delta, \gamma)$. Then IVP (1) has at least one solution on $[t_0, t_0 + \eta]$ for some positive number η .

Theorem 10. Assume that the functions f and g are Lipschitz continuous with respect to the second variable, that is, there exist positive constants L_{i_1} and L_{i_2} such that

$$\|f_i(t, x_{it}) - f_i(t, x_{i2t})\| \leq L_{i_1} \text{ and } \|g_i(t, x_{it}) - g_i(t, x_{i2t})\| \leq L_{i_2}.$$

Then there is a constant $h \in \mathbb{R}^+$ such that there exists a unique solution to the IVP(1.1) in the interval $[t_0, t_0 + h] \subseteq [a, b]$ if $\left(\frac{L_{i_1}}{\Gamma(\alpha_i+1)} (\psi(t_0+h) - \psi(t_0))_i^\alpha + L_{i_2} \right) < 1$.

Proof. For $t \in I_0$, define the function F by

$$F_i(x, t) = \phi_i(0) - g_{i1}(t_0, \phi_1, \phi_2, \dots, \phi_k) - g_{i2}(t_0, \phi_1, \phi_2, \dots, \phi_k) + g_{i1}(t, x_t) + g_{i2}(t, x_t) + \frac{1}{\Gamma(\alpha_i)} \int_{t_0}^t \psi'(s) (\psi(t) - \psi(s))^{\alpha_i-1} f_i(s, x_s) ds.$$

Let $U = \{x_i \in C([t_0 - r, t_0 + a], \mathbb{R}^n) : {}^C D_{t_0}^{\alpha_i, \psi} x_i(t)$ exists and is continuous in $[t_0, t_0 + h]\}$. It is enough to prove that $F_i : U \rightarrow U$ is a contraction.

Let us see that F_i is well defined, i.e., $F_i(U) \subseteq U$.

Given the function $x_i \in U$, we see that ${}^C D_{t_0}^{\alpha_i, \psi} (F_i(x_i)(t) - g_i(x_{it})) = f_i(t, x_{it})$ is continuous and

$$F_i(x_i)(t) = I_{t_0}^{\alpha_i, \psi} f_i(t, x_{it}) + g_i(t, x_{it}).$$

Now let $x_{i1}, x_{i2} \in U$ be arbitrary, then by assumptions H_1, H_2 , we have

$$\begin{aligned} \|F_i(x_{i1}) - F_i(x_{i2})\| &\leq \|I_{t_0}^{\alpha_i, \psi} (f_i(t, x_{i1t}) - f_i(t, x_{i2t}))\| + \|g_i(t, x_{i1t}) - g_i(t, x_{i2t})\| \\ &\leq \left[\frac{L_{i1}}{\Gamma(\alpha_i + 1)} (\psi(t_0 + h) - \psi(t_0))_i^\alpha + L_{i2} \right] \|x_{i1} - x_{i2}\|, \end{aligned}$$

which proves that F_i is a contraction. By the Banach fixed point theorem, we get the result of the theorem. \square

4 Example

Here we give an example to demonstrate our results.

Consider the 3-dimensional system of ψ -Caputo neutral fractional differential equations

$$\begin{cases} D^{\frac{1}{2}, x} \left(x_1(t) - \frac{e^{-3t}}{12\sqrt{6400+t^4}} (\sin x_1(t) + \cos x_2(t) + \sin x_3(t)) \right) \\ = \frac{\Gamma(\frac{3}{4})}{\Gamma(\frac{1}{4})} (t + 3)^{-\frac{3}{4}} \frac{\sin^4(x_1(t))}{1+|(x_2(t))|} \times \frac{(x_3(t))^2}{1+|x_3(t)|^3} \\ D^{\frac{1}{4}, x} \left(x_2(t) - \frac{1}{12\sqrt{3600+t^2}} \left(\cos x_1(t) + \frac{|x_2(t)|}{2+|x_2(t)|} + \frac{|x_3(t)|}{4+|x_3(t)|} \right) \right) \\ = \frac{\Gamma(\frac{3}{8})}{\Gamma(\frac{1}{8})} (t + \frac{3}{2})^{-\frac{7}{8}} \frac{\cos^2(x_1(t))}{1+\sin^4(x_3(t))+|x_2(t)|^2} \\ D^{\frac{1}{3}, x} \left(x_3(t) - \left(\frac{e^t}{18} + \frac{\cos^2 x_1(t)}{9} + \frac{25|x_2(t)|}{10+|x_2(t)|} \right) \right) \\ = \frac{\Gamma(\frac{5}{6})}{\sqrt{\pi}} (t + 1)^{-\frac{1}{2}} \frac{|x_1(t)|}{1+(x_1(t))^2+6|x_2(t)|^5} \end{cases}$$

for $t \in (0, 1)$

$$x_{i_0} = t, i = 1, 2, 3, t \in [-1, 0].$$

Define the maps

$$\begin{aligned}
f_1(t, x_1, x_2, x_3) &= \frac{\Gamma(\frac{3}{4})}{\Gamma(\frac{1}{4})} (t+3)^{-\frac{3}{4}} \frac{\sin^4(x_1(t-1))}{1+|(x_2(t-1))|} \times \frac{(x_3(t-1))^2}{1+|x_3(t-1)|^3} \\
f_2(t, x_1, x_2, x_3) &= \frac{\Gamma(\frac{3}{8})}{\Gamma(\frac{1}{8})} (t+\frac{3}{2})^{-\frac{7}{8}} \frac{\cos^2(x_1(t-1))}{1+\sin^4(x_3(t-1))+(x_2(t-1))^2} \\
f_3(t, x_1, x_2, x_3) &= \frac{\Gamma(\frac{5}{6})}{\sqrt{\pi}} (t+1)^{-\frac{1}{2}} \frac{|x_1(t)|}{1+(x_1(t))^2+6|x_2(t)|^5} \\
g_1(t, x_1, x_2, x_3) &= \frac{e^{-3t}}{12\sqrt{6400+t^4}} (\sin x_1(t) + \cos x_2(t) + \sin x_3(t)) \\
g_2(t, x_1, x_2, x_3) &= \frac{1}{12\sqrt{3600+t^2}} \left(\cos x_1(t) + \frac{|x_2(t)|}{2+|x_2(t)|} + \frac{|x_3(t)|}{4+|x_3(t)|} \right) \\
g_3(t, x_1, x_2, x_3) &= \frac{e^t}{18} + \frac{\cos^2 x_1(t)}{9} + \frac{25|x_2(t)|}{10+|x_2(t)|}
\end{aligned}$$

with $\alpha_1 = \frac{1}{2}$, $\alpha_2 = \frac{1}{4}$, $\alpha_3 = \frac{1}{3}$, $\psi(x) = x$ and if $m_1(t) = \frac{\Gamma(\frac{3}{4})}{\Gamma(\frac{1}{4})} (t+3)^{-\frac{3}{4}}$, $m_2(t) = \frac{\Gamma(\frac{3}{8})}{\Gamma(\frac{1}{8})} (t+\frac{3}{2})^{-\frac{7}{8}}$, $m_3(t) = \frac{\Gamma(\frac{5}{6})}{\sqrt{\pi}} (t+1)^{-\frac{1}{2}}$, it is easy to check that $|f_1(t, x_{t_1}, x_{t_2}, x_{t_3})(t)| \leq m_1(t)$, $|f_2(t, x_{t_1}, x_{t_2}, x_{t_3})(t)| \leq m_2(t)$, $|f_3(t, x_{t_1}, x_{t_2}, x_{t_3})(t)| \leq m_3(t)$.

Also $g_1(t, x_{t_1}, x_{t_2}, x_{t_3})(t)$, $g_2(t, x_{t_1}, x_{t_2}, x_{t_3})(t)$ and $g_3(t, x_{t_1}, x_{t_2}, x_{t_3})(t)$ satisfy Lipschitz condition with $l_1 = \frac{1}{320}$, $l_2 = \frac{1}{240}$ and $l_3 = \frac{1}{18}$ respectively.

Thus, all conditions of Theorem (7) hold and so this system of ψ -Caputo fractional functional differential equation has a solution.

5 Conclusion

The main reason behind the unpopularity of fractional calculus is that there are many nonequivalent definitions for integral and differential operators in it. Hence nowadays many researchers concentrate on defining generalized operators, from which the classical definitions can be obtained. Different phenomena can be interpreted with the help of systems of equations more effectively than with single equation. In this paper we concentrated on generalized fractional differential operators in k -systems and proved the existence and uniqueness of solutions of a k -systems of ψ -caputo fractional neutral functional differential equations under the specified conditions using Krasnoselskii's Fixed Point theorem and Banach's Fixed Point theorem respectively. Finally, we give an example to illustrate our results.

References

- [1] A. A. Kilbas, H. M. Srivastava and J. J. Trujillo. "Theory and applications of Fractional Differential equations", North-Holland Mathematics Studies, 204, 1st ed., Elsevier Science B. V., Amsterdam, 2006.
- [2] S. G. Samko, A. A. Kilbas and Marichev, "Fractional Integrals and Derivatives, Theory and Applications", Gordon and Breach, Yverdon, 1993.
- [3] J. A Tenreiro Machado, Manuel F. Silva, Ramiros S. Barbosa, Isabel S. Jesus, Cecilia M Reis, Maria G. Marcos and Alexandra F. Galhano, Some applications of Fractional calculus in Engineering, *Mathematical Problems in Engineering* **639801** (2010).
- [4] Mehdi Dalir and Majid Bashour. Applications of Fractional Calculus, *Applied Mathematical Sciences* **4** (2010),1021-1032.

- [5] Yong Zhang and Samantha E. Hansen. A review of applications of fractional calculus in Earth system dynamics, *Chaos, Solitons and Fractals* **102** (2017), 29-46.
- [6] Yong Zhou, Jinrong Wang and Lu Zhang, “Basic Theory of Fractional Differential Equations”, 3rd ed., WSPC World Scientific Co. Pte, Ltd, 2017.
- [7] O. P. Agarwal, Some generalized fractional calculus operators and their applications in integral equations, *Frac. Cal. Appl. Anal* **15** (4) (2012), 700-711.
- [8] Ricardo Almeida. A Caputo fractional derivative of a function with respect to another function, *Communications in Nonlinear Science and Numerical Simulation* **44** (2017), 460-481.
- [9] U. N. Katugampola, New fractional integral unifying six existing fractional integrals, *arxiv.org/abs/1612.08596*, (2016).
- [10] U. N. Katugampola, A new approach to generalized fractional derivatives, *Bull. Math. Anal. Appl.* **6** (4) (2014), 1-15.
- [11] J. Vanterler Da C. Sousa, E. Capelas De Oliveira, On the ψ -Hilfer Fractional Derivative, *Commun. Nonlinear Sci. Numer. Simulat.* **60** (2018), 72-91.
- [12] Dumitru Baleanu, Sayyedeh, Zahra Nazemi and Shahram Rezapour, A k - Dimensional System of Fractional Neutral Functional Differential Equations with Bounded Delay, *Hindawi Publishing Corporation, Abstract and Applied Analysis* **524761** (2014).
- [13] R. P. Agarwal, Yong Zhou and Yunyun He. Existence of fractional neutral functional differential equations *Computers and Mathematics with Applications* **59** (2010), 1095-1100.
- [14] W. R. Melvin. A class of Neutral Functional Differential Equations, *Journal of Differential Equations* **12** (1972), 524-534.
- [15] Runping Ye and Guowei Zhang, Neutral Functional Differential Equations of Second order with infinite Delays, *Electronic Journal of Differential Equations* **36** (2010), 1-12.
- [16] Shabna.M.S and Ranjini.M.C. Fractional Impulsive Neutral functional Differential Equations involving ψ -Caputo fractional derivative, *Malaya Journal of Mathematik* **1** (2019), 493-499.
- [17] D.Baleanu, S. Z. Nazemi, and Sh. Rezapour. Attractivity for a k -dimensional system of fractional functional differential equations and global attractivity for a k -dimensional system of nonlinear fractional differential equations, *Journal of Inequalities and Applications* **31**, (2014).
- [18] Ricardo Almeida, Agnieszka B. Malinowska and M. Teresa T. Monteiro, Fractional differential equations with a Caputo derivative with respect to a Kernel function and their applications, *Mathematical Methods in the Applied Sciences* **41** (2018), 336-352.
- [19] Ricardo Almeida, Fractional differential equations with mixed boundary conditions, *The Bulletin of the Malaysian Mathematical Society* **2** (2018).
- [20] William R. Melvin. Some extensions of Krasnoselskii Fixed point theorem, *Journal of Differential Equations* **11** (1972), 335–348.

Title	Acta Universitatis Matthiae Belii Series Mathematics
Volume	28
First Edition	
Number of copies	110
Pages	98
Design and layout	Ján Karabáš
Published by	Belianum, vydavateľstvo UMB
Printed by	Equilibria, s.r.o., Košice
Typeset with \LaTeX	
ISSN	1338-712X
ISBN	978-80-557-1786-9

Contents

H. Cheriha, Y. Gati and V. P. Kostov
Degree 5 polynomials and Descartes' rule of signs 3

M. Izadi
**An accurate approximation method for solving fractional
order boundary value problems** 23

K. Kotul'ová and M. Haviar
Recent developments on gracefulness of graphs.
A survey complemented with chessboard representations 39

S. Kurtulík
New descriptions of certain classes of graceful graphs 67

M. S. Shabna and M. C. Ranjini
**A k -dimensional systems of fractional neutral functional
differential equations involving ψ -Caputo fractional derivative** 85